Transformative Science and Engineering for Nuclear Decommissioning

Off-Gas Emissions From Vitrification of Nuclear Waste

Alex Stone, Sheffield Hallam University

Transcend Theme Meeting 2020

For a Low Carbon Future

The Problem

- The UK has 133,000 m^3 of radioactive waste in storage and an estimated 4,420,000 m^3 arising in the future[1]
- A majority of this waste is from (or will arise from) site decommissioning and legacy (eg. Sellafield, Magnox)
- Vitrification has been considered as a waste treatment technique for ILW which involves the heating of waste to high temperatures up to 1400°C which may volatilise some of the components of the waste[2]

1. NDA. (2020). *The 2019 Inventory*. NDA Department for Business, Energy and Industrial Strategy. https://ukinventory.nda.gov.uk/the-2019-inventory/2019-uk-data/
2. Caurant, D. (2009). *Glasses, glass-ceramics and ceramics for immobilization of highly radioactive nuclear wastes*. Nova Science Publishers, Inc.

The Project

Develop technologies for real time emission monitoring

Establish techniques for reduction of emissions from melts

Create an off-gas system for measuring emissions and trial previous steps

Scale up and apply to industrial size vitrification tanks

Experimental Procedure

- To establish a baseline for validation of the real time system and emission reduction firstly another method must be used to quantify the target gaseous compound
- Impingement[3] in various absorption solutions from furnace exhaust and subsequent analysis

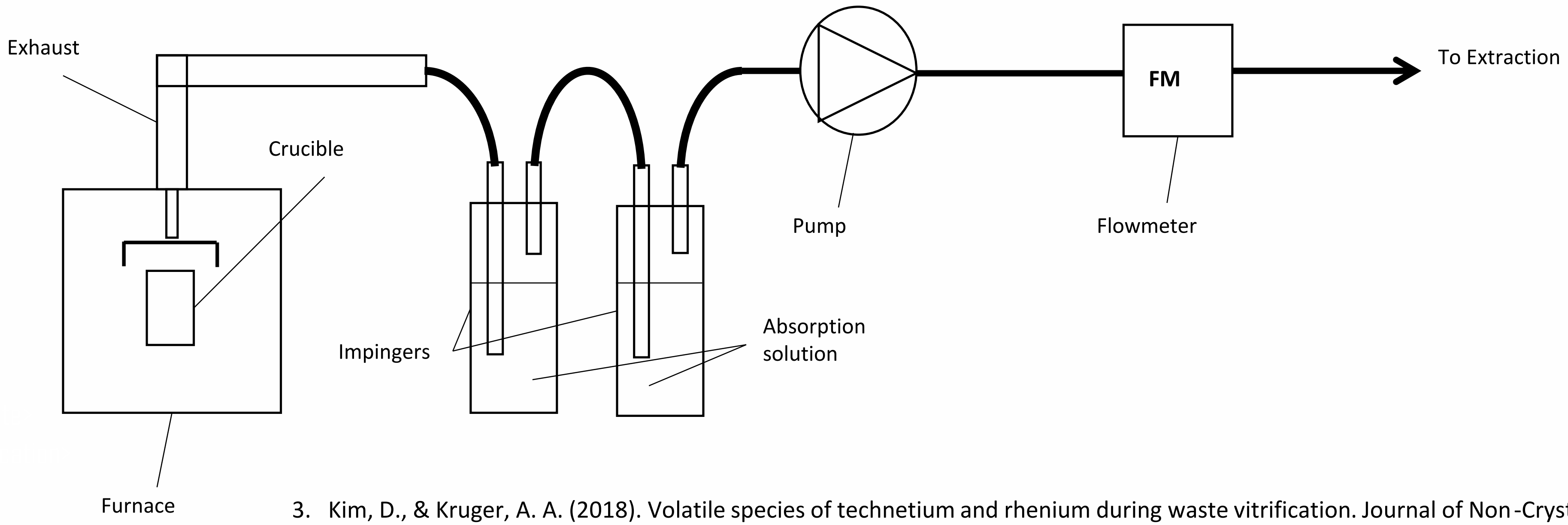

3. Kim, D., & Kruger, A. A. (2018). Volatile species of technetium and rhenium during waste vitrification. Journal of Non-Crystalline Solids, 481(October 2017), 41–50. https://doi.org/10.1016/j.jnoncrysol.2017.10.013

Experimental Procedure

Borosilicate

Magnesium Aluminosilicate

Mixture Windscale

SIXEP Sludge

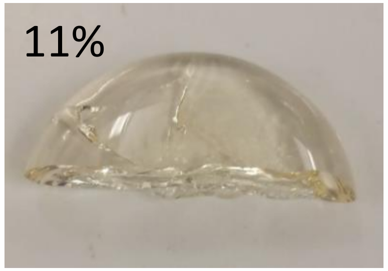

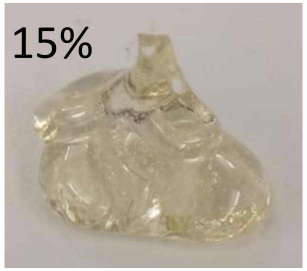

Clinoptilolite/Sand Mixture

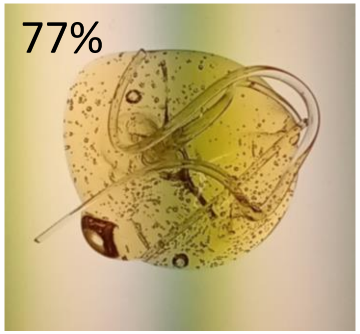

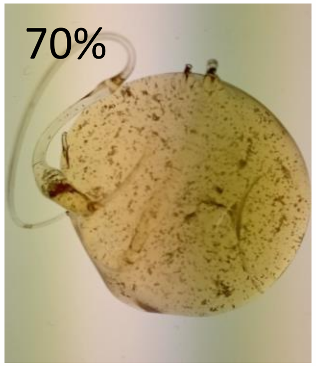

Waste Loading is indicated in the top left of the image.

4. Cassingham, N. J., Corkhill, C. L., Stennett, M. C., Hand, R. J., & Hyatt, N. C. (2016). Alteration layer formation of Ca- and Zn-oxide bearing alkali borosilicate glasses for immobilisation of UK high level waste: A vapour hydration study. Journal of Nuclear Materials, 479, 639–646. https://doi.org/10.1016/j.jnucmat.2016.06.009

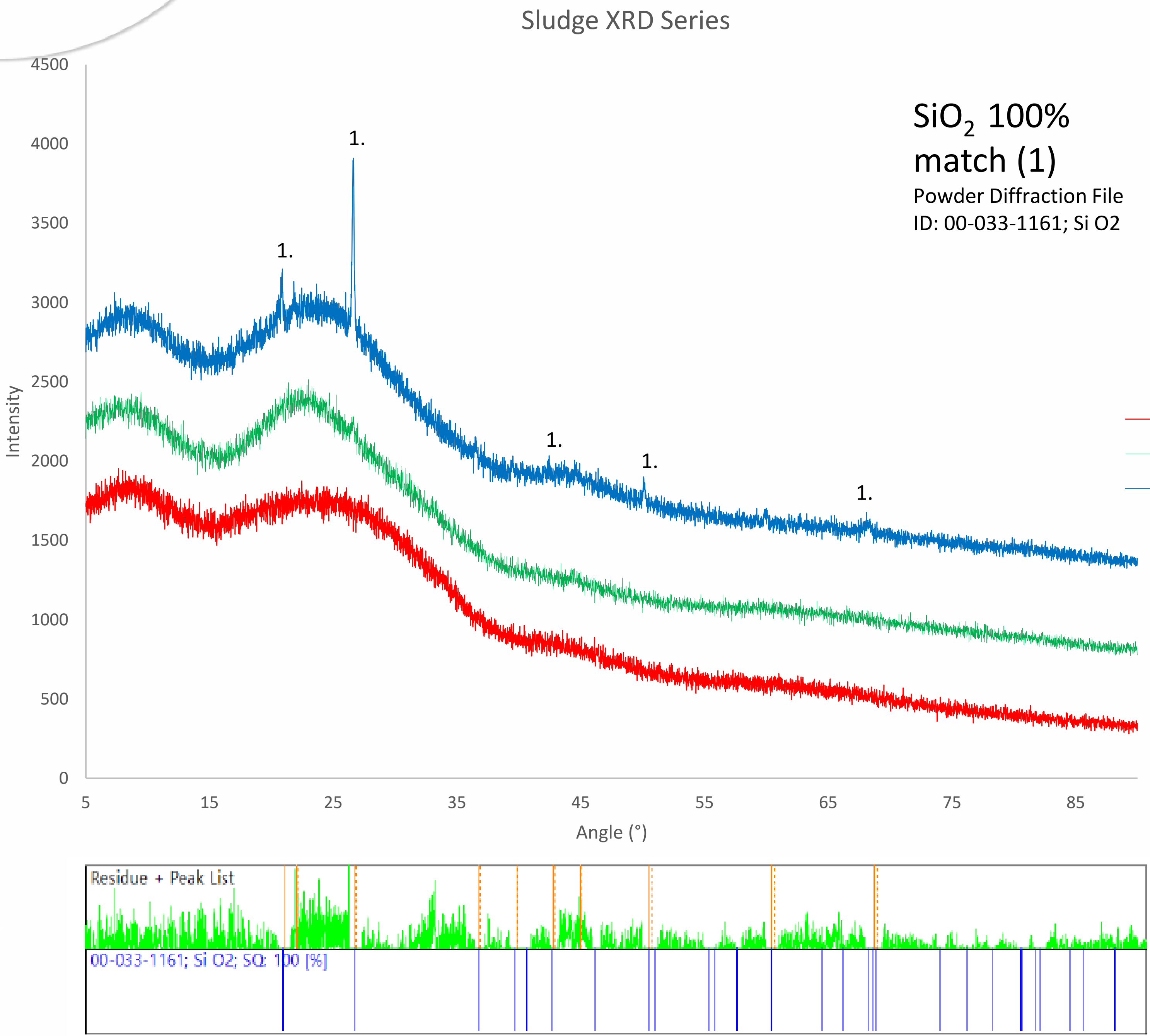
Sludge XRD Series
SiO2 100% match (1)
Powder Diffraction File ID: 00-033-1161; Si O2
Intensity
Angle (°)
Borosilicate
MgAlSilicate
Mixture Windscale
Residue + Peak List
00-033-1161; Si O2; SQ: 100 [%]

Conclusion and Future Work

- Off Gas system almost ready for trial runs
- Initial waste glass trials complete with:
  - Simulant contaminated SIXEP sand/clinoptilolite
  - SIXEP sludge
- Good waste loading shown in a number of samples
- Real time system selection and installation into off-gas system
- Collaboration with real time system developers

TRANSCEND

Transformative Science and Engineering for Nuclear Decommissioning

Simulation of behavioural modification effects in suspension waste pipe flow

Bisrat Wolde, University of Leeds

TRANSCEND Virtual Conference Meeting

2nd December 2020
Virtual Conference

Energy
For a Low Carbon Future

A brief overview of my project:

- Modelling and simulating for Understanding Pond and Silo Sludge Behaviour
- In the decontamination of legacy ponds and silos, the provision of a predictive capability to understand how sludges will behave is crucial to successful retrieval and completion of post operational clean out (POCO) operations
- Develop and validate multiphase direct numerical simulation in a horizontal pipe of radius R, axial length 25R in turbulent flows at Re_{τ}= 361 and 180
- Both polydispersed and irregular shaped particles will be tracked
- Apply behavioural modification effects to the fluid and solid particle properties to promote the desired outcome

- Supervisors: Professor Michael Fairweather

  Dr Lee Mortimer

Governing Equations:

The Navier Stokes equation can be expressed as follows for constant density:

$$\nabla . u^* = 0$$

$$\frac{\partial u^*}{\partial t^*} + (u^* . \nabla) u^* = -\nabla p^* + \frac{1}{Re_b} \nabla . \tau^* + f_i \, ,$$

Here, $u^*(x^*, t^*)$is the fluid velocity vector, non-dimensionalised using the bulk velocity, $\mathrm{u_b}$, the position vector, x^* and time, t^* non-dimensionalized as $x^* = \frac{x}{D}$ and $t^* = \frac{t}{D/\mathrm{u_b}}$ respectively, p^* is the non-dimensionalised pressure term for high-velocity flow, $p^* = \frac{p}{\rho \mathrm{u_b}^2}$, The bulk Reynolds number Re_b is already a non-dimensional and defined as $\mathrm{u_b D}/\nu$, where, D is the pipe diameter, ν is the kinematic viscosity and $\mathrm{u_b}$ is the mean bulk velocity, τ^* is the non-dimensionalized stress tensor, $\tau^* = \nabla u^* + \nabla u^{*T}$ and f_i is arbitrary forcing terms used in multiphase flows

A solution for the unknow $p, u, v \text{ and } w$ is sought using continuity equation, $\nabla . \boldsymbol{u} = 0$ and boundary conditions

The non-dimensional particle equations of motion is given by:

$$u_p^* = \frac{\partial x_p^*}{\partial t^*}$$

$$\frac{\partial u_p^*}{\partial t^*} = \underbrace{\frac{3 C_D |\boldsymbol{u_s^*}|}{\boldsymbol{4 d_p^*} \, \rho_{\boldsymbol{p}}^*}}_{\text{Drag}} \boldsymbol{u_s^*} + \boldsymbol{g} * \underbrace{(\mathbf{1} - \rho_{\boldsymbol{p}}^*)}_{\text{Gravity}} + \underbrace{\frac{3 \, C_L}{4 \rho_{\boldsymbol{p}}^*} (\boldsymbol{u_s^*} \, \boldsymbol{x} \, \boldsymbol{\omega_f^*})}_{\text{Lift}} + \underbrace{\frac{\mathrm{D}' \boldsymbol{u_f^*}}{\mathbf{2} \rho_{\boldsymbol{p}}^* \, \boldsymbol{Dt*}}}_{\text{Virtual Mass}} + \underbrace{\frac{\mathrm{D} \boldsymbol{u_f^*}}{\rho_{\boldsymbol{p}}^* \, \boldsymbol{Dt*}}}_{\text{Pressure Gradient}}$$

Methods:

To solve the descriptive equations numerically a computational fluid dynamics solver Nek5000 used. This solver is based on spectral element method (SEM) – that is a high order weighted residual technique

Nek5000 is favourable for:

- ✓High spectral accuracy
- ✓Very little numerical dispersion and dissipation
- ✓High parallelisation

The high-level computational algorithm is:

- To integrate the Navier Stokes equations, split the controlled volume into small cells (meshing)
- Numerically integrate the Navier-Stokes equations throughout the cells
- Solve numerical equations for u, v, w and p in combination with boundary conditions
- Save the solutions for post processing

(a)

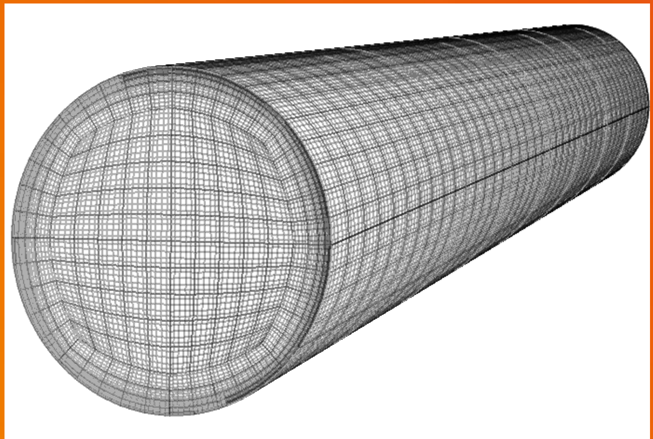

(b)

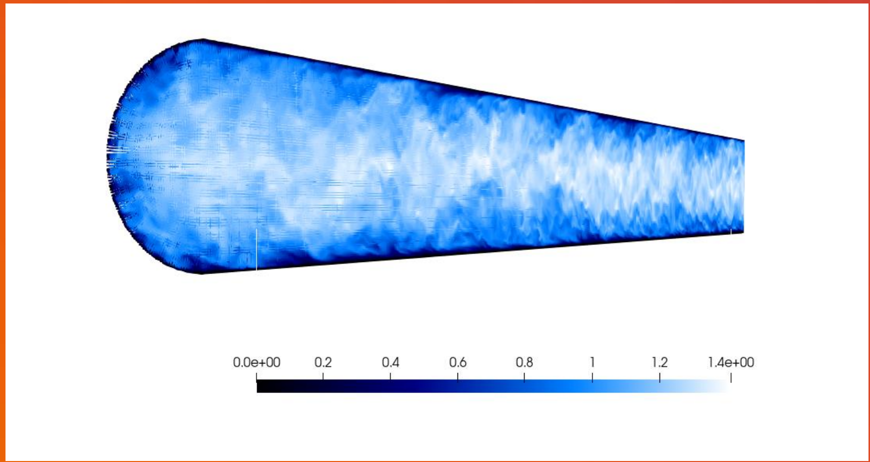

(c)

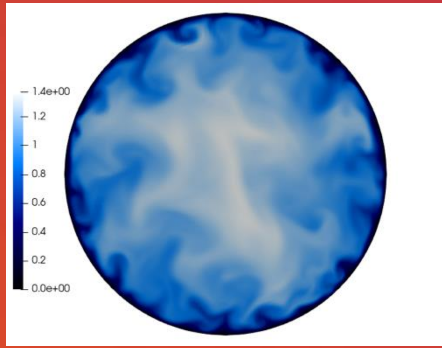

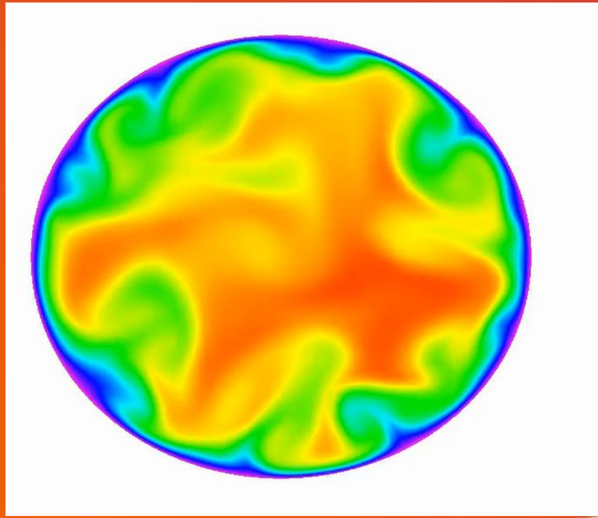

Computational mesh and pseudo-colour visualisation of the instantaneous axial velocity:

Panels: (a) is the computational mesh with Gauss–Lobatto–Legendre quadrature points (N = 7) for both simulations at Re_τ = 180 and Re_τ = 361, (b) instantaneous streamwise velocity normalized by bulk velocity, U_b , (c) a computational mesh clipped at the centreline and pseudo-colour visualisation of the instantaneous axial velocity in 3D

Fluid flow results:

$\mathbf{Re_\tau = 180}$

(a) Validation of mean axial velocity profiles at $Re_\tau = 180$. u_z^* , stream wise direction, __ solid lines are present DNS contrasted with, – – dashed lines are El Khoury's DNS, + cross markers are Den Toonder experiment at Re_τ≈ 170 and ○ open circle markers are Eggels experiment at Re_τ≈ 180. (c) Validation of statistical root mean square velocity fluctuation profiles of DNS at $Re_\tau = 180$. The axial z^*_{rms}, radial r^*_{rms}, azimuthal θ^*_{rms}, and Reynolds shear stress $< u_z \ u_r >^*$ as a function of $(1-r)^*$ compared against the following DNS and experimental datasets: __ solid lines are present DNS result, – – dashed lines are El Khoury's DNS , + cross markers are Den Toonder experiment Re_τ≈ 170 and ○ open circle markers are Eggels experiment at at Re_τ≈ 180. (b and d) – log scales.

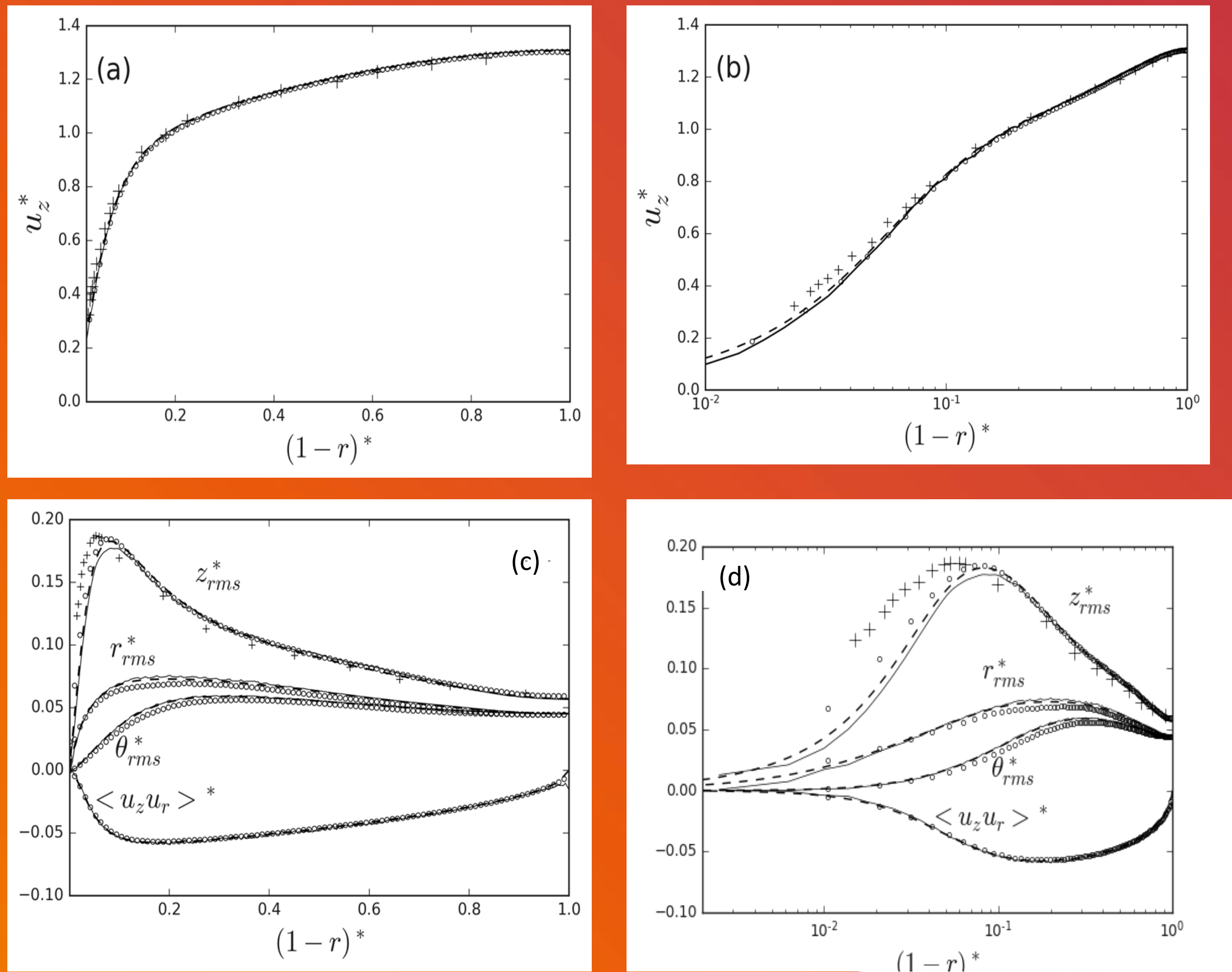

Fluid results:

$$\boldsymbol{Re_\tau = 361}$$

(a) The mean axial velocity profiles DNS validation at $Re_\tau = 361$. u_z^* __ solid lines are present DNS contrasted with, – – dashed lines are El Khoury's DNS, ○ open circle markers are Den Toonder experiment at $Re_\tau \approx 315$, + cross markers are Singh's DNS. **(b)** – log scale.

(c) Inner scaled statistical profiles root mean square of fluctuating velcoties of DNS at $Re_\tau = 361$. The axial z_{rms}^*, radial r_{rms}^*, azimuthal θ_{rms}^*, and Reynolds shear stress $< u_z\ u_r >^*$ as a function of $(1-r)^*$ compared against the following DNS and experimental datasets. __ Solid lines are present DNS result, – – dashed lines are El Khoury's DNS, ○, open circle markers are Den Toonder experiment at $Re_\tau \approx 315$ and + cross markers are Singh DNS at $Re_\tau \approx 323$. **(d)** log scale.

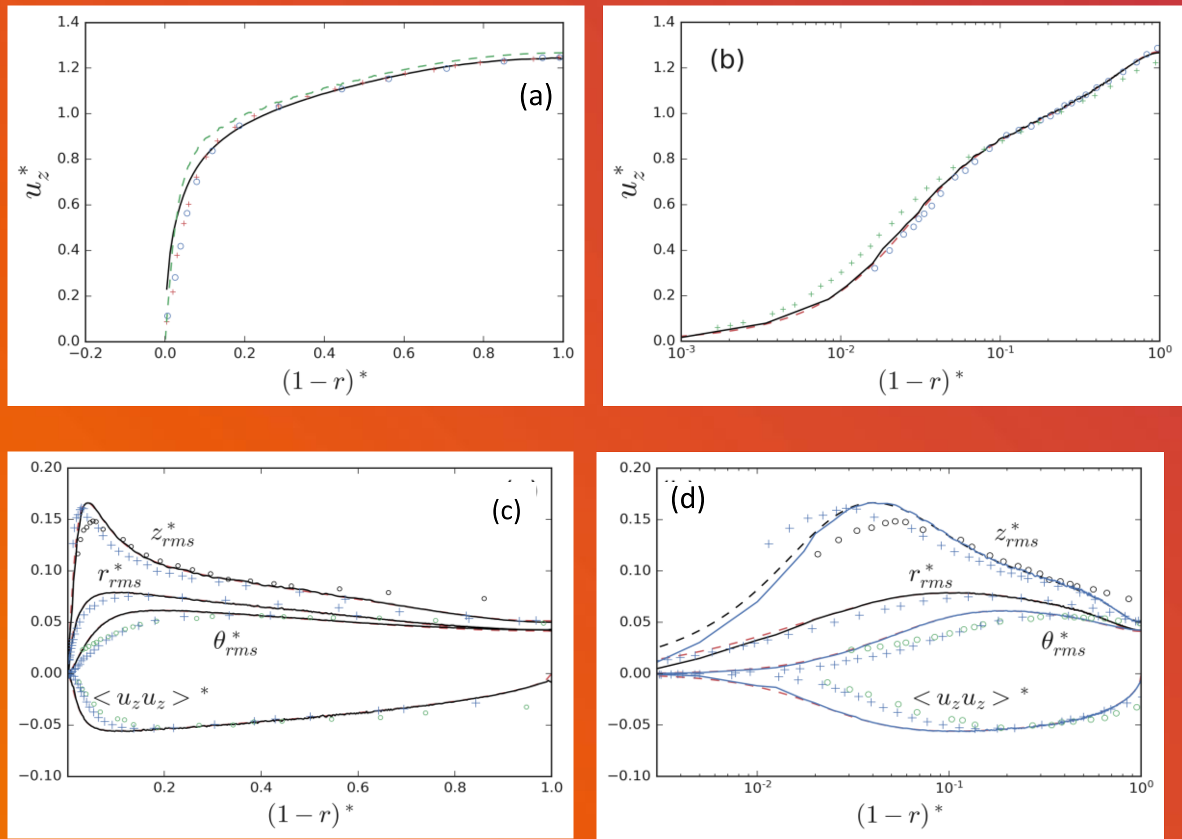

To investigate the bulk behaviour of high concentration dispersions, a Lagrangian particle tracker has been developed to model large quantities of dispersed solids

- The particles are injected at random position within the fully developed fluid flow domain
- Assigned the fluid velocity at that location
- Particle collision with the pipe wall considered to be elastic
- A fourth order Runge-Kutta method implemented to solve the particle equation of motion for each particle at every time-step
- Statistical data gathered for analysis after letting a few response times to adjust to the surrounding fluid

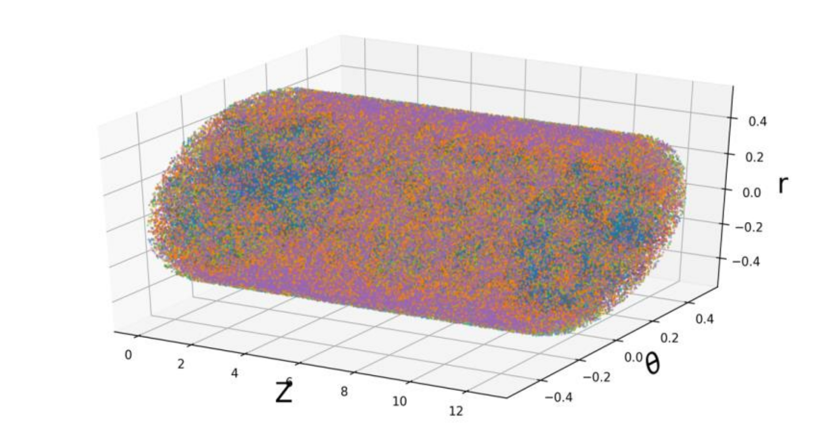

Particles simulation configurations:

Parameters	Shear Reynolds number, $Re_\tau = 361$	
	$St^+ \cong 14$	$St^+ \cong 29$
Particle diameter, d_p^+	0.72	0.72
Particle diameter, d_p^*	$2.0E^{-03}$	$2.0E^{-03}$
Axial length	25R	25R
Number of particles, N_p	$42.0E^{+04}$	$21.0E^{+04}$
Shear stokes number, St_τ	14.4	28.96
Bulk stokes number, St_b	1.3	2.6
Density ratio, ρ_p^*	$5.0E^{+02}$	$1.0E^{+03}$
Volume fraction, ϕ	$1.79E^{-04}$	$8.96E^{-05}$
Particle and fluid timestep, Δt^*	$1.0E^{-03}$	$1.0E^{-03}$

Parameters	Shear Reynolds number, $Re_\tau{}^1 = 140$, $Re_\tau{}^2 = 180$,	
	$St^+ \cong 33$	$St^+ \cong 75$
Particle diameter, $d_p\,[\mu m]$	60	90
Particle diameter, d_p^*	$3.0E^{-03}$	$4.5E^{-03}$
Axial length	25R	25R
Number of particles, N_p	$29.4E^{+03}$	$43.6E^{+03}$
Shear stokes number, St_τ	33.3	75.06
Bulk stokes number, St_b	4.0^1; 5.45^2	9.0^1; 12.27^2
Density ratio, ρ_p^*	$2.058E^{+03}$	$2.058E^{+03}$
Volume fraction, ϕ	$4.24E^{-05}$	2.12^{-04}
Particle and fluid timestep, Δt^*	$1.0E^{-03}$	$1.0E^{-03}$

Transformative Science and Engineering for Nuclear Decommissioning

Particle results:

$$Re_\tau = 180$$

(a) LPT validation of inner scaled statistical particle mean velocity profiles of a DNS at $Re_\tau = 180$, (b) log scale, (c) statistical particle profiles, root mean square of velocity fluctuations of a DNS at $Re_\tau = 180$ for axial z^*_{rms}, radial r^*_{rms}, azimuthal θ^*_{rms} and Reynolds shear stress $< u_z \ u_r >^*$ shown. For $St^+ \cong 33$, — solid lines are current work, and + markers are Vreman at $Re_\tau =$ 140 DNS, (d) near wall particle concentration of $St^+ \cong$ 33 and 75 normalised by initial bulk concentration and (e) and (f) are corresponding snapshot of the last timestep

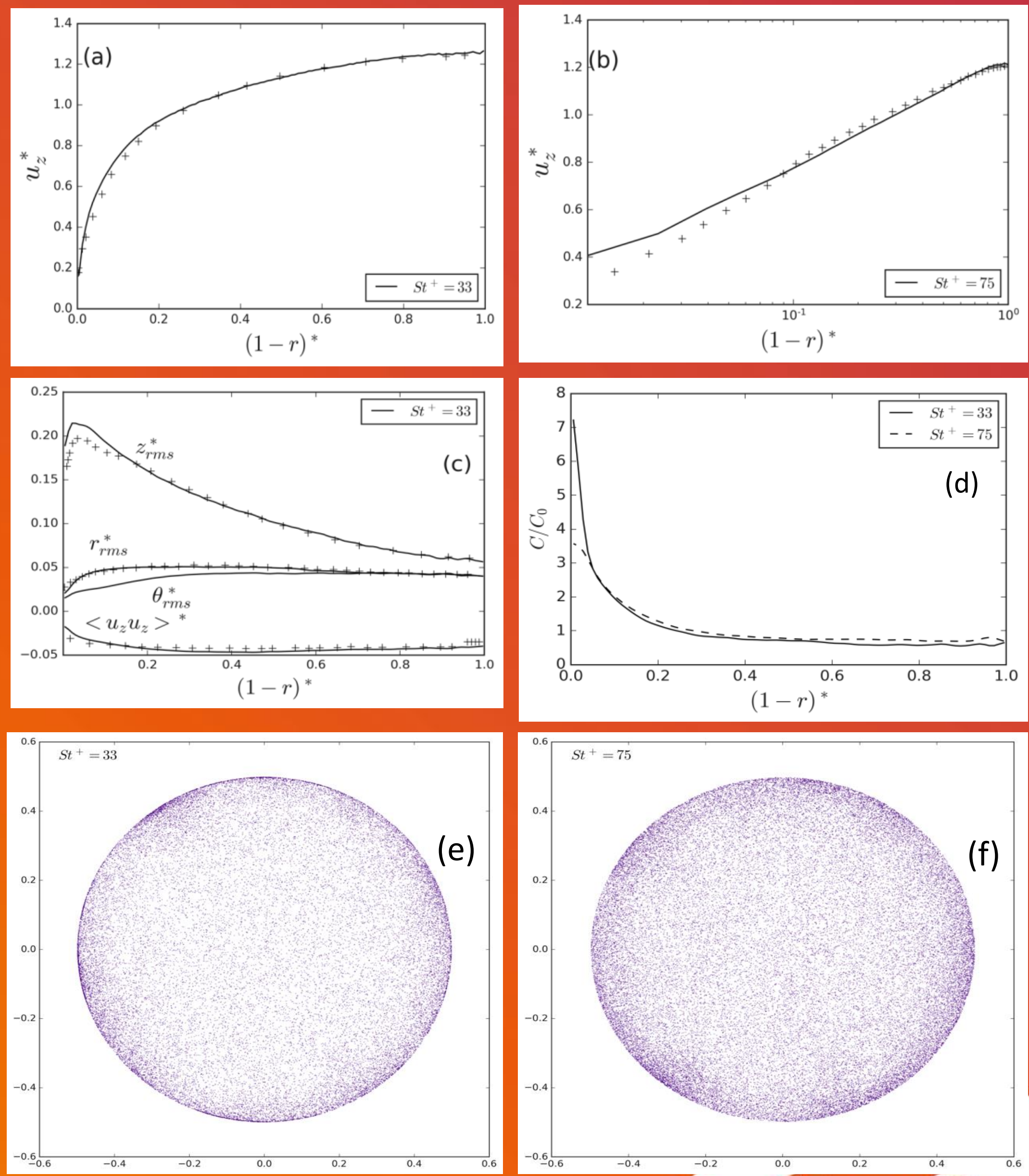

Energy For a Low Carbon Future

Particle results:

$$Re_\tau = 180$$

Probability density function for the particle Reynolds number in viscous, buffer, log-law and bulk flow regions of the pipe at $St^+ \cong 33$ and 75.

Top left is the radial and right is azimuthal. Lower left is the slip velocity and on the right is axial. Solid line: viscous sublayer; dashed: buffer layer; dotted: log-law region; dot- dashed: bulk flow

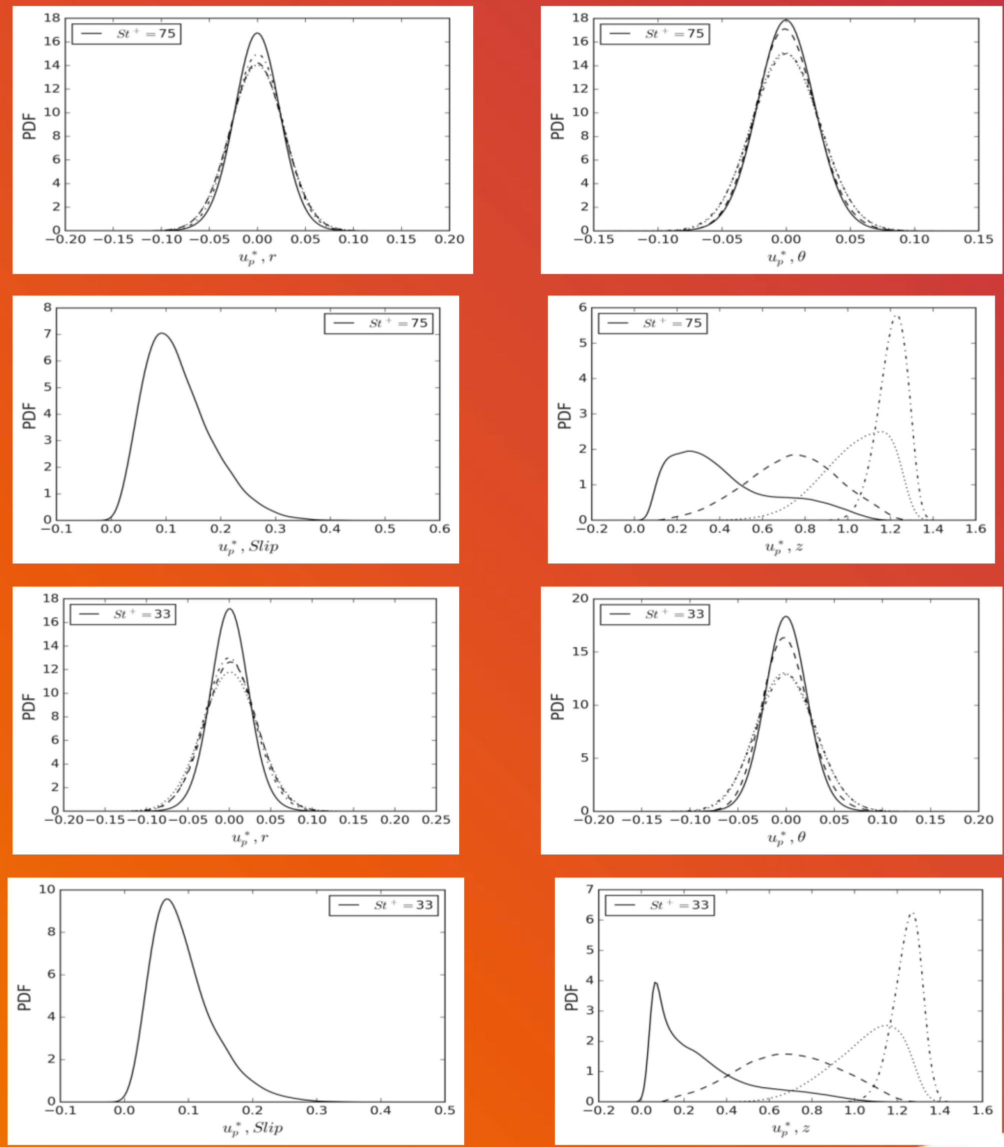

TRANSCEND

Transformative Science and Engineering for Nuclear Decommissioning

Particle results:

$$Re_\tau = 361$$

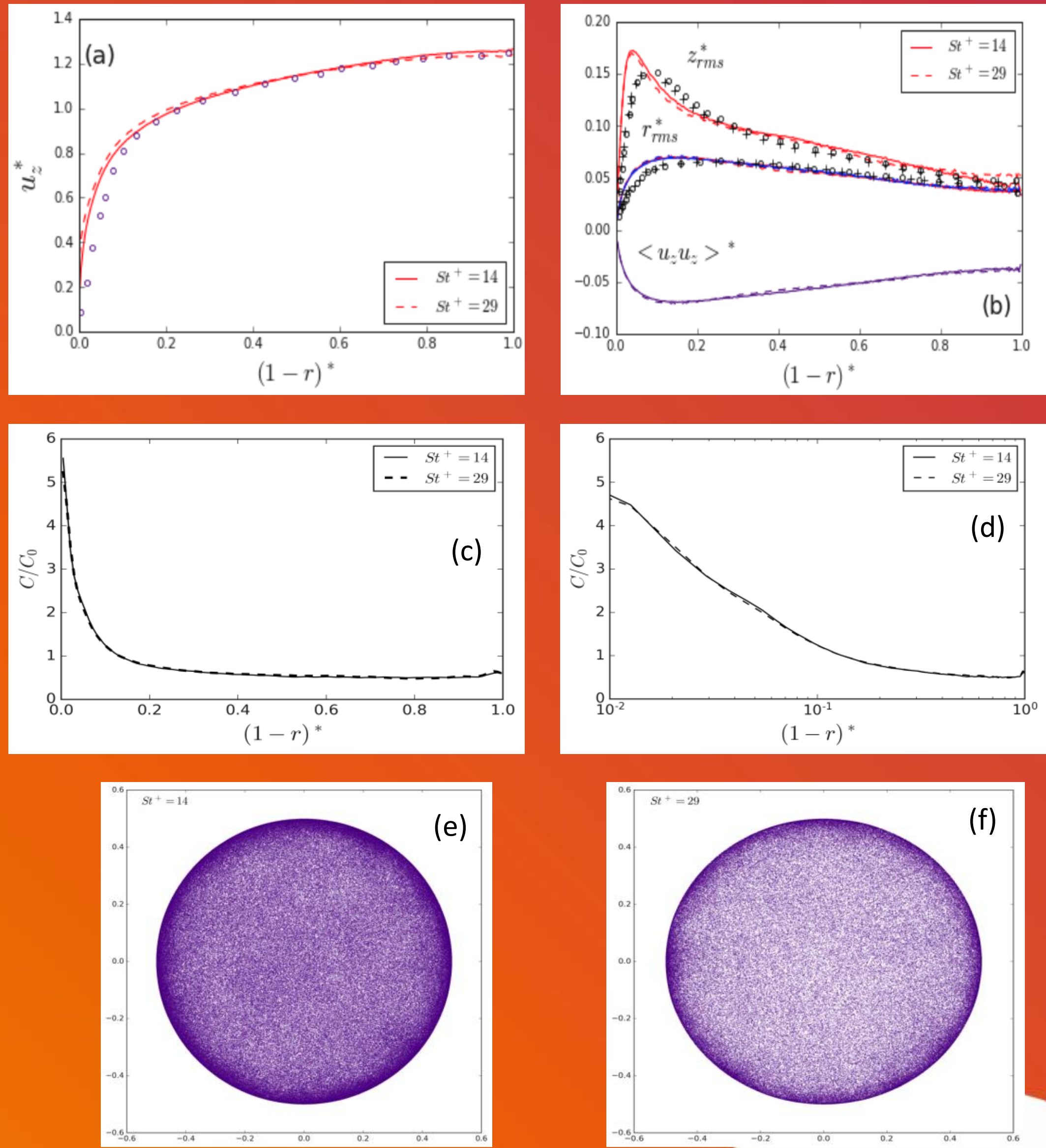

(a) Inner scaled statistical particle mean velocity profiles of a DNS at $Re_\tau = 361$, (b) statistical particle profiles, root mean square of velocity fluctuations of a DNS at $Re_\tau = 361$ for axial z^*_{rms}, radial r^*_{rms} and Reynolds shear stress $< u_z \ u_r >^*$. —— Solid line and – – dashed lines are current work, and o and + markers are Sarma DNS, (c) near wall particle concentration of $St^+ \cong 14$ and 29 particles, normalised by initial bulk concentration, (d) log scale, and (e) and (f) are corresponding snapshot of the last timestep

Energy

For a Low Carbon Future

Particle results:

$$Re_\tau = 361$$

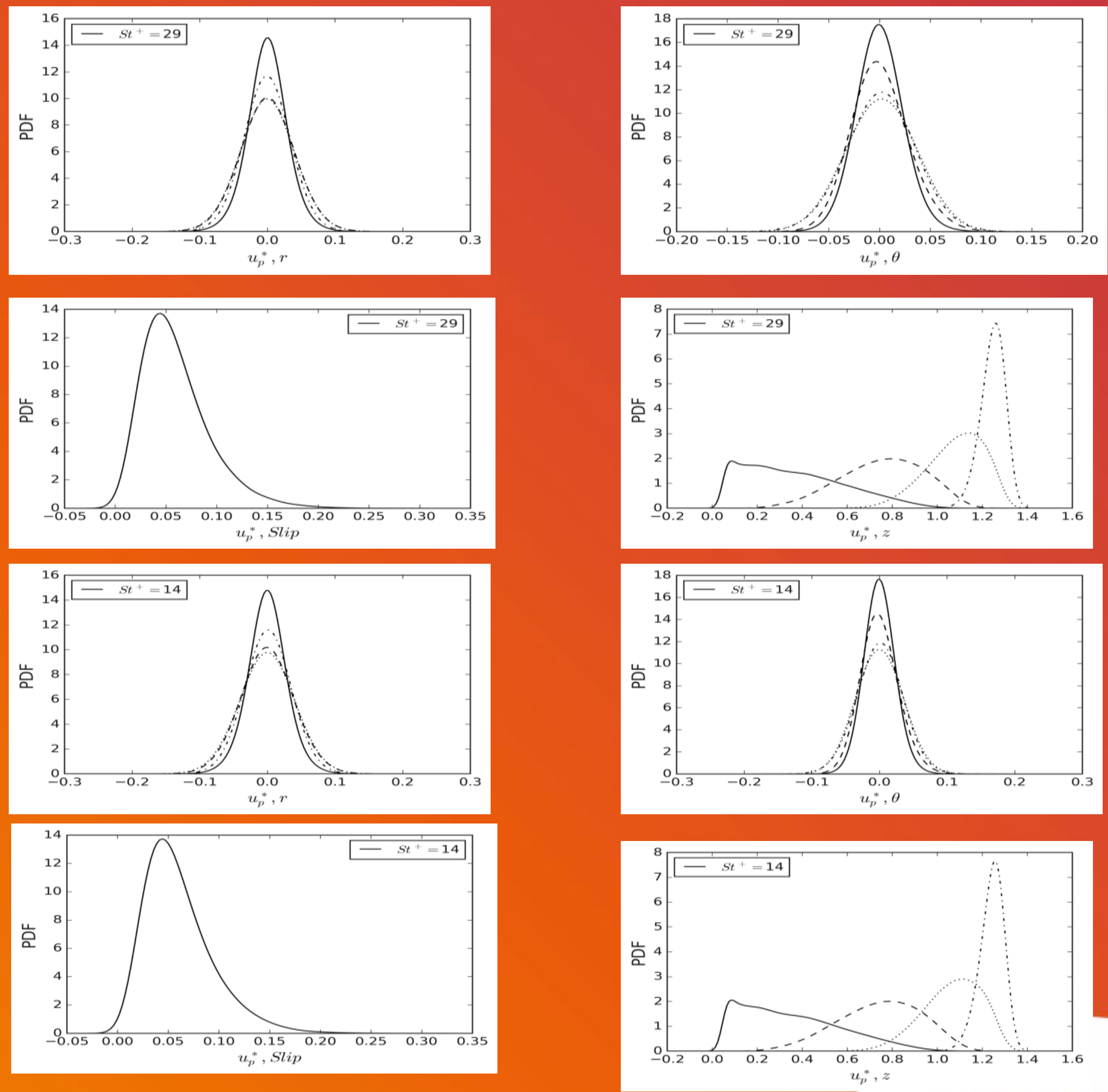

Probability density function for the particle Reynolds number in viscous, buffer, log-law and bulk flow regions of the pipe at $St^+ \cong 14$ and 29

Top left is the radial and right is azimuthal. Lower left is the slip velocity and on the right is the axial. Solid line: viscous sublayer; dashed: buffer layer; dotted: log-law region; dot- dashed: bulk flow.

Transformative Science and Engineering for Nuclear Decommissioning

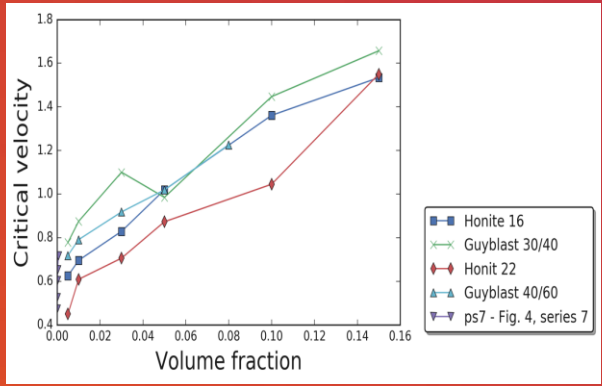

Dimensional analysis:

$V_c = f(d, D, \phi, (\rho_s - \rho_f)g, \rho_f, \mu\,)$

Where,

$\mu = [ML^{-1}T^{-1}]$ – Dynamic viscosity

g $= [LT^{-2}]$ Acceleration due to gravity

$V_c = [LT^{-1}]$ critical velocity

d $=$ [L] particle diameter

D $=$ [L] pipe diameter

$Q_s = [L^3T^{-1}]$ solid-phase volumetric flow rate

$Q_f = [L^3T^{-1}]$ solid-phase volumetric flow rate

$\rho_s = [ML^{-3}]$ Density of solid phase

$\rho_f = [ML^{-3}]$ Density of fluid phase

Side note: - $\phi = \frac{Q_s}{Q_s+Q_l} = [M^0L^0T^0] = [1]\ and\ s = \frac{\rho_s}{\rho_f}[M^0L^0T^0] = [1]$

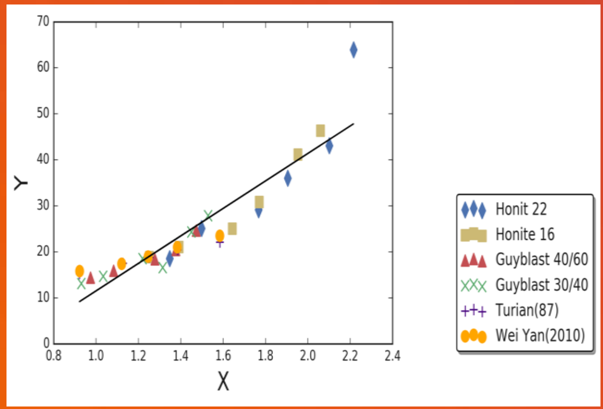

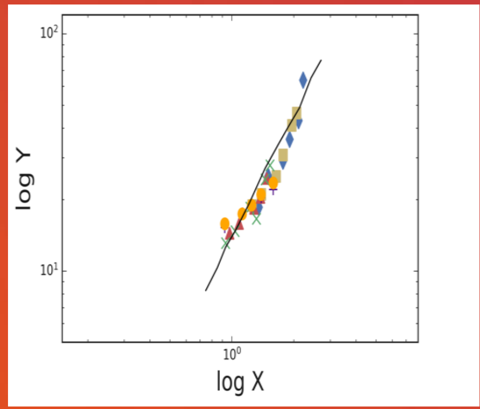

To develop a functional relationship the above equation set to:

$$\frac{V_c}{\sqrt{gd(s-1)}} = i_0(\frac{d}{D})^{i_1}\,\phi^{i_2}\,(1-\phi)^{i_3}\,(\frac{\mu}{d\rho_f\sqrt{gd(s-1)}})^{i_4}$$

$i_0 - i_4$ values determined by regression using experimental data.

The following model derived using linear regressor is:

$$\frac{V_c}{\sqrt{gd(s-1)}} = 1.85(\frac{d}{D})^{-0.18}\,\phi^{0.154}\,(1-\phi)^{0.16}\,(\frac{\mu}{d\rho_f\sqrt{gd(s-1)}})^{0.09} \qquad \text{(Eq 1)}$$

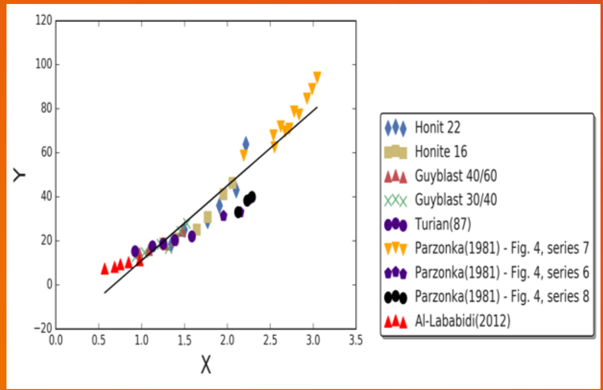

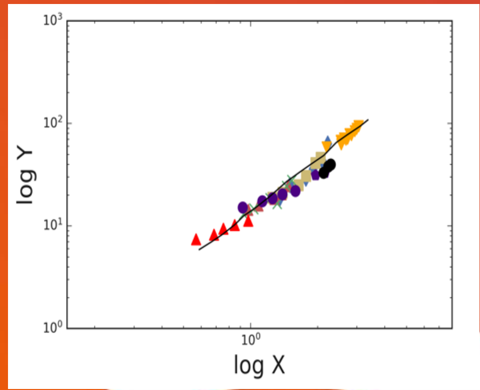

Experimental deposition data were also plotted against the same empirical correlation (equation 1.) Deposition based dataset plotted against the same empirical correlation.

Planned work:

- Validation of particle deposition
- Deploy two-way coupling
- Investigate the settling and deposition behaviour of suspensions of dense particles
- Implement four-way coupling
- Implement four-way coupling with agglomeration
- ➢ DLVO theory will be applied

- Modelling and understanding pond and silo sludge behaviour
- Apply behavioural modification effects to the fluid and solid particle properties to promote the desired outcome such as reducing particle agglomeration, and hence, the likely deposition of particles during processing
- The behavioural modification effects to be studied includes changes in:
- ❖ Temperature
- ❖ Ionic strength
- ❖ Polymers and pH of the liquid phase

Any questions?

TRANSCEND

Transformative Science and Engineering for Nuclear Decommissioning

Thank you

pmbw@leeds.ac.uk

Characterisation of Thermal Treatment Products

Project Overview and First Year Review (January 2020-December 2020)

Daniel Parkes, University of Sheffield

(dparkes2@sheffield.ac.uk)

TRANSCEND November 2020

TRANSCEND

Project Drivers

- NDA strategy - integrated and optimised waste management strategy
- **HLW (High Level Waste)**–encapsulate in borosilicate glass. No Change.
- **ILW (intermediate Level Waste)**–fragmented, mostly compaction and cement. Thermal treatment advantages – reduction in volume and reactivity. Main Focus.
- **LLW (Low Level Waste)** –compaction, incineration and metal decontamination. No Change. but interest due to ILW/LLW boundary waste.

<Date>

Compacted and cemented PCM waste


Integrated Waste Management
Radioactive Waste Strategy
September 2019


Integrated Waste Management
NDA Higher Activity Waste Strategy
May 2016

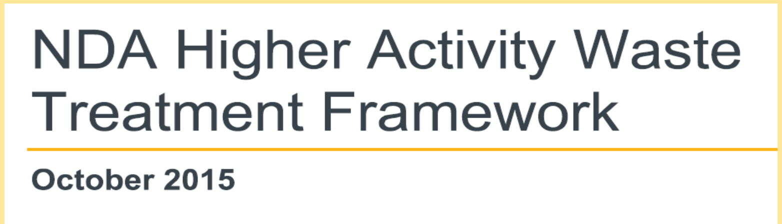
NDA Higher Activity Waste Treatment Framework
October 2015

Key NDA Strategy Reports

ILW and Thermal Treatment

- Thermal technologies - plasma vitrification, joule heating (JHCM and Geomelt), induction melting, incineration, SHIVA, PIVIC.
- UK ILW - Sand-Clino, Magnox Sludge, Plutonium Contaminated Material (PCM) and mixed alpha and beta waste.

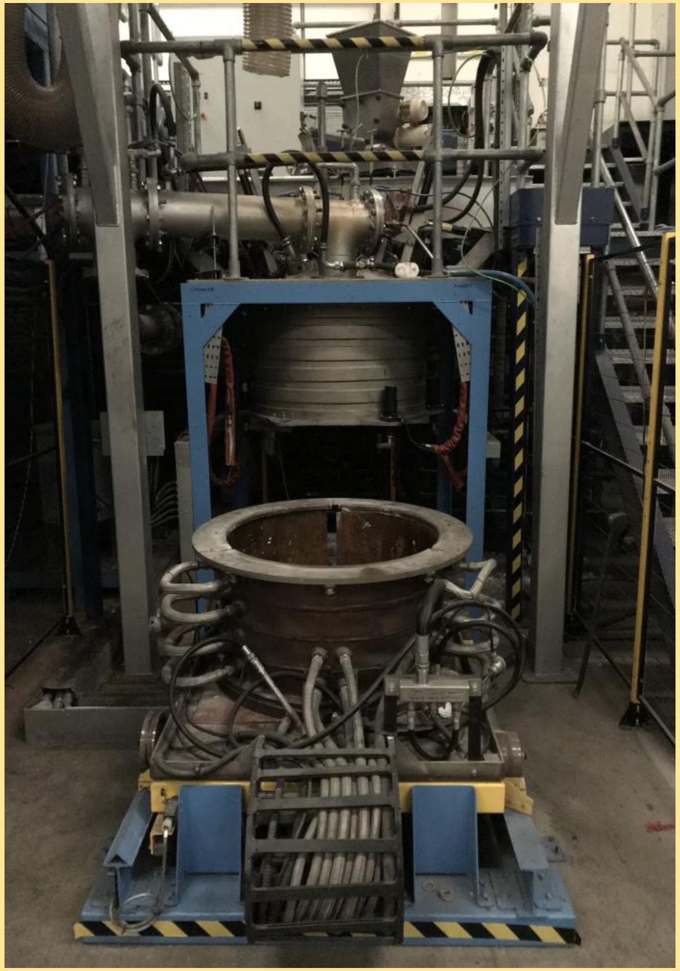

Plasma Vitrification set up at Valingar, Swindon

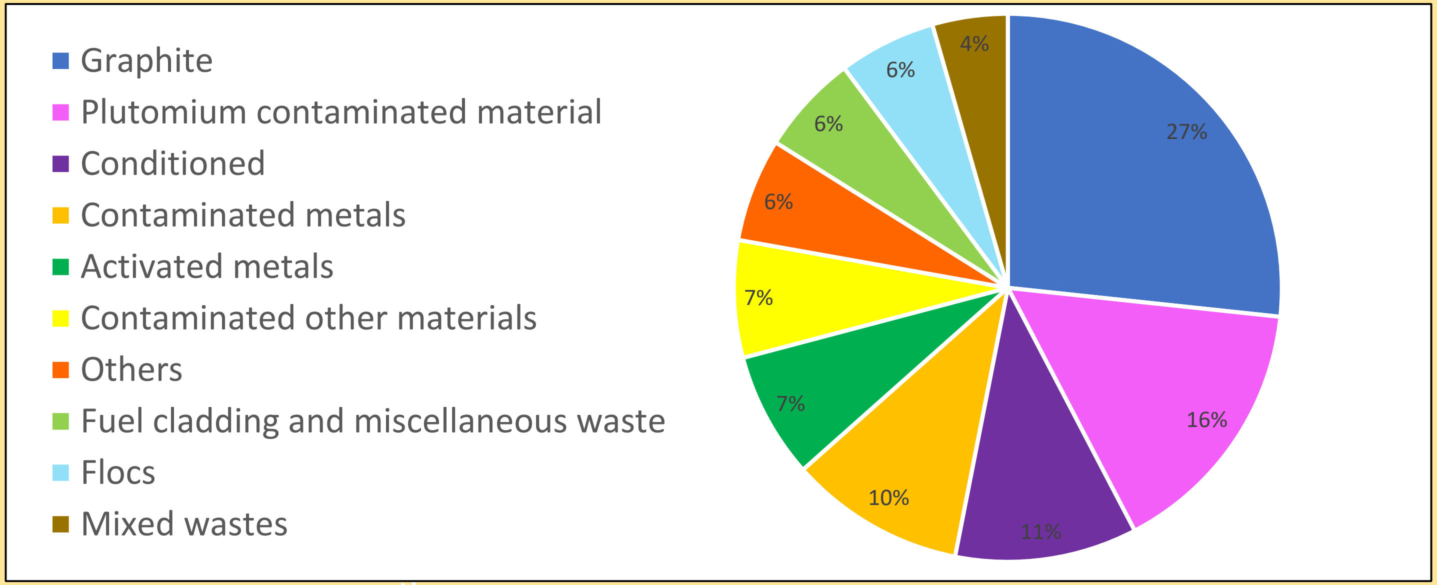

UK ILW compositional percentage mix

TRANSCEND

Aims

- **Treatment process** –experiments, processing temperature, waste composition, glass frit composition, processing time- literature review.
- **Composition** – non reactive, durable, homogenous.
- **Radionuclide distribution** – concentration, glass, metal, crystalline material, homogenous.
- **Long term durability** – dissolution, disposal safety case.

Nuclear Waste Life Cycle

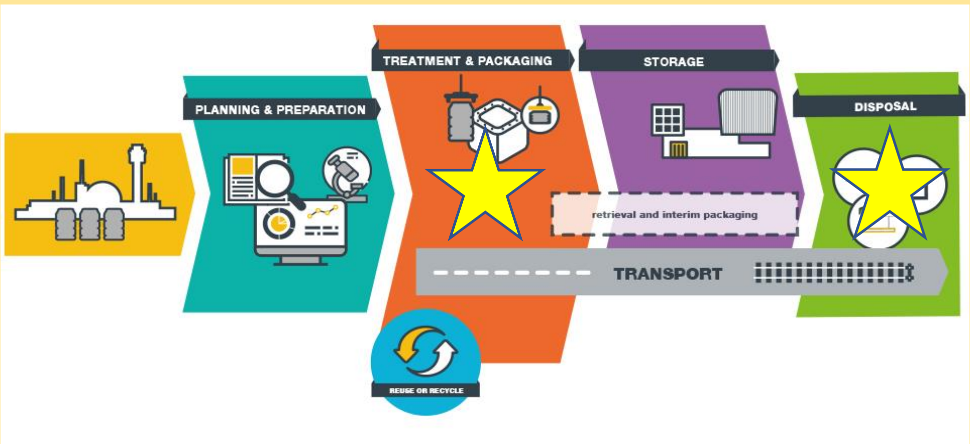

Plans

Samples

- **Lab simulants** – build on previous studies (*L.Boast PhD* and *Hyatt 2013*) – create lab simulants of previous studies for comparison to industry/archaeological samples. Create new samples with updated glass frit.

- **Industrial samples** – Valingar for Sellafield.

- **Archaeological samples** - Hayle, Cornwall. Copper smelting slag immersed in saline waster for 209 years. Previous analysis shows slag analogous to PCM, investigate long term dissolution behaviour.

Techniques

- **Characterisation** – Sample composition – glass and crystalline composition (SEM, XRD, XRF, Mossbauer) radionuclide distribution, partitioning, oxidation state (SEM, XANES, XRF) , metal composition – decontamination and oxidation.

- **Dissolution Experiments** – standard PCT to look at bulk dissolution but also VCI (Vertical Scanning Interferometry) to look at dissolution of different glass and crystalline elements of the waste form.

Examples - Samples

- COVID issues with lab access
- Other samples WANTED – please email dparkes2@sheffield.ac.uk

Industrial samples

Lab samples

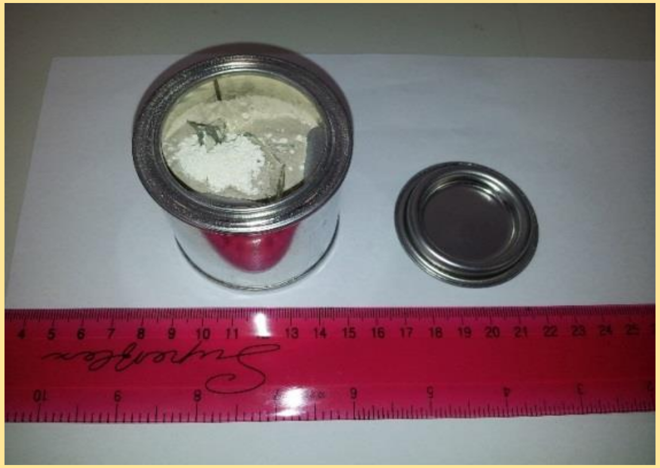

Archaeological Samples

Examples – Techniques

- COVID issues with lab access – examples from L.Boast PhD.

- SEM images show mixed Xc and glass.
- EDX maps – potential even radionuclide distribution.
- EDX data - 1.2 mol% CeO_2 in amorphous phase – upper limit 2 mol%.

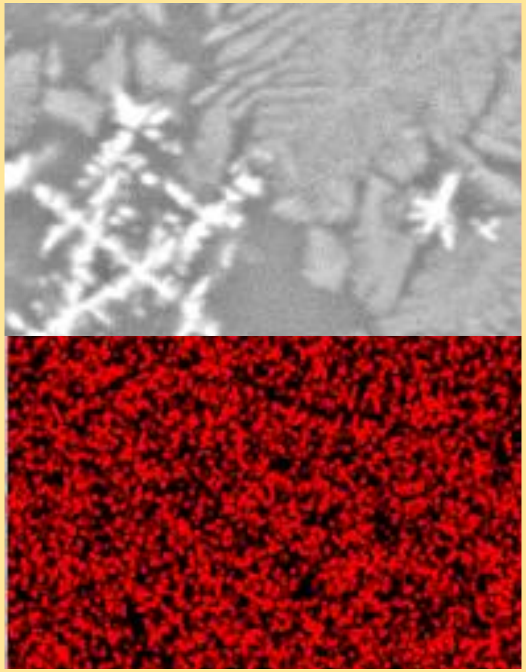

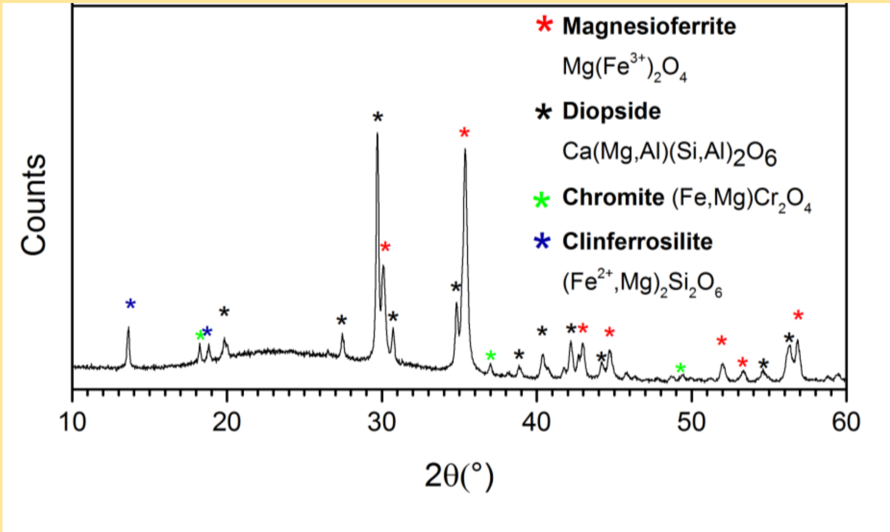

- XRD identifies mineral phases

- XANES date shows trivalent Ce. Important as radionuclide is more soluble in trivalent state.

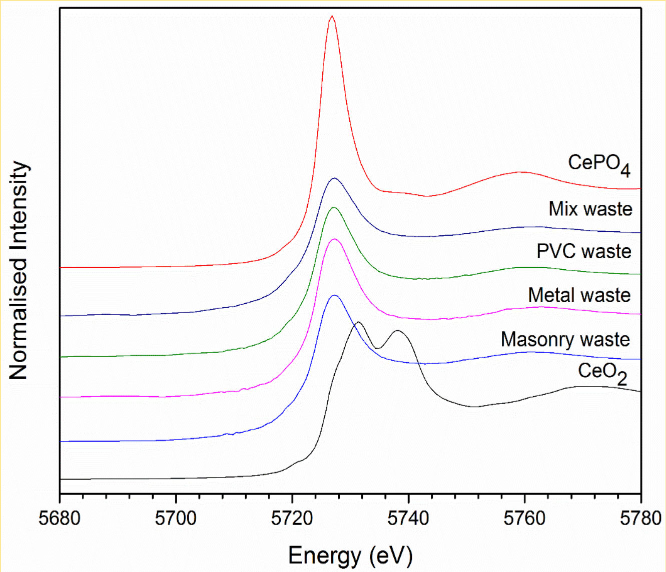

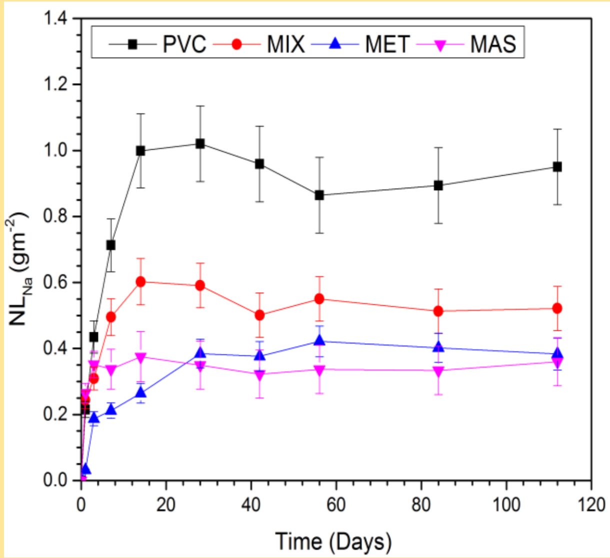

- PCT dissolution tests with normalised loss for Si
- PVC waste – reduced durability due to lower SiO_2 so reduced network connectivity.

Thankyou for listening

And thankyou to:

Dr Claire Corkhill (UoS)
Dr Clare Thorpe (UoS)
Mike Harrison (NNL)

Thank you

Contact Details : dparkes2@sheffield.ac.uk

TRANSCEND

Transformative Science and Engineering for Nuclear Decommissioning

Processes at and across Nanoparticle-Water Interfaces

Ella Schaefer, UoM

Integrated Waste Management Theme

2.12.20

ella.schaefer@postgrad.manchester.ac.uk

Energy
For a Low Carbon Future

Background

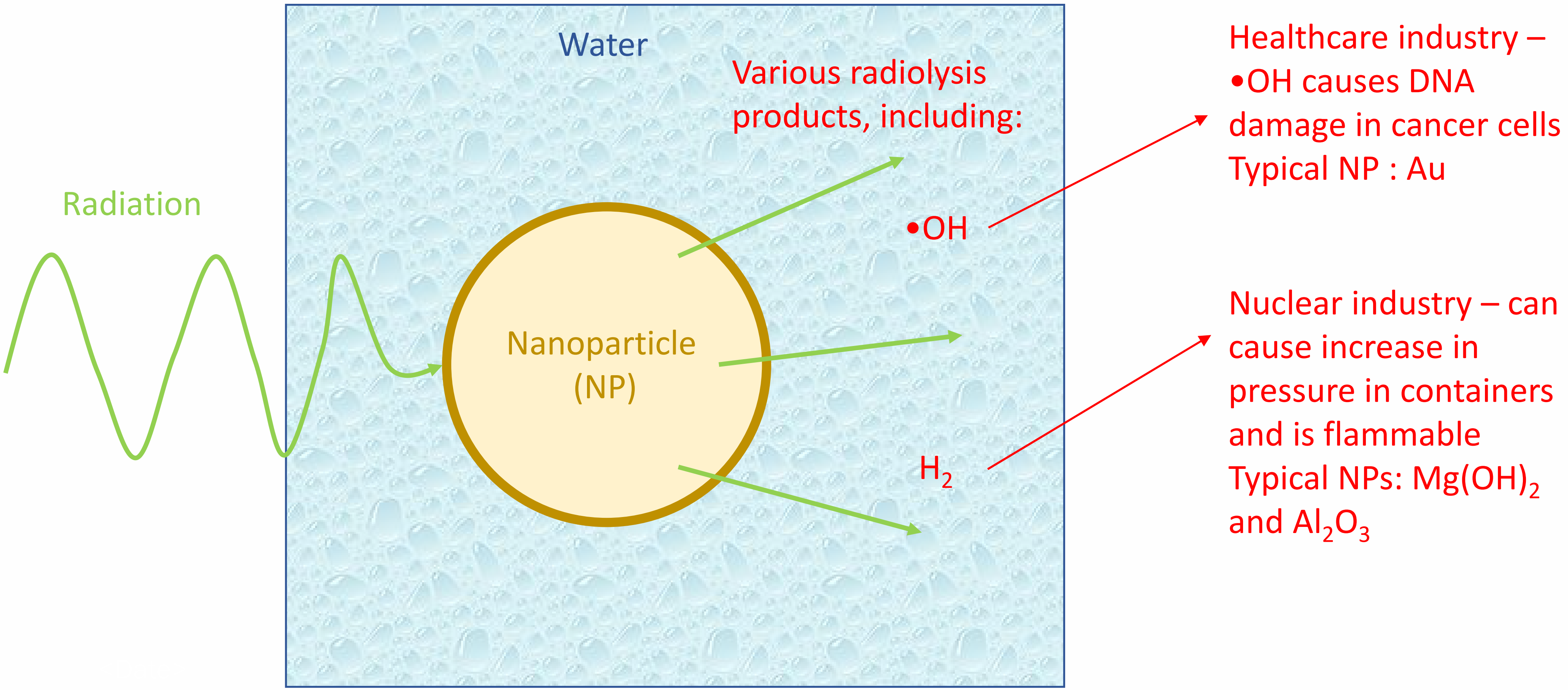

Figure 1 – Diagram showing the irradiation of a NP resulting in various radiolytic species, noting two of interest; the hydroxyl radical and gaseous dihydrogen, and their relevance to key fields.

Aims

- Develop simulations where energy is directly deposited into NPs
- Model energy transfer at the NP-water interface
- Cultivate an integrated account of all processes

Background

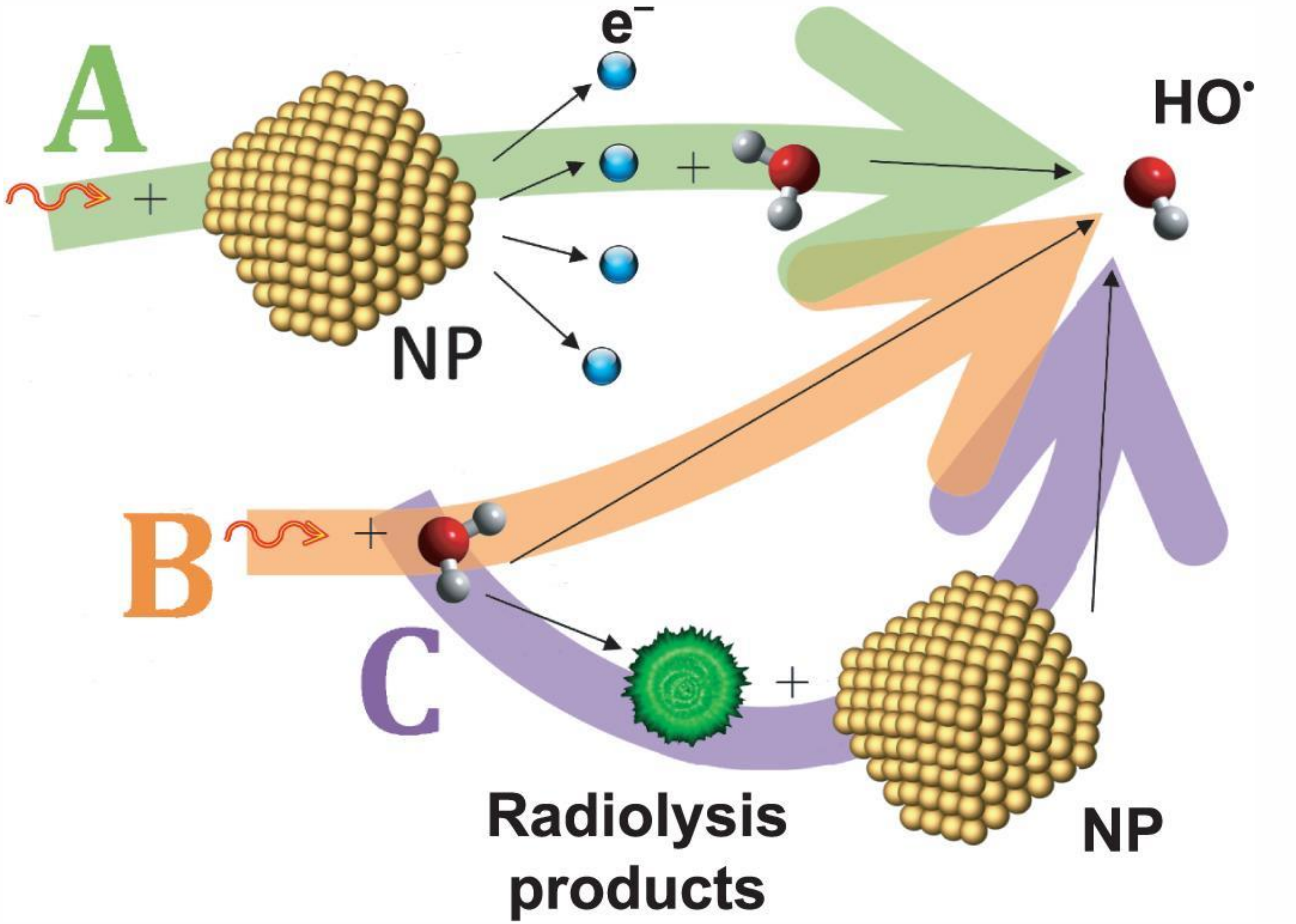

Figure 2 –The three classes of pathways for irradiated NP solutions [Sicard-Roselli, et al Small. 2014;10(16):3338–46.].

Background

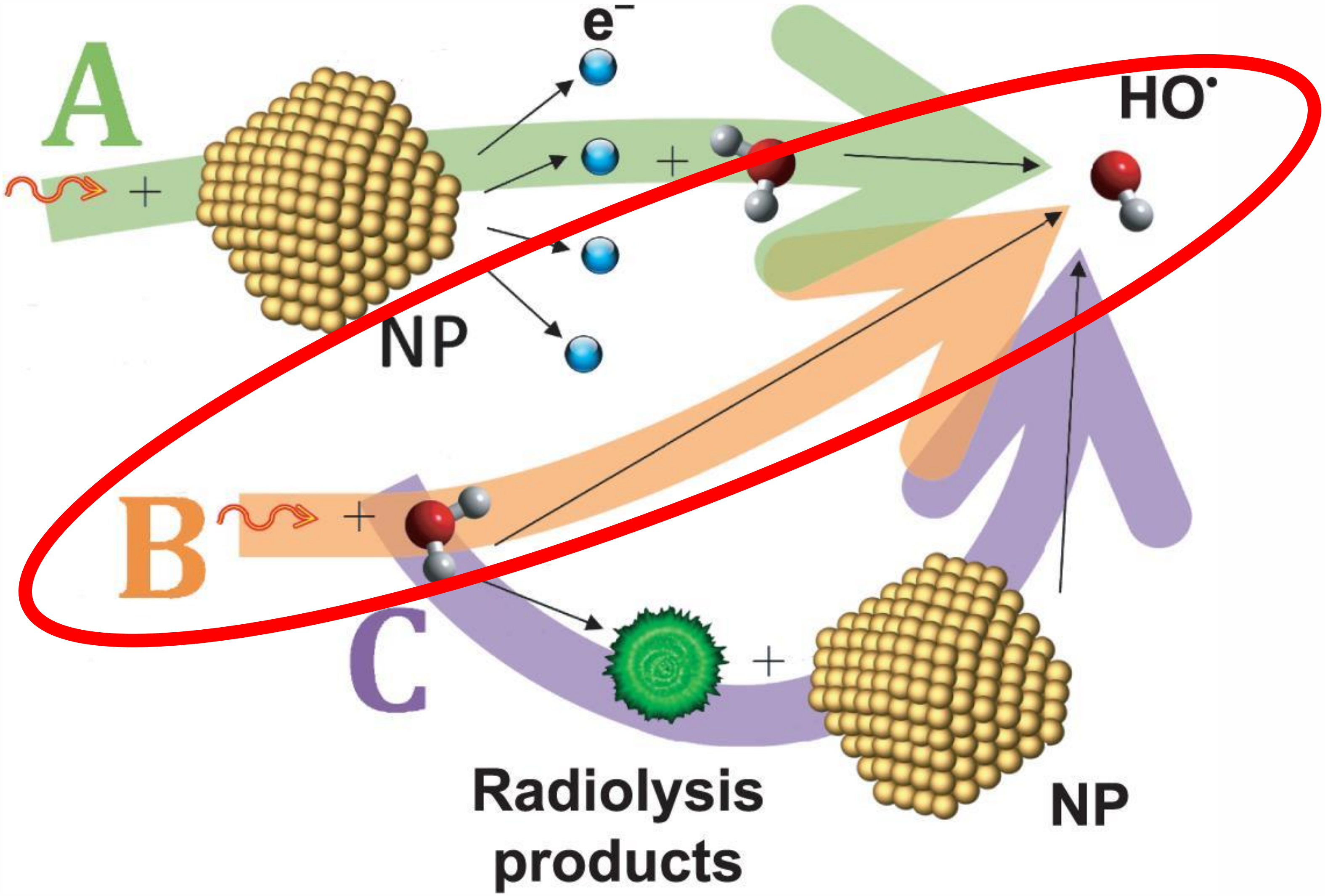

Figure 2 – The three classes of pathways for irradiated NP solutions.

Pathway B – Water Radiolysis

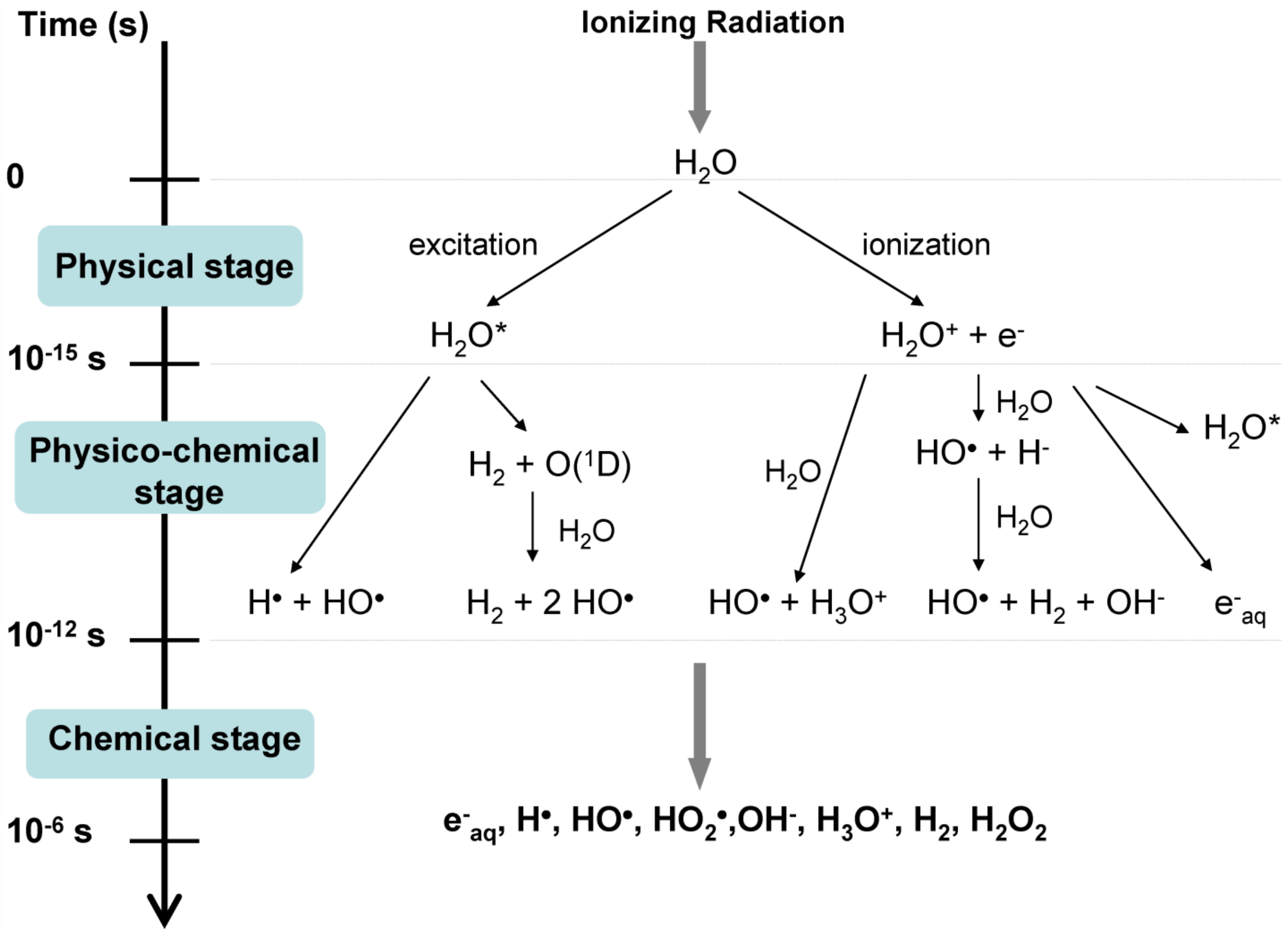

Figure 3 – The three stages of water radiolysis. [Le Caër S, 2011;3(1):235–53.].

Background

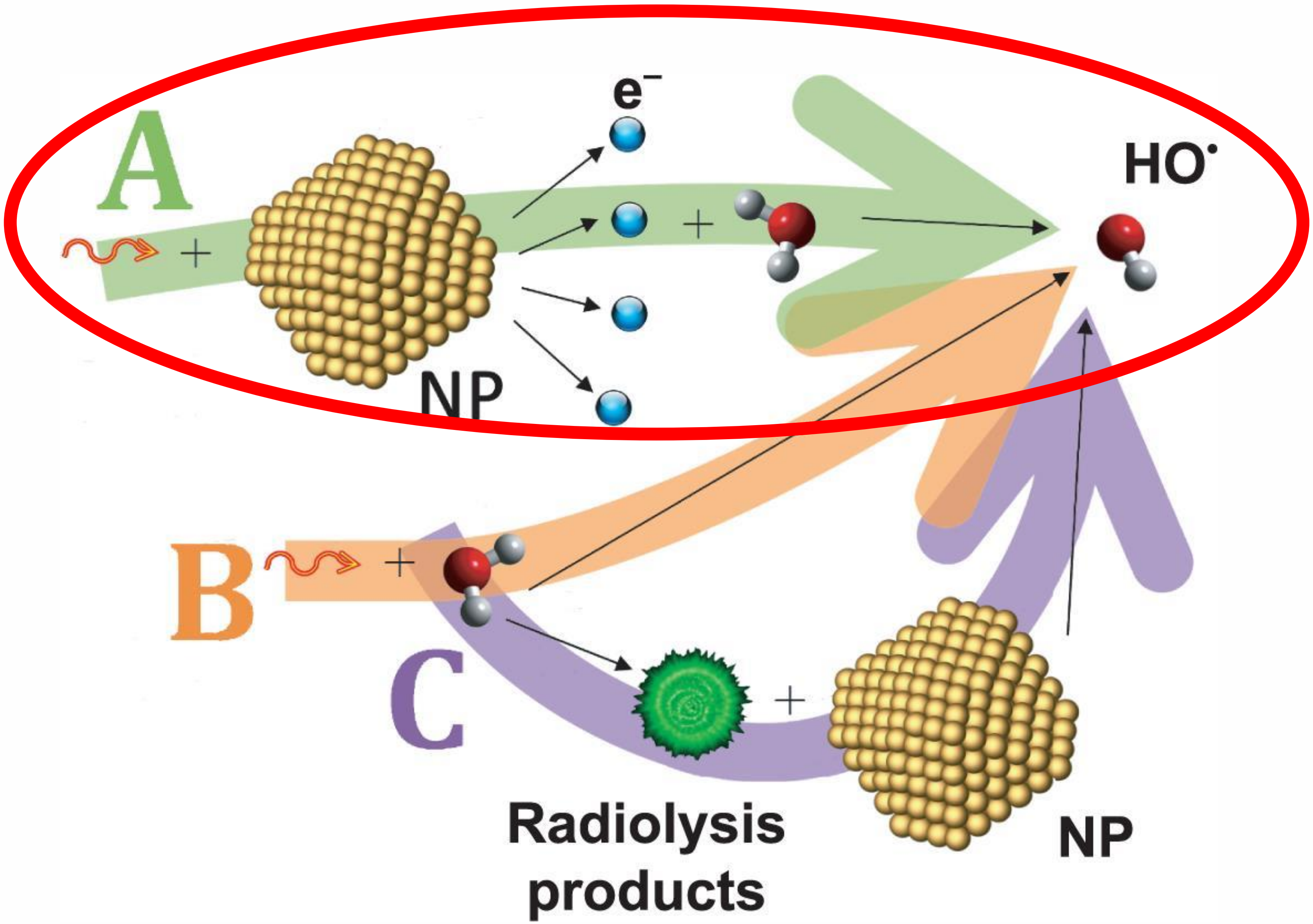

Figure 2 – The three classes of pathways for irradiated NP solutions.

Pathway A – Interaction with the NP

NP is irradiated creating a range of energetic species:

- Photoelectric effect
  - Esp. Auger cascade
- Excitons
- Water radiolysis as in Pathway B

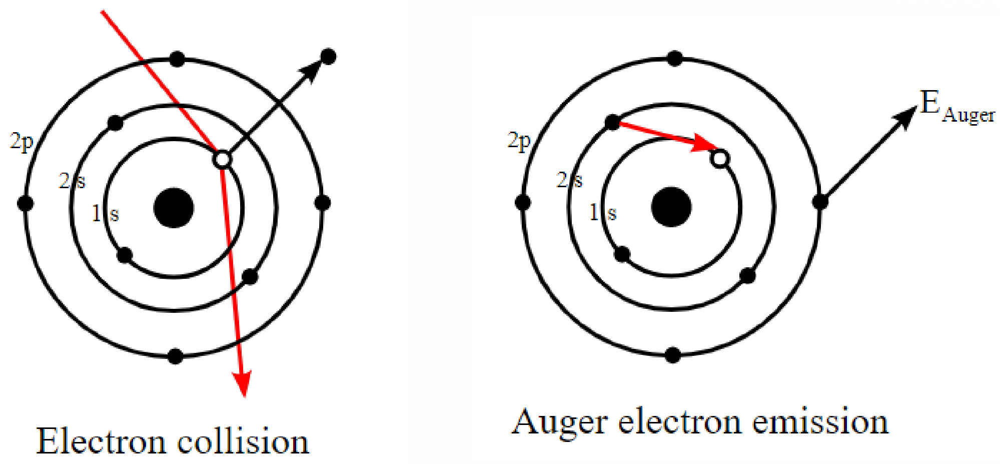

Figure 4 – Auger emission diagram [A. Carlson, 2007]

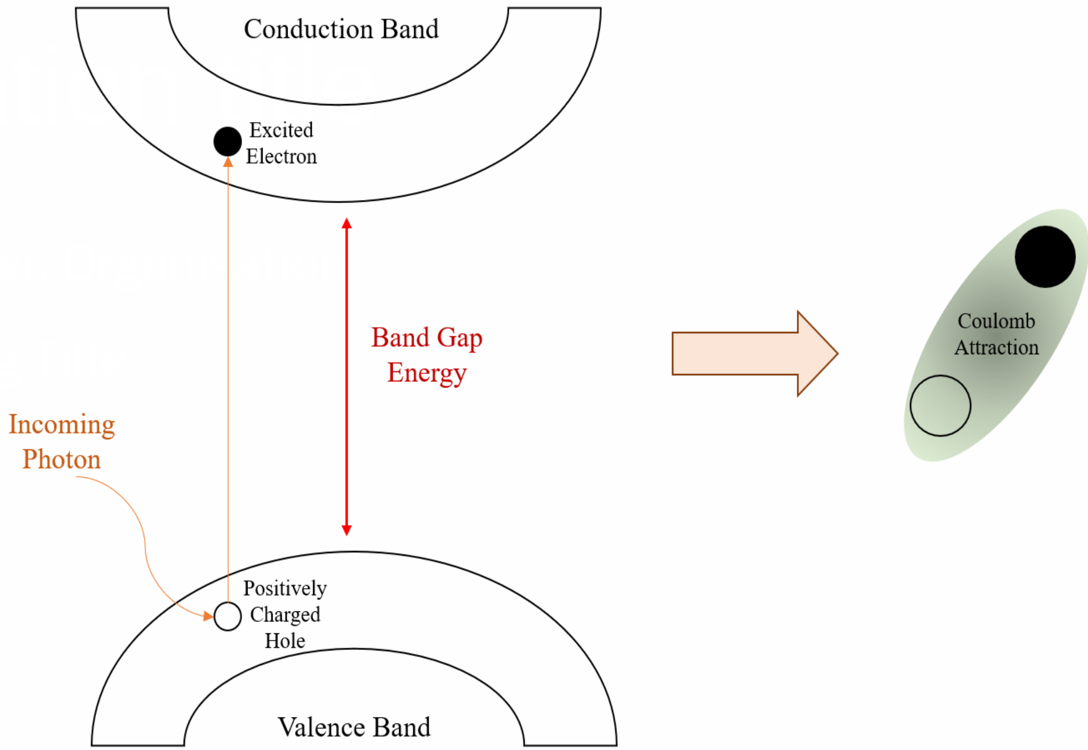

Figure 5 – Diagram depicting the formation of an exciton by the excitation of an electron from the valence band to the conduction band.

Background

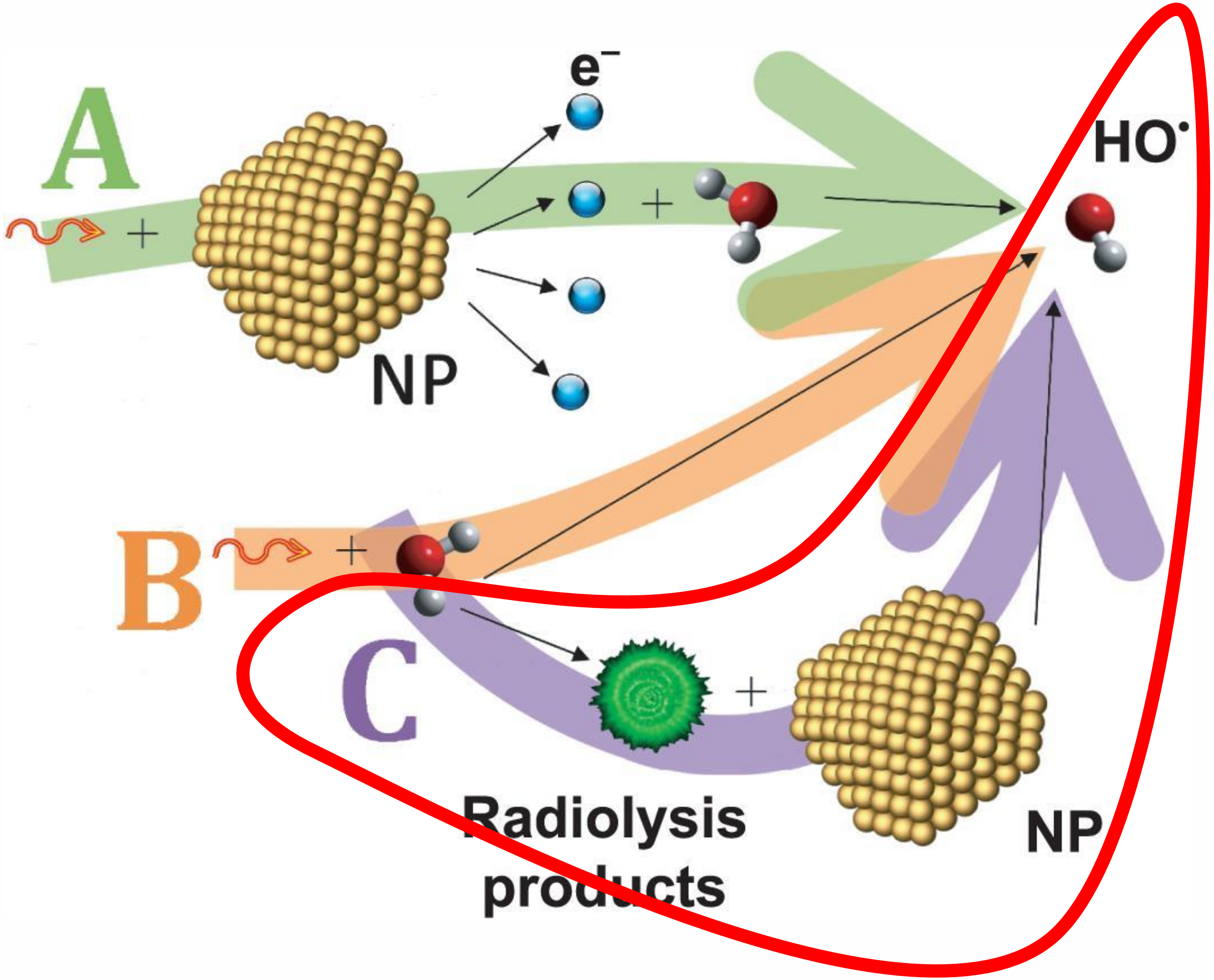

Figure 2 – The three pathways for irradiated NP solutions.

Pathway C – NP interface

Mechanisms that occur at the NP-water interface which lead to water radiolysis:

- Structured water layers – lengthen H-OH bonds
- Energy carrying species interact with surface
- Pathways A and B still occur

Aims

- Develop simulations where energy is directly deposited into NPs
- Model energy transfer at the NP-water interface
- Cultivate an integrated account of all processes

Method Development

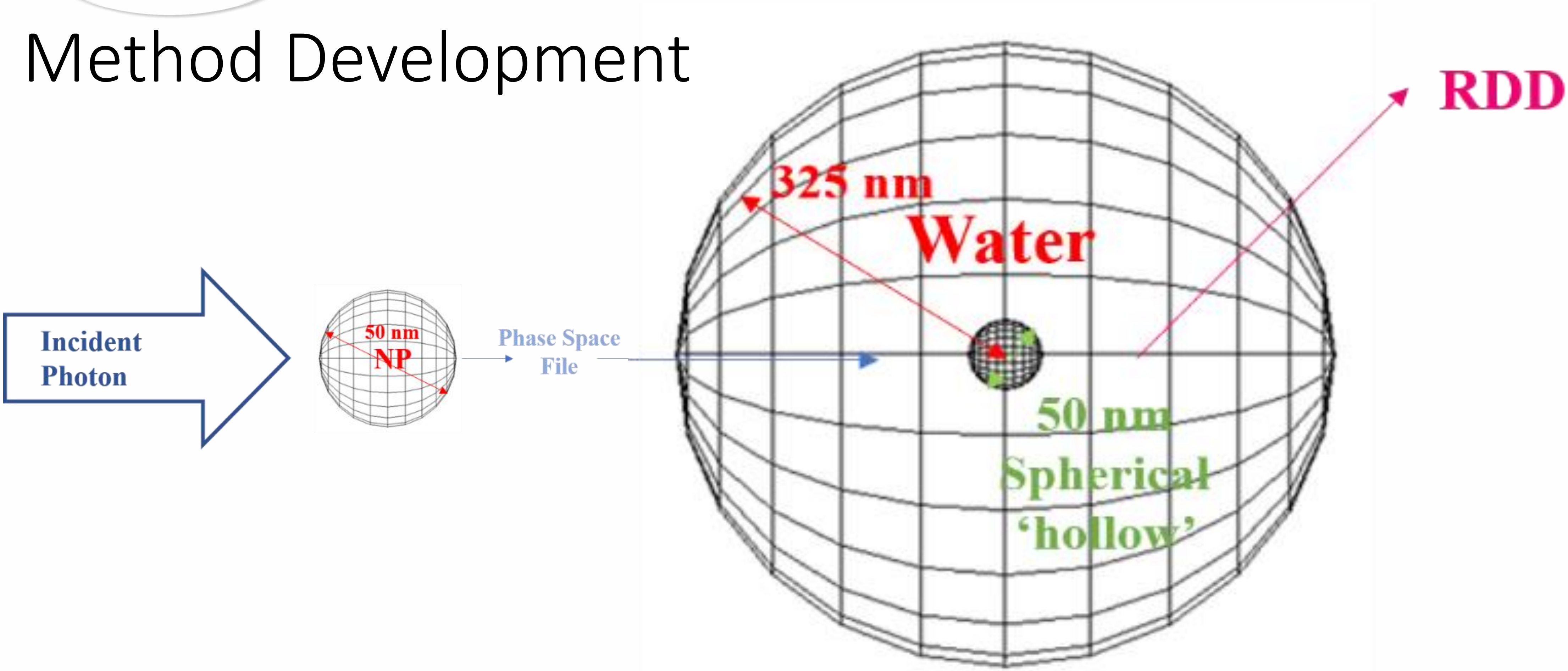

50 nm spherical hollow – any particles that re-enter this space can be tracked, and are effectively killed

Figure 6 – A visualisation of the simulation procedure for the second model

Preliminary Results

0.1 Gy – comparable to accepted models

Lower energy keV have the longest range in water

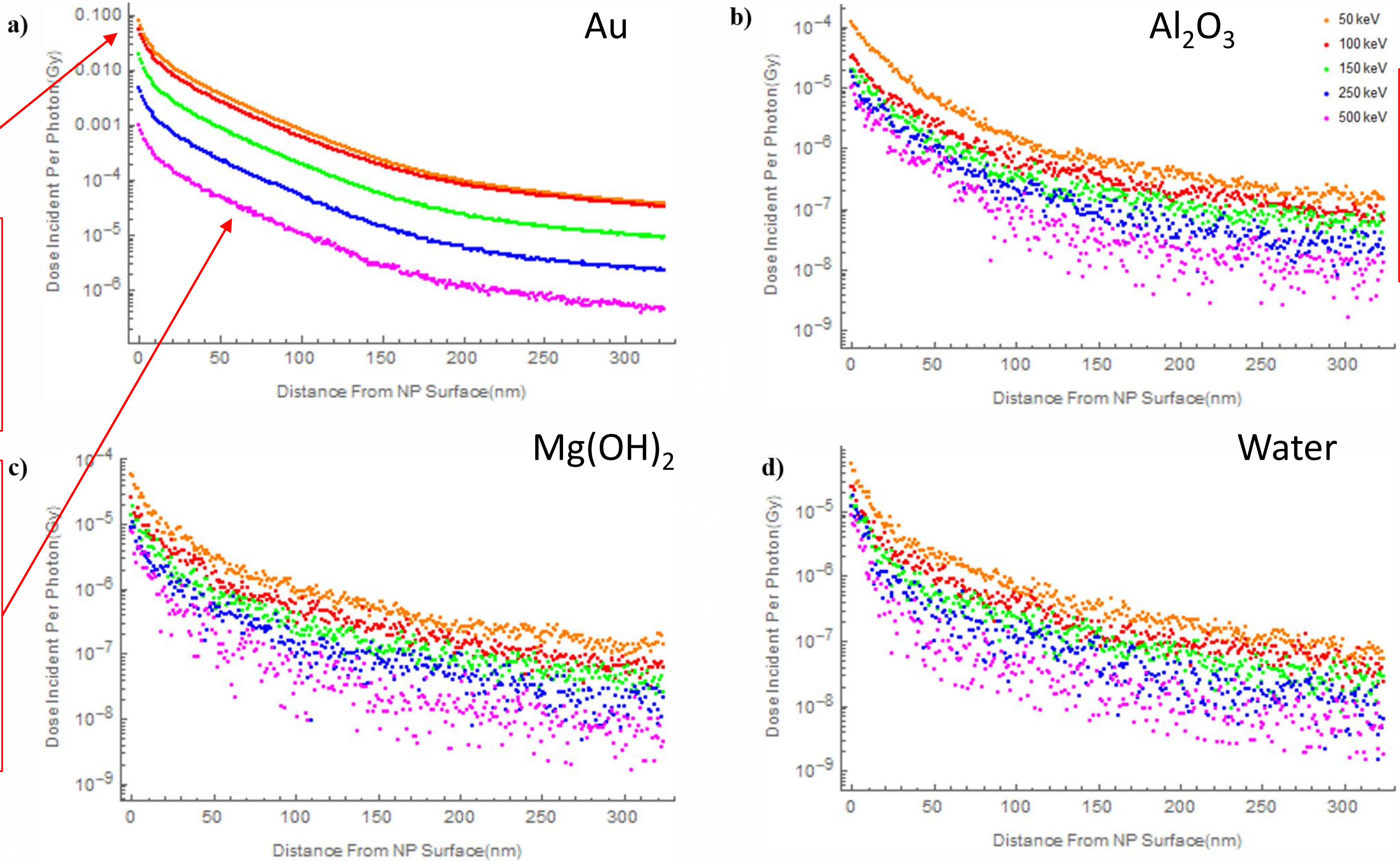

Al_2O_3 and $Mg(OH)_2$ are very similar to water

Although they are expected to be lower than Au as they have a lower density

Figure 7 – Graphs showing the radial dose distributions per incident photon for a) Au, b) Al_2O_3, c) $Mg(OH)_2$ and d) Water NPs irradiated by 50, 100, 150, 250 and 500 keV photon beams.

Preliminary Results

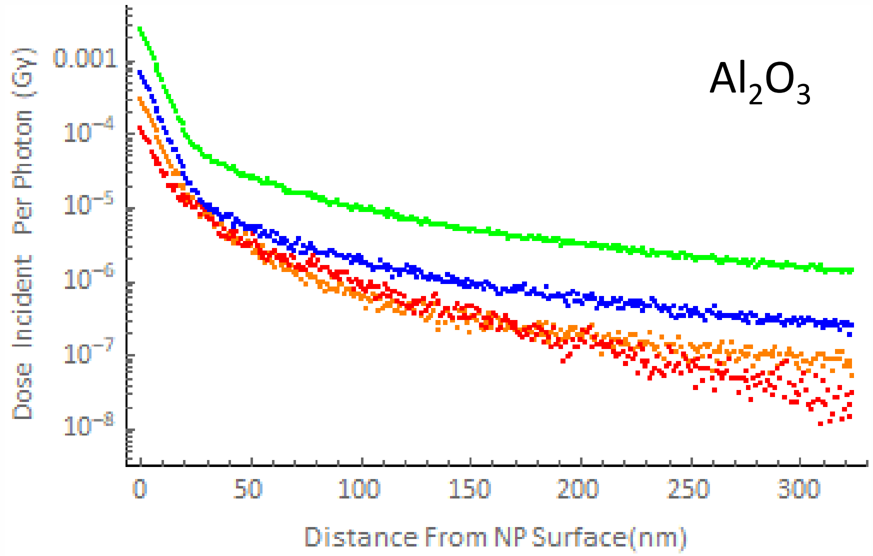

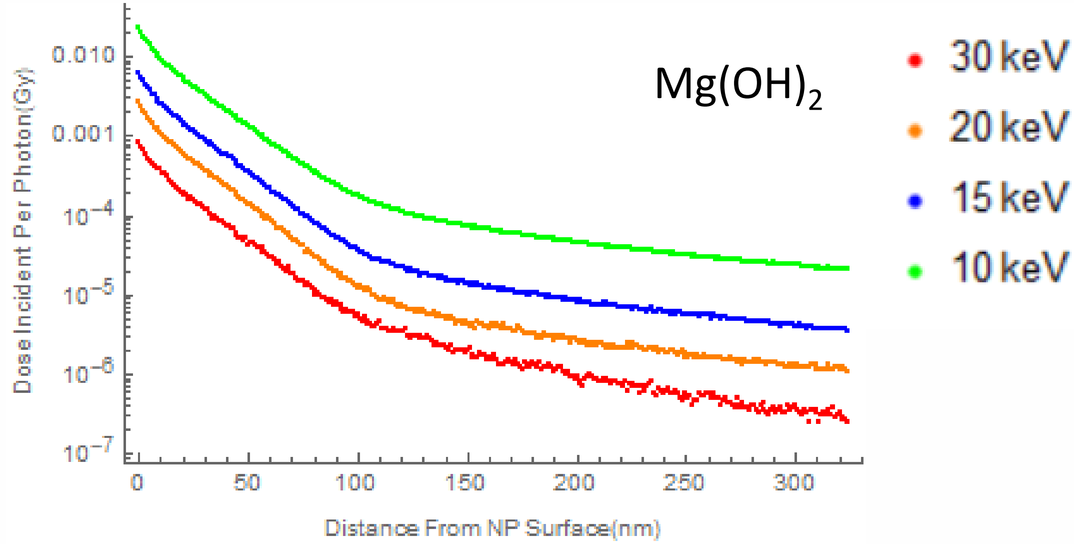

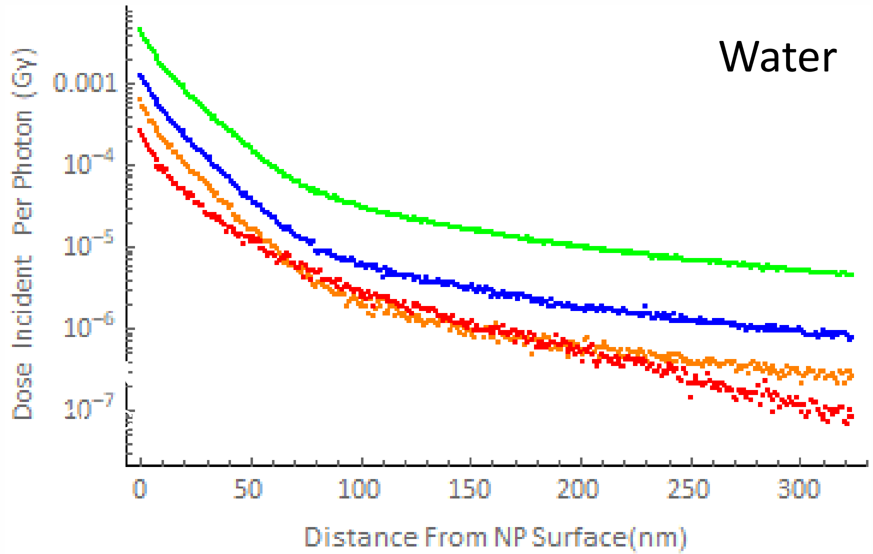

Figure 8 – Graphs showing the radial dose distributions per incident photon for a)Al_2O_3, b) $Mg(OH)_2$ and c) Water NPs irradiated by 10, 15, 20 and 30 keV photon beams.

Future Work

- Investigate which effects are dominant in Al_2O_3 and $Mg(OH)_2$
  - Photon energy
  - Density
  - Atomic number
  - NP size
- Develop scorer that can detect and track ionisations and excitations
- Model water radiolysis
- Simulate exciton mechanism for energy transfer

TRANSCEND

Transformative Science and Engineering for Nuclear Decommissioning

Thank you

Ella Schaefer
ella.schaefer@postgrad.manchester.ac.uk

TRANSCEND

Transformative Science and Engineering for Nuclear Decommissioning

Imperial College London

Nanotechnology for effluent treatment and radionuclide assay

Dr. Gurpreet Singh

Imperial College London

Supervisors: Prof. Luc Vandeperre & Prof. Mary Ryan

02/12/2020
TRANSCEND Project

Energy
For a Low Carbon Future

Previous Works

- Fortner's group (ref 1) had reported since 2015 about magnetic nanoparticles of mixed Mn/Fe oxide nanocrystals covered with a bilayered oleyl phosphate to adsorb/exchange uranyl ions in solution.
- Adsorption Capacity reported to be 1667 mg/g of mixed oxide nanocrystals.
- In 2018 Imperial's PhD student (Ref 2) further enhanced the work by using pure magnetite coated with oleic acid (12nm in size).

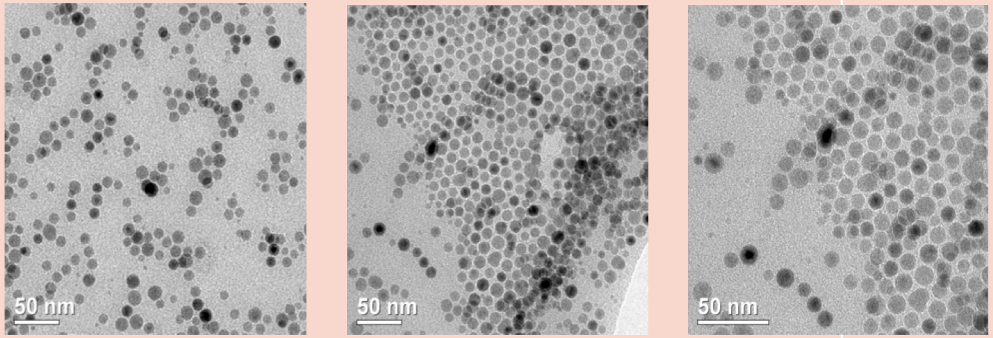

- The nanoparticles were further functionalised with phosphate groups to sequester uranium.
- The reported uptake capacity of Uranyl ions at neutral pH 7 was 1700 mg/g of Fe in 200ppm U(VI) nitrate solution
- This is the highest ever to be reported in the lit...

Proposed developments

The TRANSCEND project is aimed at the following:

1. To understand the mechanism of adsorption
2. To extend the application at acidic pH
3. To target other radionuclides with new functionalised coatings
4. To investigate magnetic steering of nanoparticles for repairing cracks in concrete

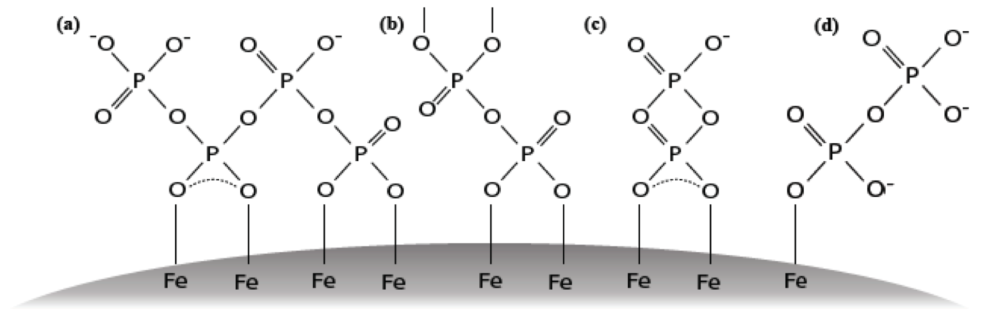

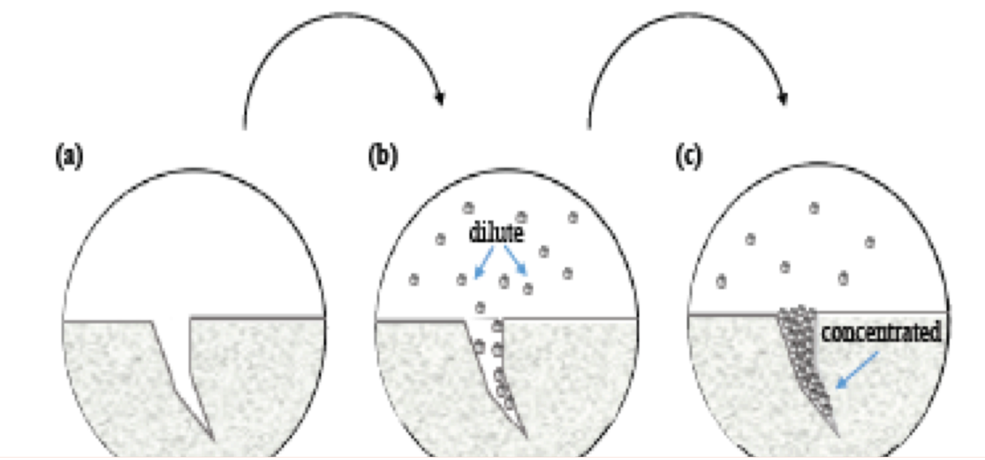

Work so far

- Previous method has limitations to upscale, especially due to tedious synthesis protocols and time frame. Hence, a new methodology is investigated using co-precipitation and microemulsion processes.
- The new process under investigation is lacking homogeneity, as currently the size of particles is between 5nm to 25nm, with a higher degree of aggregation.
- Current synthesis time is 3 hours from scratch, in regard to the 30+ hours of previous work.
- Current synthesis is easily up-scaled to any volumes required.
- The cost of production is presumed to cheaper, if the protocol is perfected.
- Yet to Validate the protocols and perform further analysis and adsorption experiments.

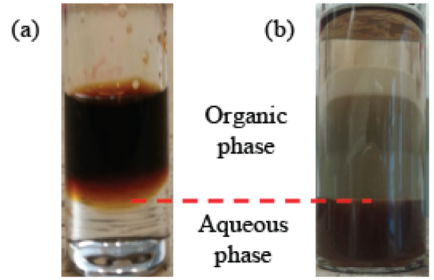

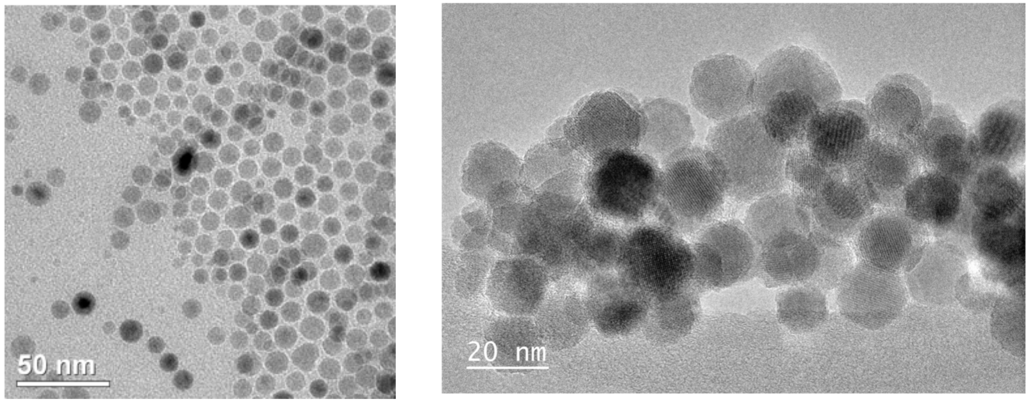

Top Image: Previous work of oleic acid coated (left) & phosphate-coated magnetite (right)

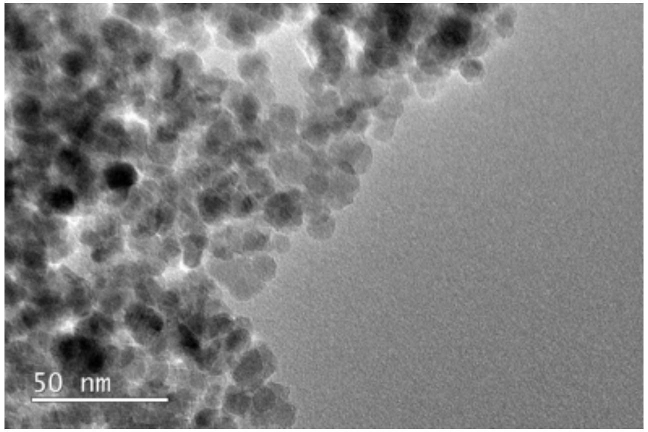

Bottom Image: Current work of bare-magnetite

TRANSCEND

Transformative Science and Engineering for Nuclear Decommissioning

REFERENCES

1. Wenlu Li, John T. Mayo, Denise N. Benoit, Lyndsay D. Troyer, Zuzanna A. Lewicka, Brandon J. La↵erty, Je↵rey G. Catalano, Seung Soo Lee, Vicki L. Colvin, and John D. Fortner. Engineered superparamagnetic iron oxide nanoparticles for ultra-enhanced uranium separation and sensing. J. Mater. Chem. A, 4(39):15022–15029, 2016.

2. Calì, E. & Qi, Jiahui & Preedy, O. & Chen, S. & Boldrin, D. & Branford, Will & Vandeperre, L. & Ryan, M.. (2018). Functionalised magnetic nanoparticles for uranium adsorption with ultra-high capacity and selectivity. Journal of Materials Chemistry A. 6. 10.1039/C7TA09240G.

Thank you

Email: gsuri@ic.ac.uk

Scoping studies of ion exchange materials

James Reed, University of Birmingham

2.12.2020
Virtual conference

About Me

- Msci Chemistry graduate, University of Birmingham.
- Particular interest in ion-exchange materials and materials chemistry.
- Enjoy running
- Keen cricketer

Msci Project: Magnetisation of tin umbites

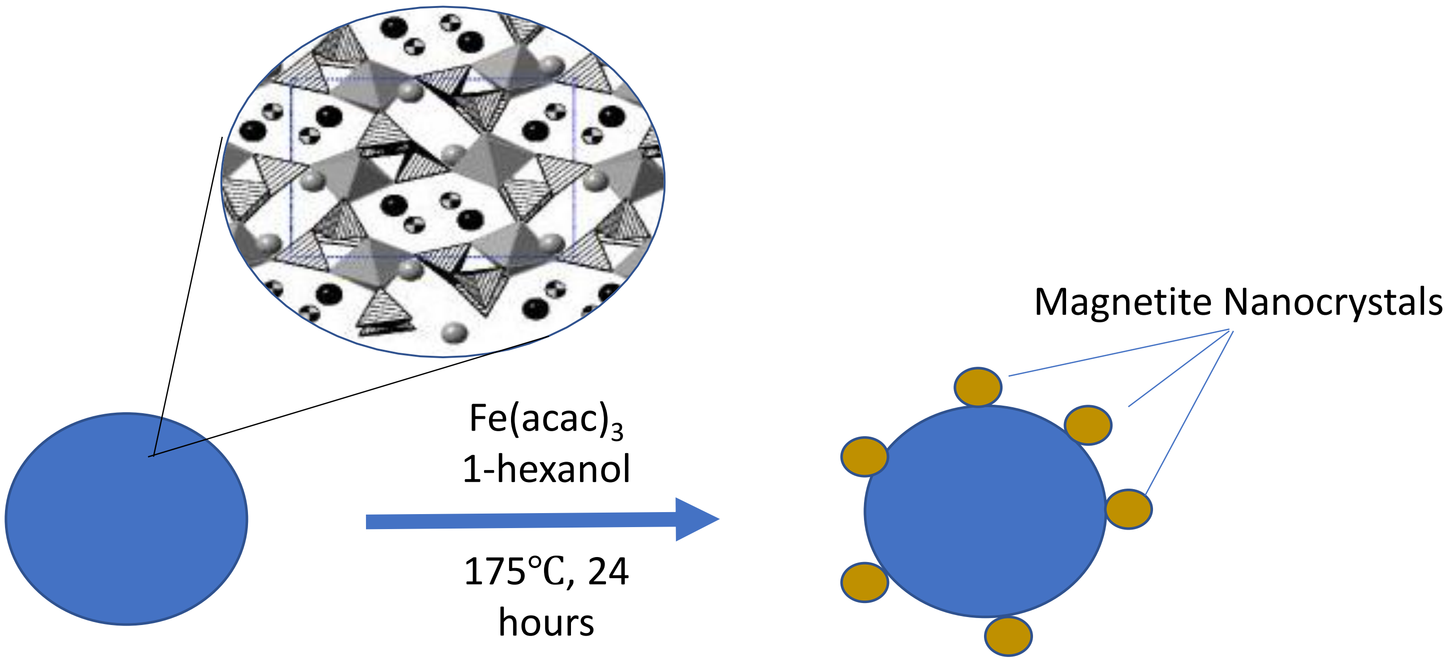

Current work: 2nd year PhD student, Hriljac/ Allan group

- 3 ½ years supported by Sellafield Ltd and NNL.
- Aim: to improve ion-exchange characteristics of naturally sourced zeolites by chemical treatments.
- Includes desilication and dealumination of the zeolite framework and phase transformations to improve uptake.

Sellafield Ltd

NATIONAL NUCLEAR LABORATORY

Why caesium and strontium?

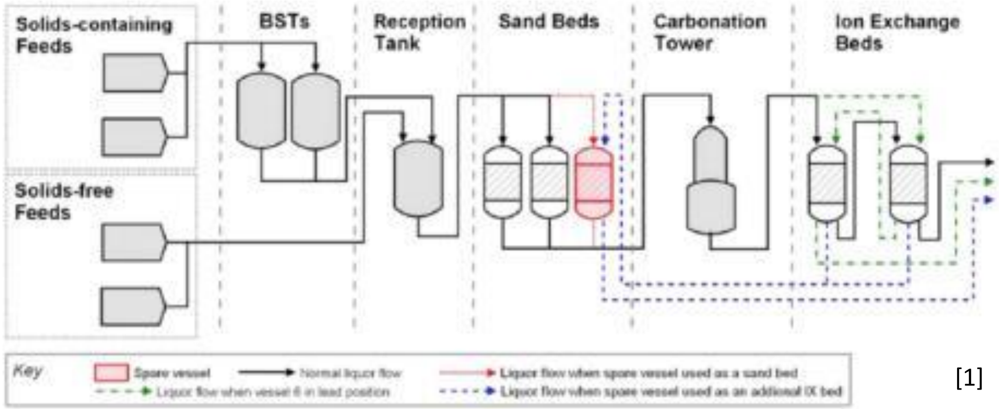

[1]

- Cs-137 and Sr-90 are key targets in removal from nuclear waste streams worldwide.
- At the Sellafield site, SIXEP treats 100s m^3 per day.
- Currently utilises a clinoptilolite sourced from Mud Hills in California.
- Supply limited, new materials must be sourced.

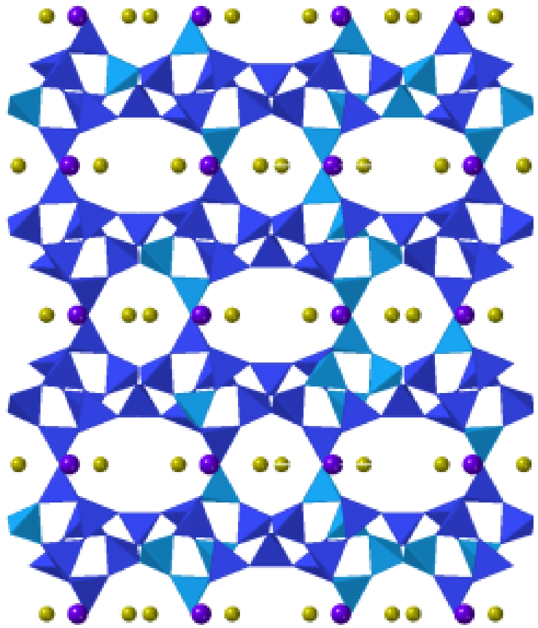

Zeolites

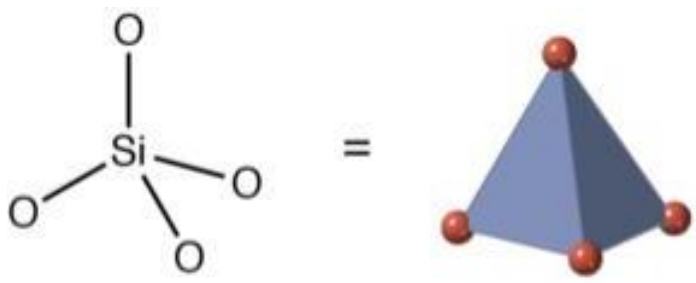

(Or Al)

FAU

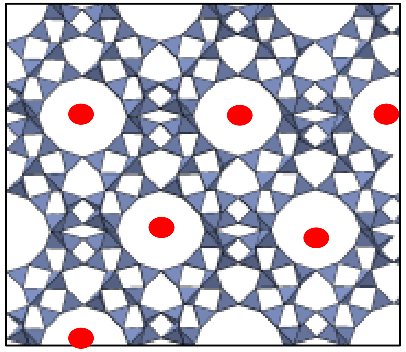

CHA

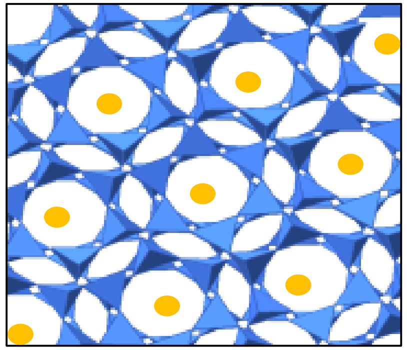

- Al tetrahedra carry negative charge.
- Cations balance this charge by sitting in spaces/ pores within the framework.
- These ions are free to move and can therefore take part in ion-exchange processes.

Si/Al ratio

Low Al content: low capacity
Used in catalysis

High Al content: high cation capacity

Used in ion-exchange

Zeolite Synthesis

Silica source + Alumina source $\xrightarrow[\text{SDA, } OH^-]{\text{Hydrothermal}}$ Many zeolite structures


[2]

$\xrightarrow[\text{Alkaline conditions}]{\text{High pressure}}$ Natural zeolites

- Cheap
- Inpure

Interzeolite Transformations

- Uses a zeolite framework as a starting material to form a different structure

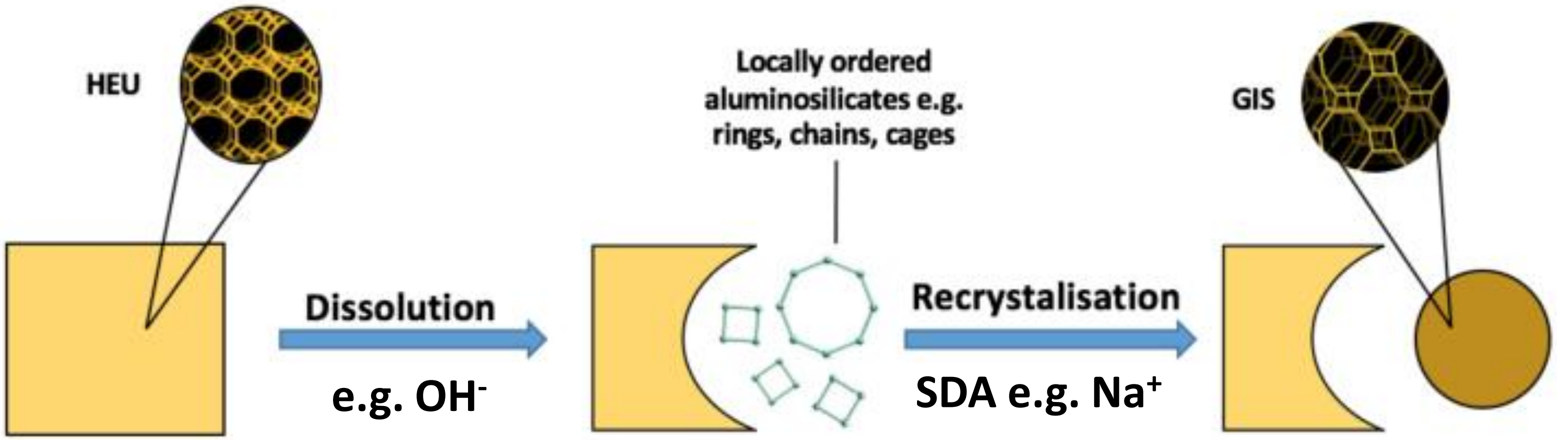

- Changes selectivity
- Increases purity
- Can add value to 'low value' materials

MH-CLINO (HEU)

Cs: 84 % uptake
Sr: 46 % uptake

Z-CLINO (HEU)

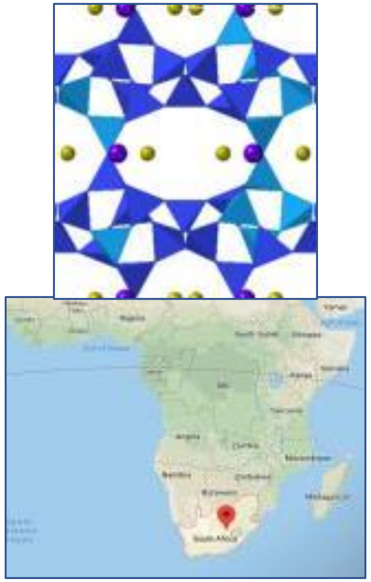

Cs: 69 % uptake
Sr: 27 % uptake

I-MORD (MOR)

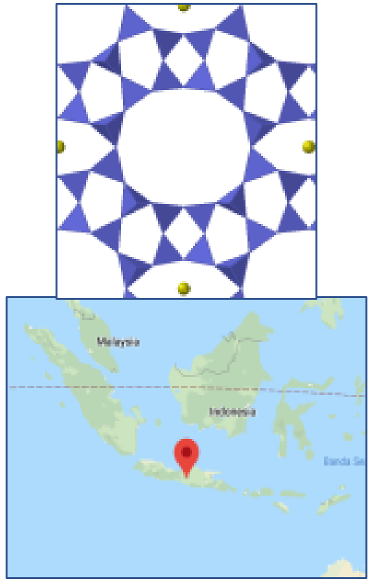

Cs: 93 % uptake
Sr: 7 % uptake

- Caesium uptake good to excellent in all systems.
- Strontium uptake poor, especially in mordenite.
- Improvement in strontium uptake required.

MH-CLINO (HEU)
Cs: 84 %
Sr: 46 %

1.0 M NaOH, 100℃, 24 h →

Chabazite (CHA)
Cs: 3 %
Sr: 98 %

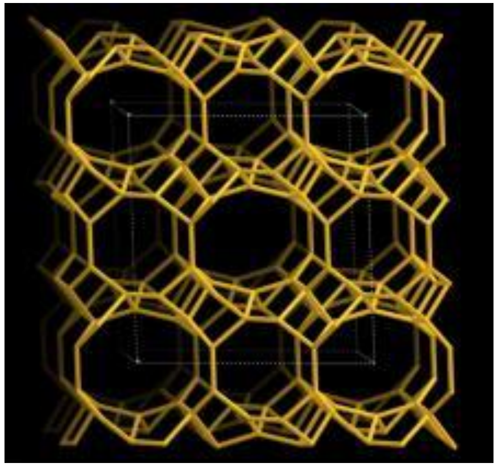

Monoclinic unit cell
a = 17.52 Å , b = 17.04 Å , c = 7.40 Å
FD = 17.5 T/1000 $Å^3$
10 and 8 ring channels along [001]

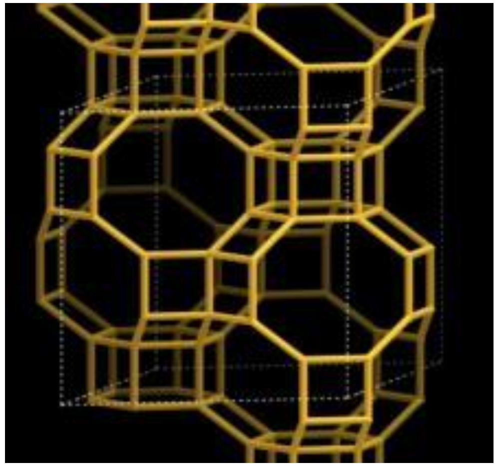

Trigonal unit cell
$a = b$ = 13.68 Å , c = 14.77 Å
FD = 15.1 T/1000 $Å^3$
8 ring channels along [100] and [010]
6 ring channels along [001]

Z-CLINO (HEU)

Cs: 69 %
Sr: 27 %

$\xrightarrow{\text{1.0 M NaOH, 100°C, 24 h}}$

Zeolite-P (GIS)

Cs: 84 %
Sr:61 %

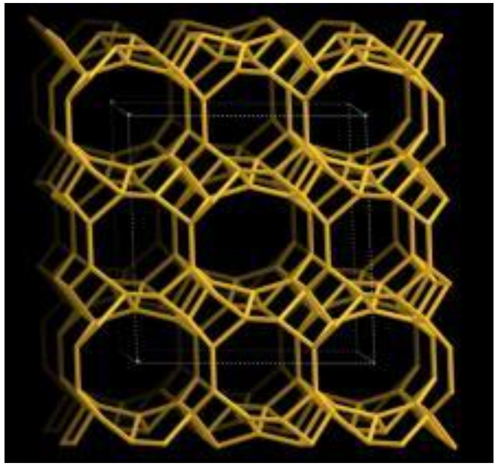

Monoclinic unit cell
a = 17.52 Å , *b* = 17.04 Å , *c* = 7.40 Å
FD = 17.5 T/1000 $Å^3$
10 and 8 ring channels along [001]

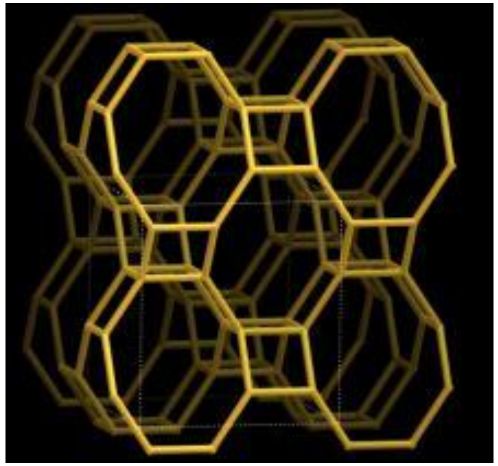

Tetragonal unit cell
a = *b* = 9.80 Å , *c* = 10.16 Å
FD = 16.4 T/1000 $Å^3$
8 ring channels along [100] and [010]

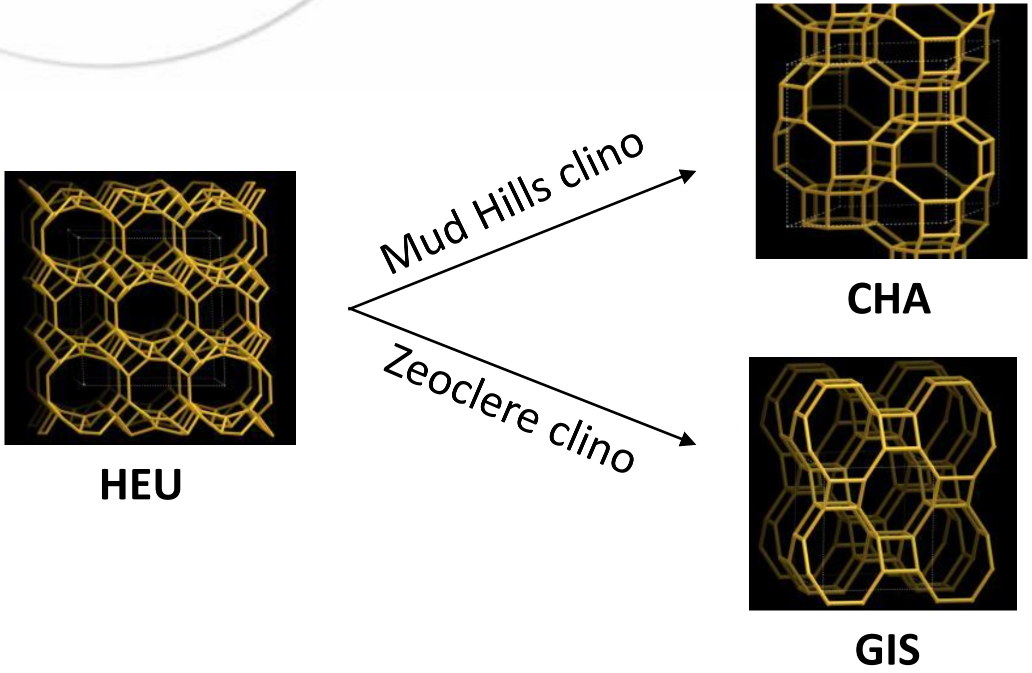

- No phase change of starting materials when KOH is used.
- Reason for this divergent phase selectivity investigated through different treatments.

Mud Hills clino $\xrightarrow{\text{Acid wash}}$ H-Mud Hills clino $\xrightarrow{\text{1M NaOH}}$ GIS

Mud Hills clino $\xrightarrow{\text{NaCl wash}}$ Na-Mud Hills clino $\xrightarrow{\text{1M NaOH}}$ CHA

I-MORD (MOR) $\xrightarrow{\text{1.5 M NaOH, 100℃, 24 h}}$ Zeolite-P (GIS)

Cs: 93 %
Sr: 7 %

Cs: 16 %
Sr: 94 %

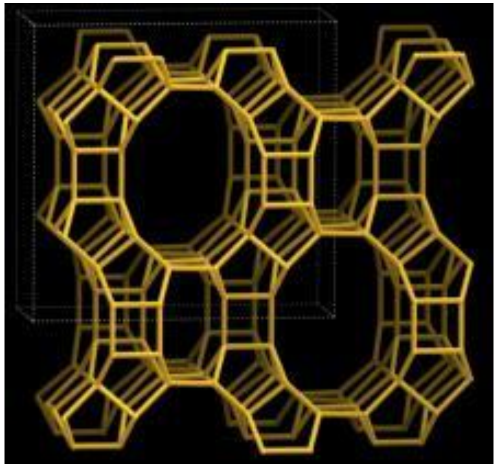

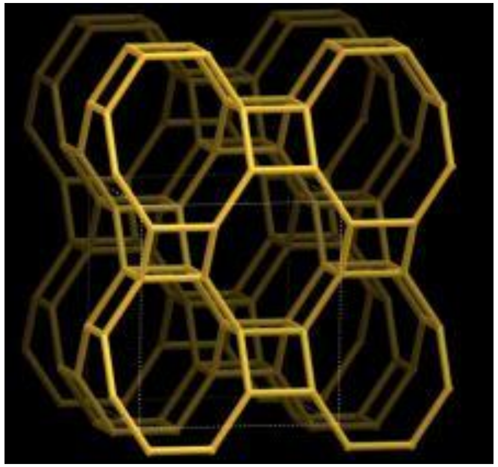

Orthombic unit cell
a = 18.26, *b* = 20.53 Å , *c* = 7.54 Å
FD = 17.0 T/1000 $Å^3$
12 and 8 ring channels along [001]

Tetragonal unit cell
a = *b* = 9.80 Å , *c* = 10.16 Å
FD = 16.4 T/1000 $Å^3$
8 ring channels along [100] and [010]

Interzeolite phase transformations of three starting materials

MH-CLINO (HEU) $\xrightarrow{\text{1.0 M NaOH, 100°C, 24 h}}$ Chabazite (CHA)

Cs: 84 %
Sr: 46 %

Cs: 3 %
Sr: 98 %

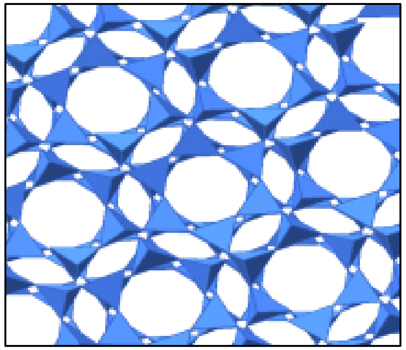

Z-CLINO (HEU) $\xrightarrow{\text{1.0 M NaOH, 100°C, 24 h}}$ Zeolite-P (GIS)

Cs: 69 %
Sr: 27 %

Cs: 84 %
Sr:61 %

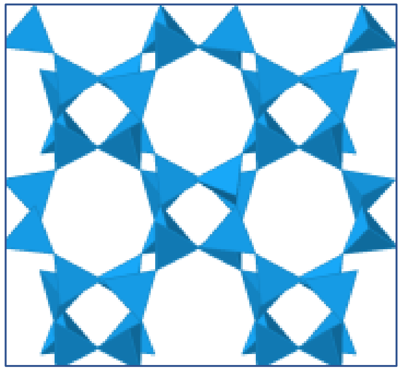

I-MORD (MOR) $\xrightarrow{\text{1.5 M NaOH, 100°C, 24 h}}$ Zeolite-P (GIS)

Cs: 93 %
Sr: 7 %

Cs: 16 %
Sr: 94 %

Partial transformations

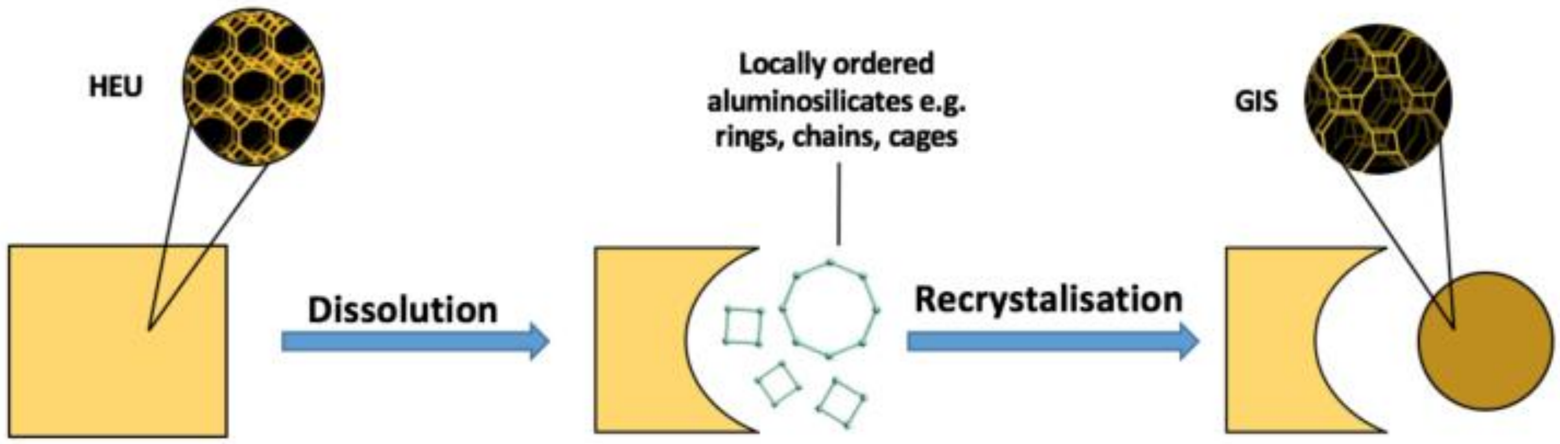

- Would this retain some selectivity from the parent zeolite?
- If so, this could lead to valuable selectivity profiles.
- Concern over physical stability of parent zeolite.

Transformative Science and Engineering for Nuclear Decommissioning

MH-CLINO (HEU)
Cs: 84 %
Sr: 46 %

0.50 M NaOH

HEU/CHA
Cs: 66 %
Sr: 95 %

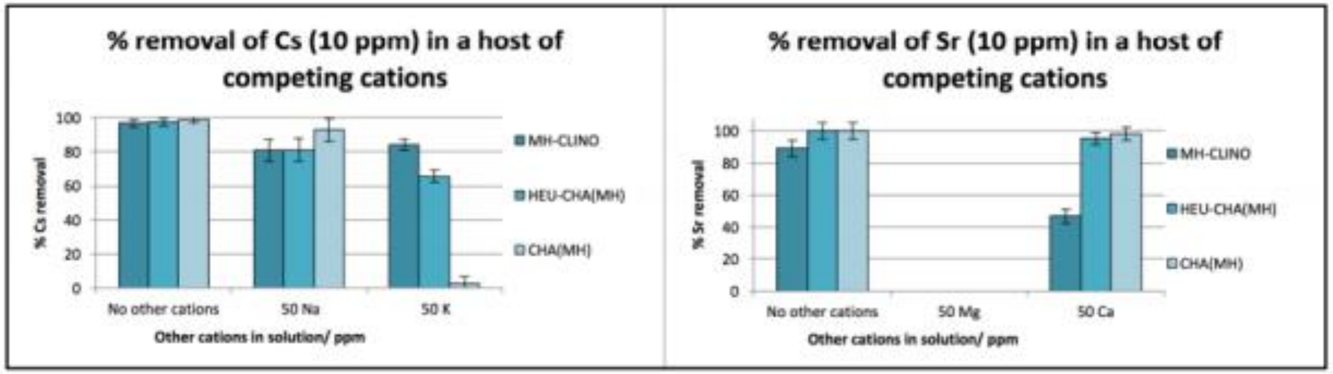

Z-CLINO (HEU)
Cs: 69 %
Sr: 27 %

0.75 M NaOH

HEU/GIS
Cs: 78%
Sr: 80%

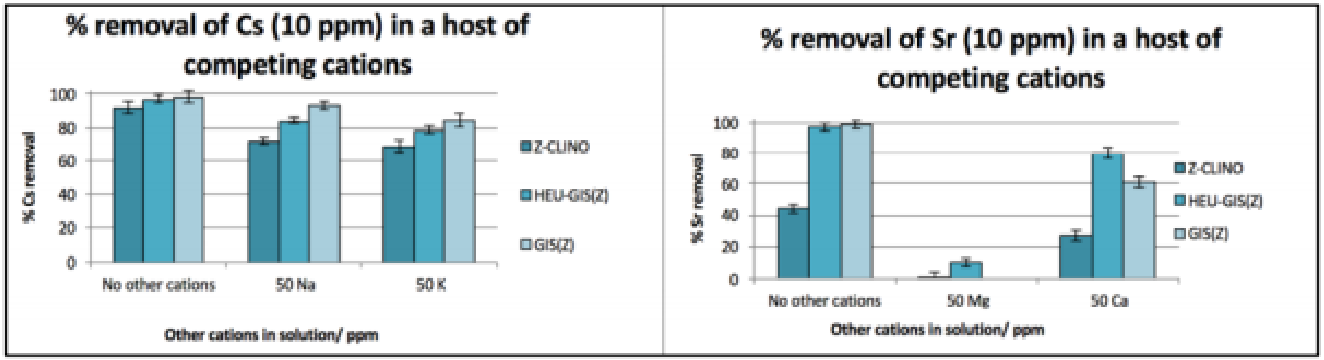

I-MORD (MOR)
Cs: 93 %
Sr: 7 %

1.00 M NaOH

MOR/GIS
Cs: 81 %
Sr: 64 %

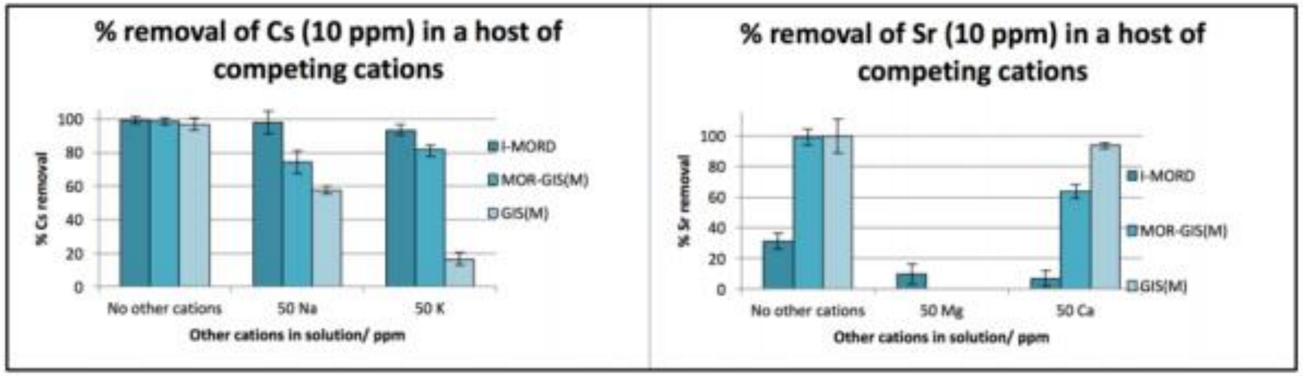

PP bottle transformations

MH-CLINO (HEU) $\xrightarrow{\text{1.0 M NaOH, 100°C, 24 h}}$ Chabazite (CHA)

MH-CLINO (HEU) $\xrightarrow{\text{0.8 M NaOH, 100°C, 24 h}}$ HEU/CHA composite

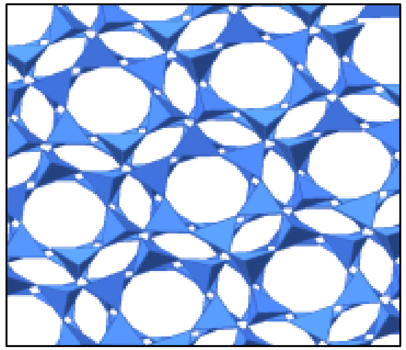

Z-CLINO (HEU) $\xrightarrow{\text{1.0 M NaOH, 100°C, 24 h}}$ Zeolite-P (GIS)

Z-CLINO (HEU) $\xrightarrow{\text{0.5 M NaOH, 100°C, 24 h}}$ HEU/GIS composite

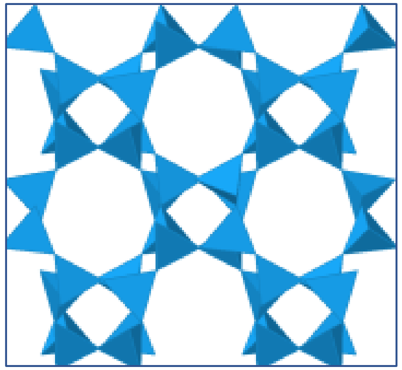

I-MORD (MOR) $\xrightarrow{\text{1.5 M NaOH, 100°C, 24 h}}$ Zeolite-P (GIS)

I-MORD (MOR) $\xrightarrow{\text{1. 1M NaOH, 100°C, 24 h}}$ MOR/GIS composite

An in-depth look at generating composites

- Series of composites generated by varying [NaOH].
- Weight fractions of each phase obtained through Rietveld refinement of powder diffraction data.
- Potential to 'tune' material for a given waste stream.

For Z-CLINO:

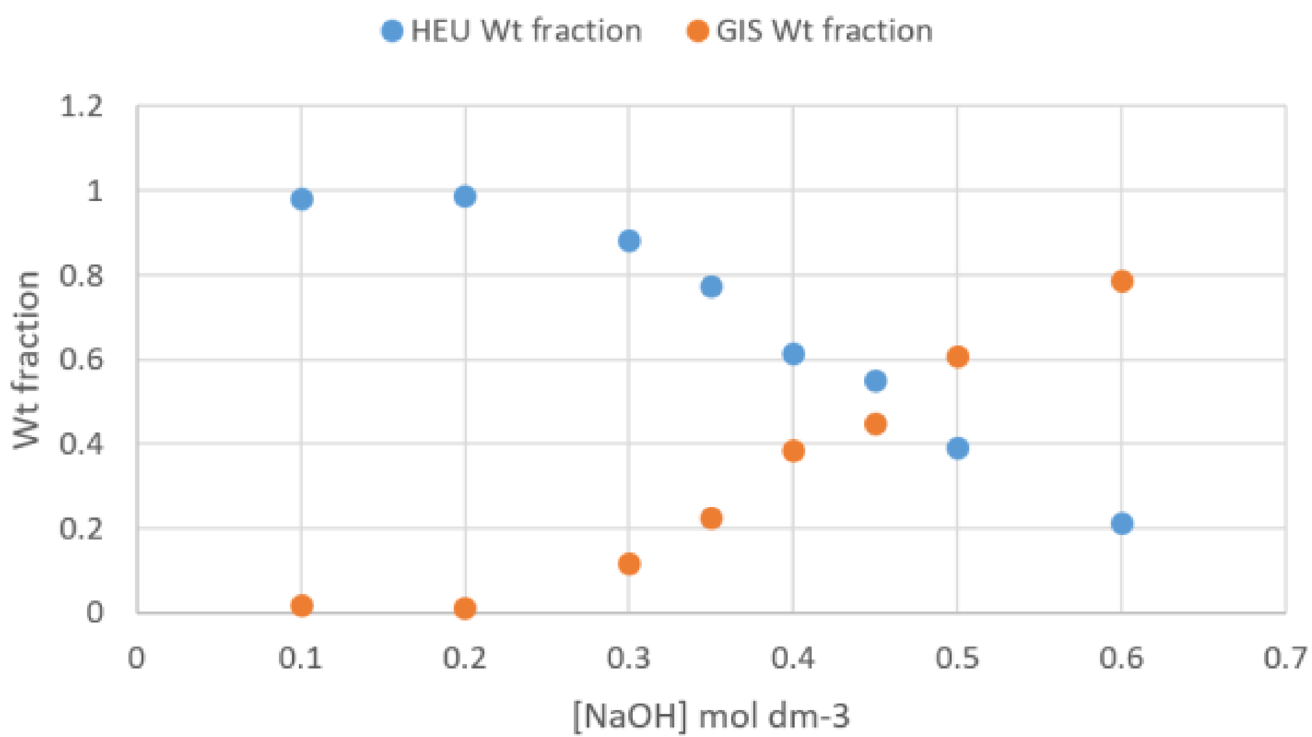

TBAH as an alternative reagent

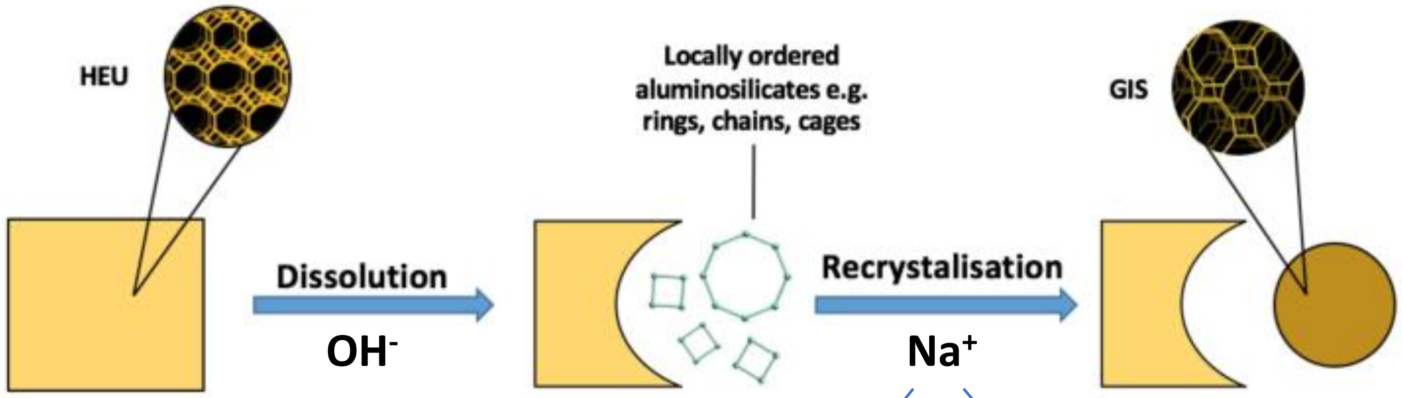

'Large cation' hysdroxide e.g. TBAH

NaOH

Na salt e.g NaCl

Z-CLINO (HEU) $\xrightarrow{\text{1.0 M TBAH/NaCl, 100°C, 24 h}}$ Zeolite-P (GIS)

Z-CLINO (HEU)	Zeolite-P (GIS)
Cs: 69 %	Cs: ? %
Sr: 27 %	Sr: ? %

Future work:

- Ion exchange data on composite studies
- Generate composite series for I-MORD
- Microscopy studies to further characterise materials
- Bring in new materials to examine
- More use of TBAH
- Active testing

References

[1] A. Dyer, J. Hriljac, N. Evans, I. Stokes, P. Rand, S. Kellet, R. Harjula, T. Moller, Z. Maher, R. Heatlie-Branson, J. Austin, S. Williamson-Owens, M. Higgins-Bos, K. Smith, L. O'Brien, N. Smith and N. Bryan, Journal of Radioanalytical and Nuclear Chemistry, 2018, 318, 2473-2491.

[2] https://theconversation.com/why-cant-we-predict-when-a-volcano-will-erupt-53898

[3] Images taken from Google earth

Transformative Science and Engineering for Nuclear Decommissioning

Thank you

jlr552@student.bham.ac.uk

TRANSCEND

Transformative Science and Engineering for Nuclear Decommissioning

Improving *in situ* acoustic characterisation of suspensions with machine learning methods

Joe Hartley, University of Leeds

Theme 1 – Integrated Waste Management

02/12/2020
Joint Nuclear Event Webinar

Energy
For a Low Carbon Future

TRANSCEND

Transformative Science and Engineering for Nuclear Decommissioning

Background

- Graduated from the University of Sheffield in 2019.
    - 2.1 - Material Science and Nuclear Engineering MEng.
    - FYP: A Dissolution Study of Thermally Treated Chabazite By Hot Isostatic Pressing.
- October 2020: Started PhD at University of Leeds:
    - Advanced Ultrasonic Characterisation of Slurry Flows

Research Challenge

- ILW legacy sludge at Sellafield needs to be pumped out of ponds to be processed.
- Characterisation data on the sludge is scarce;
  - Remote online monitoring system is needed to characterize the sludge during pipe-flow.

Figure 13: Composition of ILW by waste group

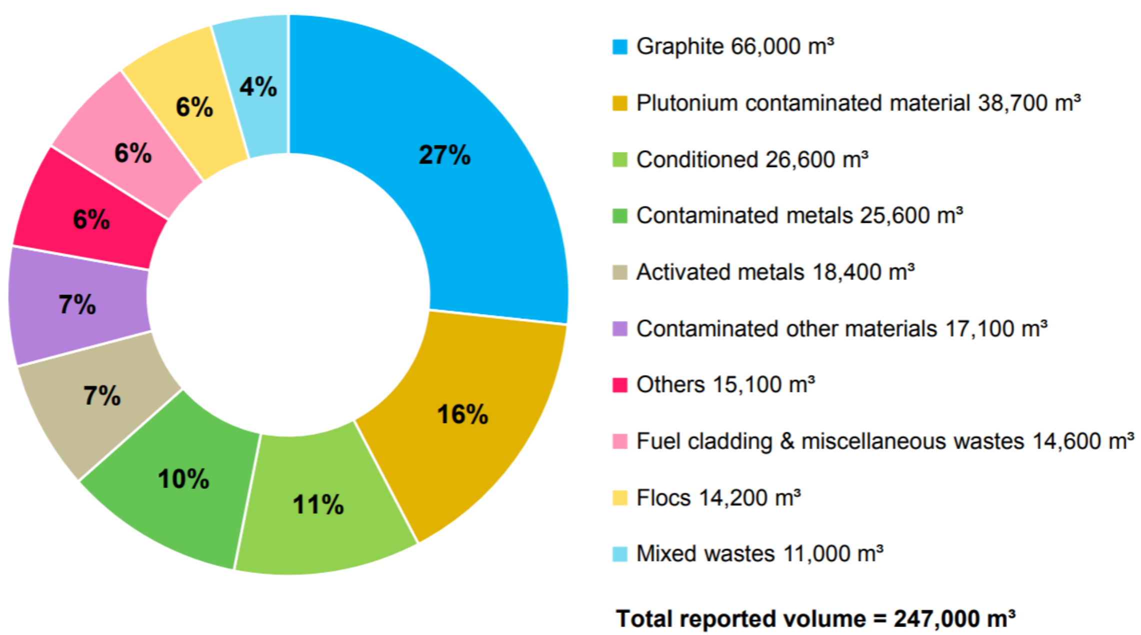

https://ukinventory.nda.gov.uk/wp-content/uploads/2020/01/2019-Waste-Report-Final.pdf https://www.youtube.com/watch?v=Yu7-D37SKOY&ab_channel=SellafieldLtd

Similar Use of Acoustics

Acoustic Backscatter System has been used industrially to characterise slurries:

P.D. Thorne, D.M. Hanes / Continental Shelf Research 22 (2002) 603–632

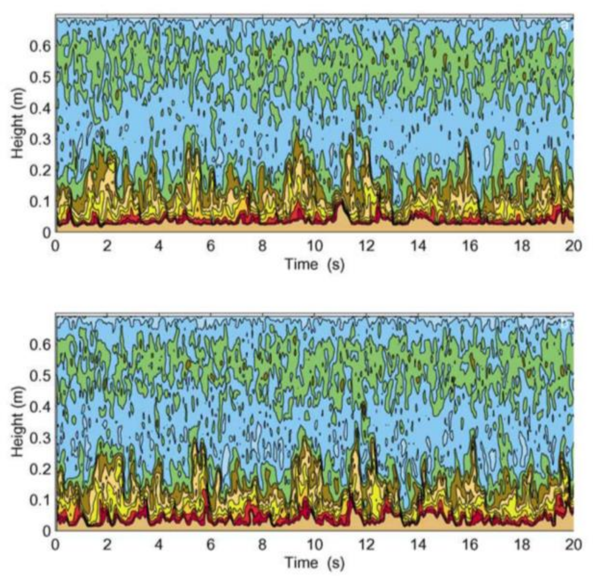

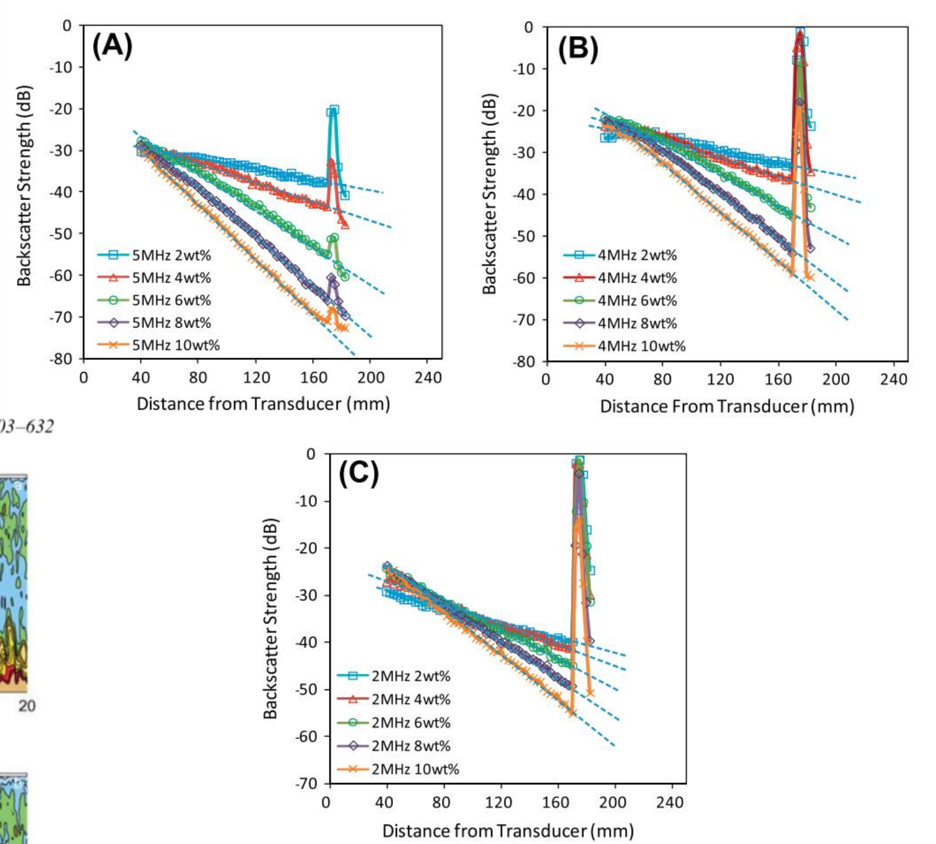

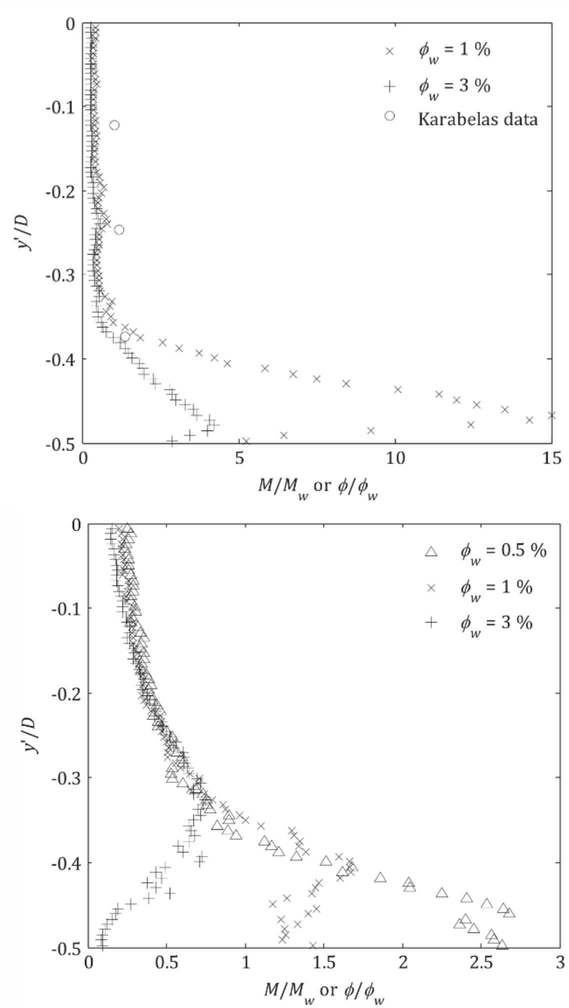

Thorne, Hanes; *A reveiw of acoustic measurement of small-scale sediment processes*

DOI:10.1016/j.mineng.2011.12.003

DOI: 10.1016/j.ces.2014.11.063

Transformative Science and Engineering for Nuclear Decommissioning

Acoustic Instrumentation

- UVP-DUO from Met-Flow.
- Has been used in the department for nearly a decade – good expertise.
- Frequency range from 1–8 MHz
- Active radii for the transducers are 2.5 – 10 mm; 2.5 or 5 mm is ideal for non-intrusive attachment on pipelines.

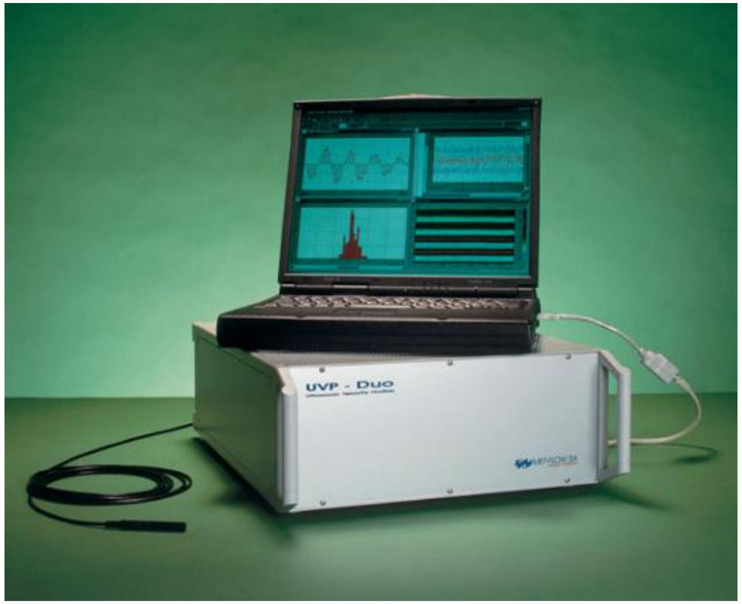

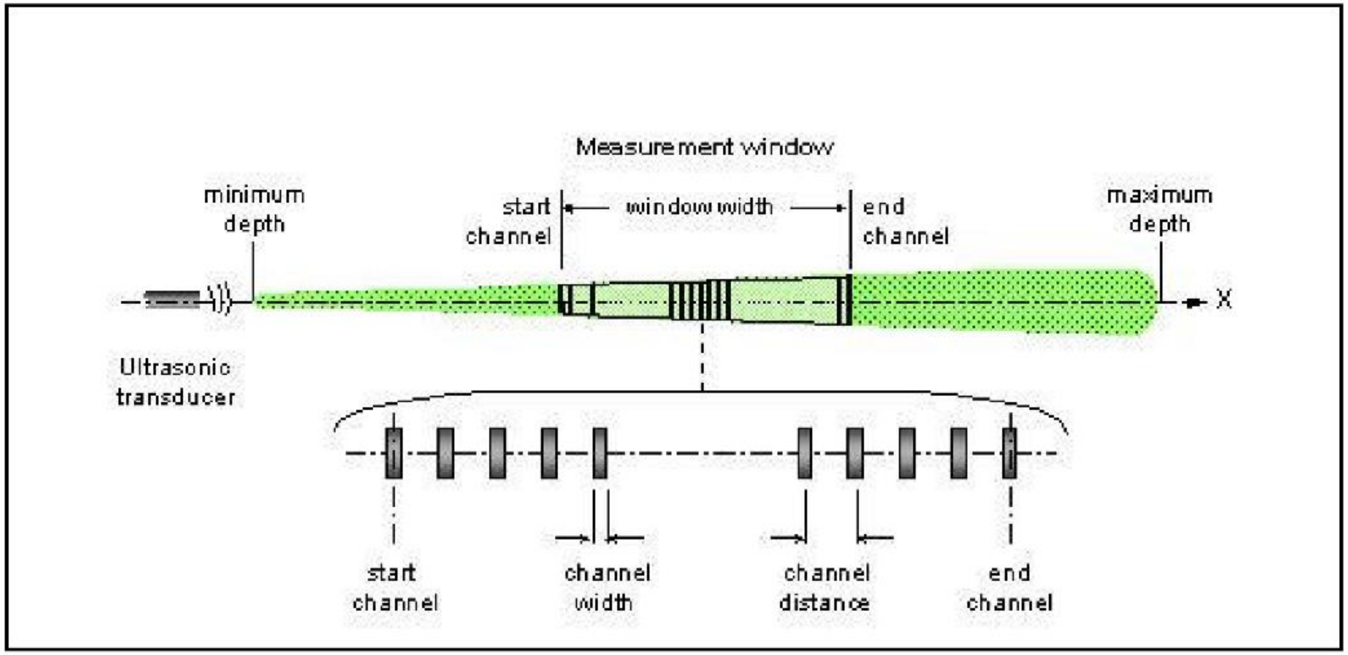

UVP Monitor Model UVP-DUO With Software Version 3, User's Guide, Draft Ed., Met-Flow, Release 5, 1/07/02.

ML and How It Will Be Applied

- Machine Learning:
  - making the computer learn from studying data and statistics.
  - a step into the direction of artificial intelligence (AI).
  - program that analyses data and learns to predict the outcome.
- Essentially pattern matching '*test*' data to the '*training*' data.

python™

Overview of Project Objectives

- Understand current Acoustic Backscatter (AB) performance of UVP for characterisation of nuclear suspension in slurry pipe-flows.
- Investigate Machine Learning (ML) methods to improve UVP particle aggregate size and concentration measurements.
- Investigate the effect of large molecular weight polymers on the AB performance of UVP.
- Compare/ combine FBRM measurements to/ with UVP-DUO and ML system.
- Understand influence of discrete size fractions, as well as varying discrete size fraction mixes, and how ML is affected.
- Optimise system to give real-time results for real-time flocculation.

Thank you

Email:
pmjha@leeds.ac.uk

Transformative Science and Engineering for Nuclear Decommissioning

Simulation of behavioural modification effects in particle-laden flows

Computational modelling of interacting polymer additives

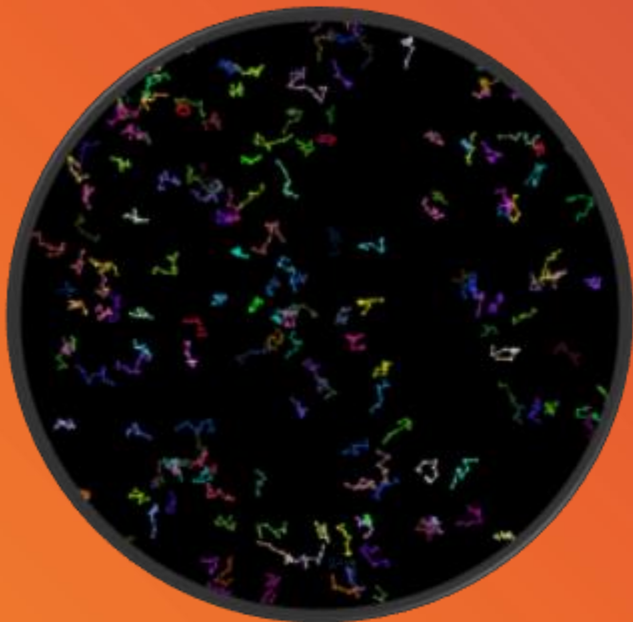

Lee Mortimer, University of Leeds

Prof. Mike Fairweather, University of Leeds

2nd December 2020
Online meeting

TRANSCEND / NDA VIRTUAL CONFERENCE 2020

MOTIVATION

- Waste suspension flows transport legacy material from historic ponds to other interim locations where they are stored safely.
- Present designs perform inefficiently, with the potential for blockages and poor flow conditions.
- Current transportive systems may not function adequately for long timeframes.
- Presence of high flow rates means systems are usually turbulent, leading to complex chaotic behaviour.
- Knowledge must be developed surrounding behaviour of waste sludges.
- Generation of this knowledge will lead to **accurate predictive capabilities** and **enhanced control over multiphase turbulent flows**.

Behavioural modification

DEVELOPMENT OF BEHAVIOURAL MODIFICATION TECHNIQUES

- Use high-fidelity simulation to predict system response to modification-capable properties.
- Temperature, ionic strength, pH, material coating, presence of other phases (particles/polymers), flow rates, turbulence intensity.
- Explore fundamental dynamics surrounding interaction mechanisms such as:

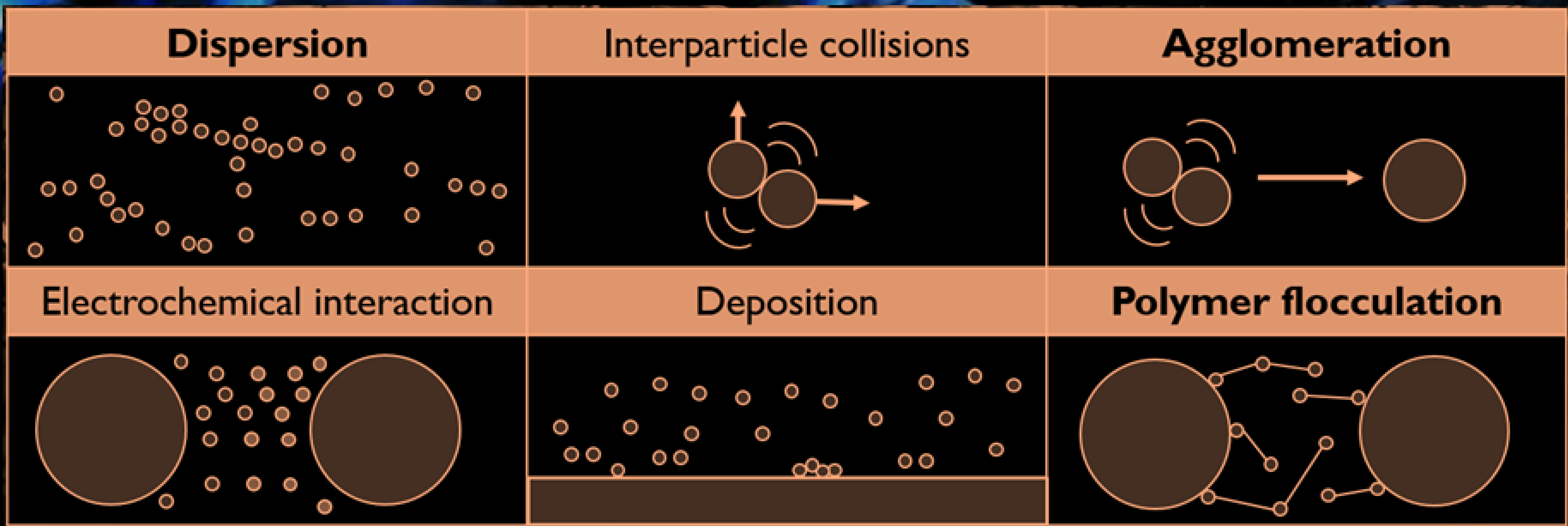

MULTIPHASE FLOW SIMULATION TECHNIQUES

Range of technical tools for both the fluid and particle phases

FLUID PHASE

Direct numerical simulation (DNS):

- All relevant turbulent length and timescales are resolved.
- Accuracy and high-fidelity allows for investigation of fundamental dynamics.
- Computationally intensive but code is parallelised (HPC at Leeds).
- NEK5000 open source spectral element method solver.

PARTICLE PHASE

Lagrangian particle tracking (LPT):

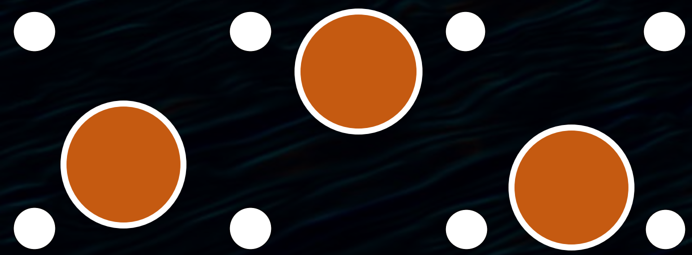

POLYMERIC PHASE

Finitely extensible nonlinear elastic (FENE) bead-spring model

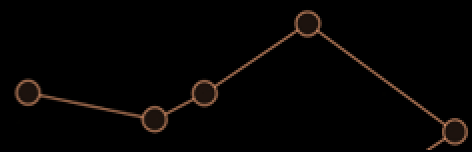

TRANSCEND

Transformative Science and Engineering for Nuclear Decommissioning

POLYMER-LADEN SHEAR AND TURBULENT FLOWS

Computational investigation into the use of polymer additives for beneficial modification of slurry flow behaviour

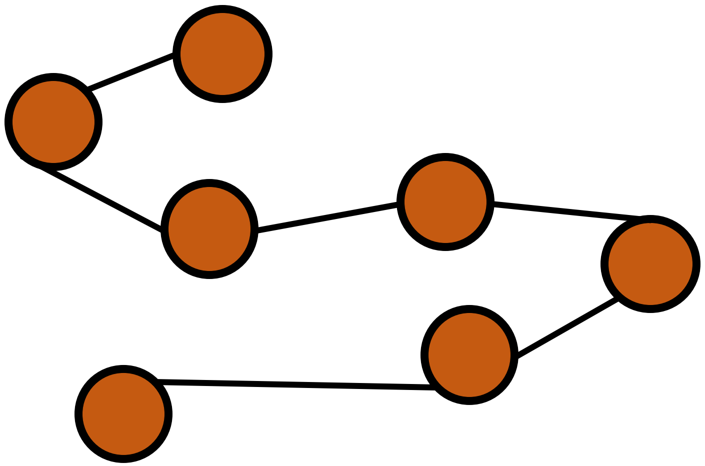

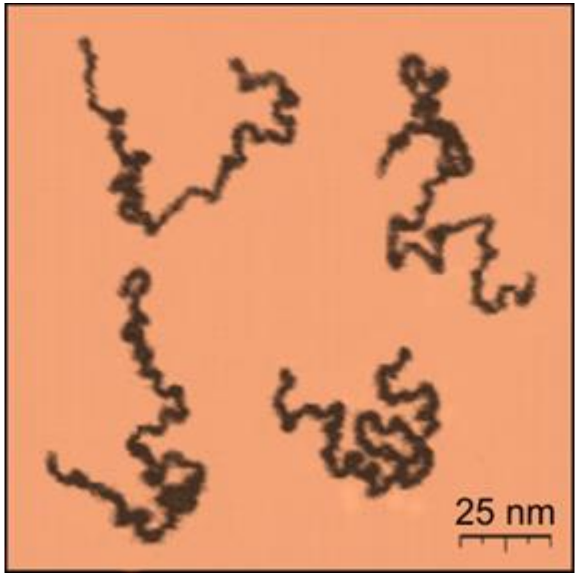

Polymers – a recap

- Polymers are chemical compounds with molecules bonded together in **long repeating chains** of monomers.
- Both **synthesized** and **naturally occurring.**
- Possess **important advantageous properties** surrounding the way in which they interact with both themselves and other materials.
- In the present case, we are interested in how they **interact** and beneficially **modify behaviour** of both the fluid and particles.

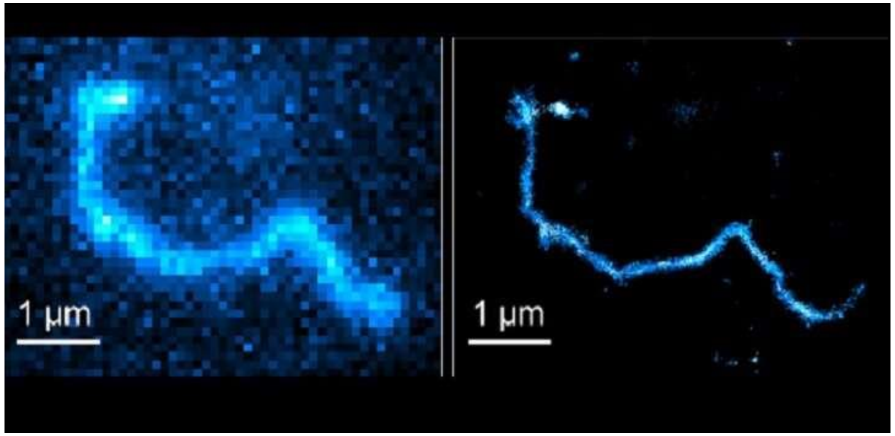

Super-resolution fluorescence microscopy of Lambda DNA.
[Abadi et al. Entangled polymer dynamics beyond reptation, *Nature Communications* (2018).]

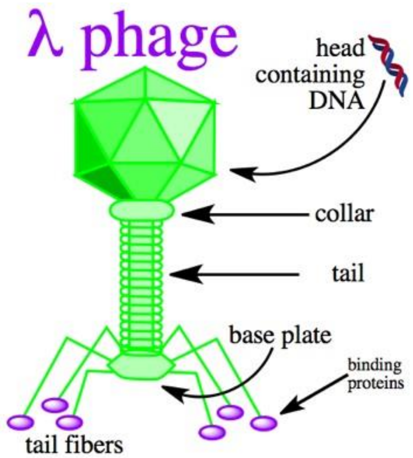

Polymer - fluid interaction

- Addition of high molecular weight polymers to a Newtonian fluid, even at low concentrations (ppm) imparts elasticity to the liquid, which can **dramatically alter the macroscopic flow behaviour**.
- E.g. drag reduction, enhanced pressure drop in porous media, inhibiting jet breakup, spray atomization.
- As polymers stretch in certain flow regions, they generate **localized elastic stresses** within the fluid. This is solved for in the model.

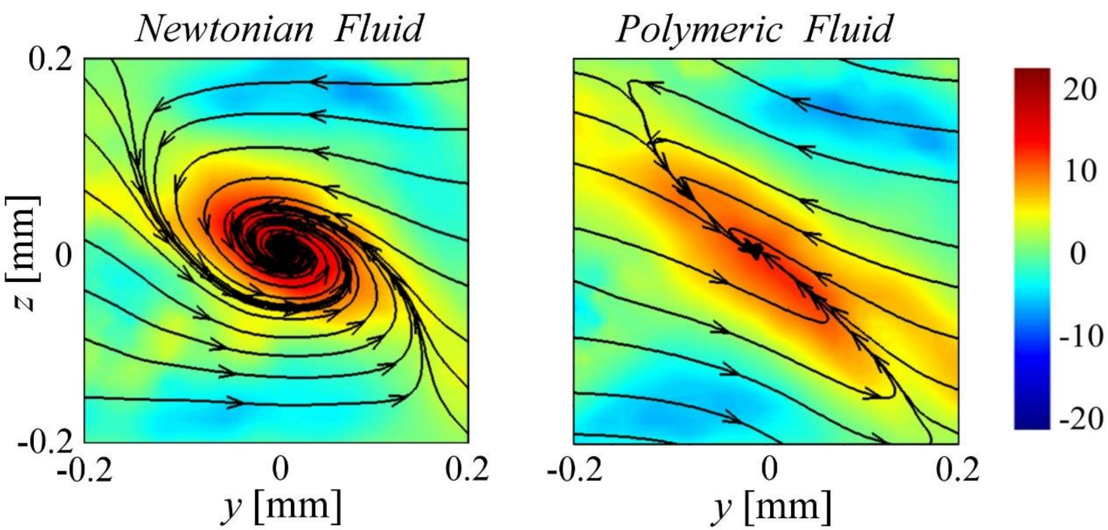

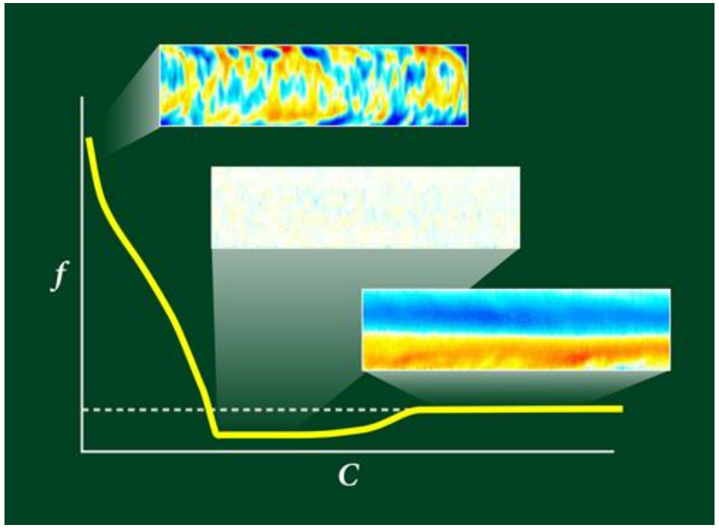

Holzner, M. (2018). Polymers reduce drag more than expected. *Physics*, 11, 29.

Polymer - particle interaction

- Polymer flocculants **induce flocculation** by neutralizing the surface charge of the particles or by forming bridges between individual particles.

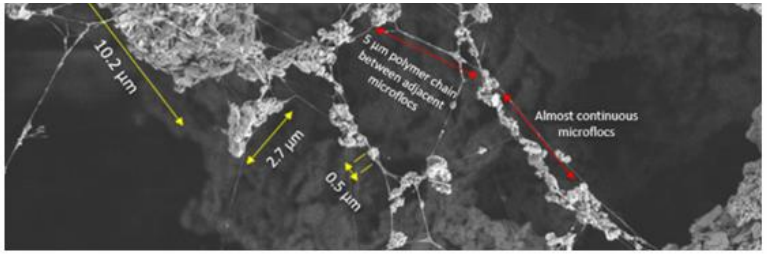

Microstructure of kaolinite floc as revealed by cryo-SEM - Sharma, S., Lin, C. L., & Miller, J. D. (2017). Multi-scale features including water content of polymer induced kaolinite floc structures. Minerals Engineering, 101, 20-29.

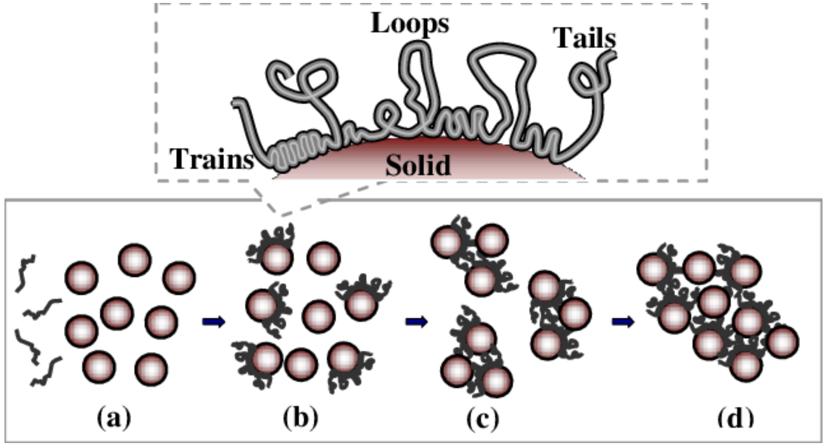

- Adsorption mechanism needs to be modelled, no current techniques available in the literature and so this needs to be developed.

- **Bridging mechanism** will hence be implicit from adsorption.

- Adsorption is determined by attachment process, **hydrophobic** or **electrostatic interaction**.

- Hence attachment mechanism upon collision will rely on **electrochemical properties** of surface of particle and the polymer head / tail.

Polymer modelling: FENE chains

- FENE (finitely extensible nonlinear elastic) chain model represents the polymer as a sequence of beads connected by nonlinear springs.
- Springs used to model individual Kuhn chains

Non-linear spring force

$$\zeta\left[v_0^* + \kappa^* \cdot r_i^* - \frac{\mathrm{d}r_i^*}{\mathrm{d}t^*}\right] + (F_i^* - F_{i-1}^*) + \sqrt{2k_\mathrm{B}T\zeta}\,\frac{\mathrm{d}W_i^*}{\mathrm{d}t^*} = 0$$

Fluid drag

Brownian

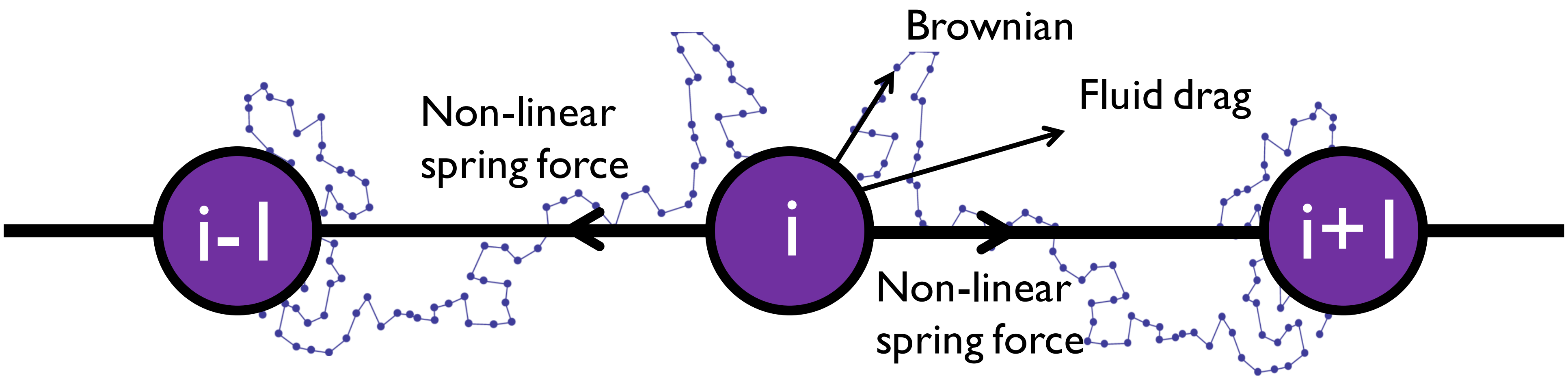

Polymer in equilibrium conditions

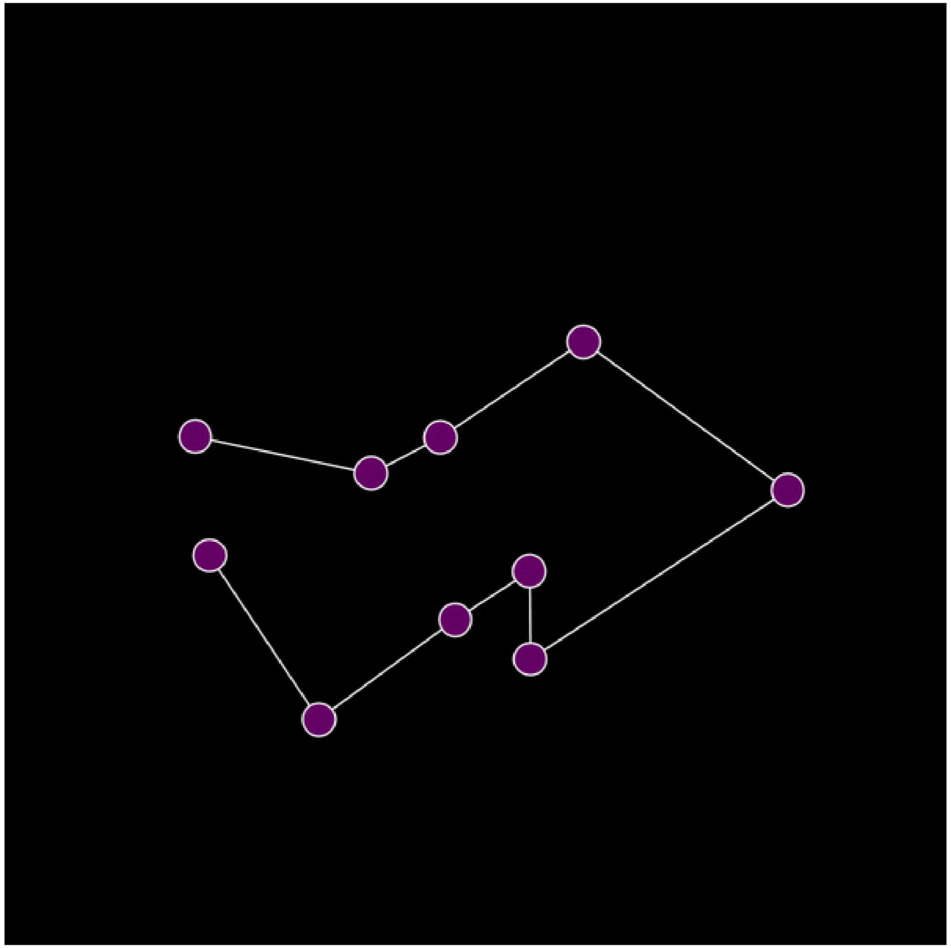

Polymer and system properties for equilibrium simulations

Property	Symbol	Value
Polymer species	-	λ-phage DNA
Contour length (μm)	l	21
Persistence length (μm)	λ_P	0.066
Effective persistence length (μm)	$\lambda_{P,eff}$	0.082
Bead radius (μm)	r_B	0.0693
Fluid dynamic viscosity ($kgm^{-1}s^{-1}$)	μ_F	0.001
Fluid temperature (K)	T	296
Simulation Euler timestep (ms)	Δt	0.01

Ensemble of polymers in equilibrium conditions

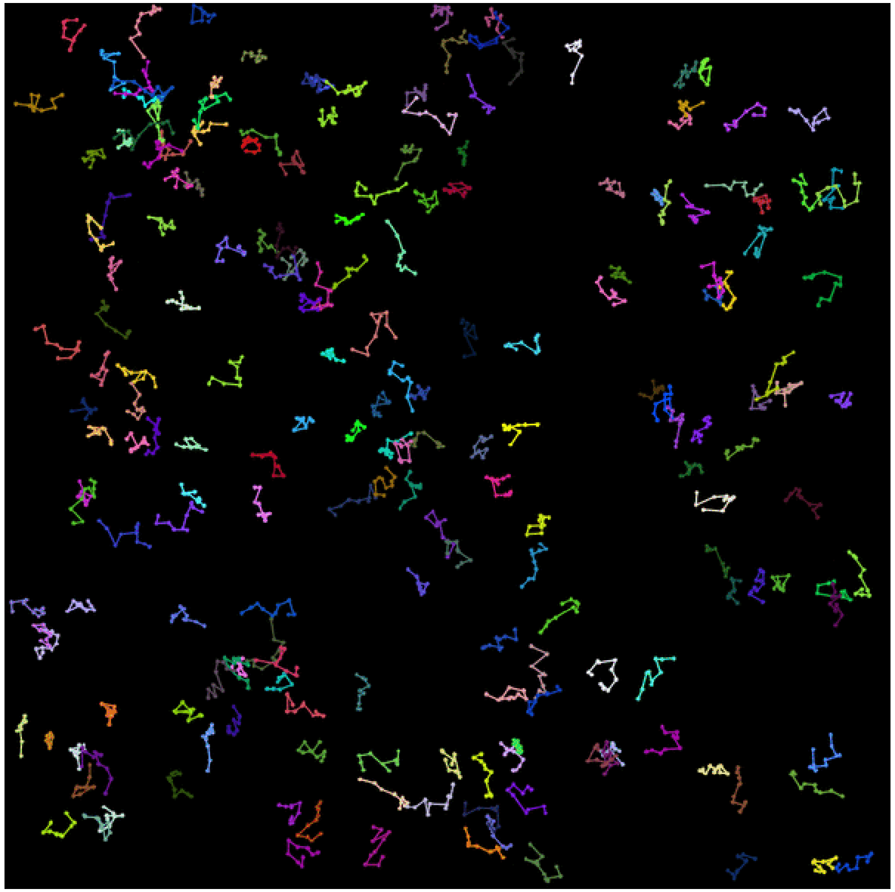

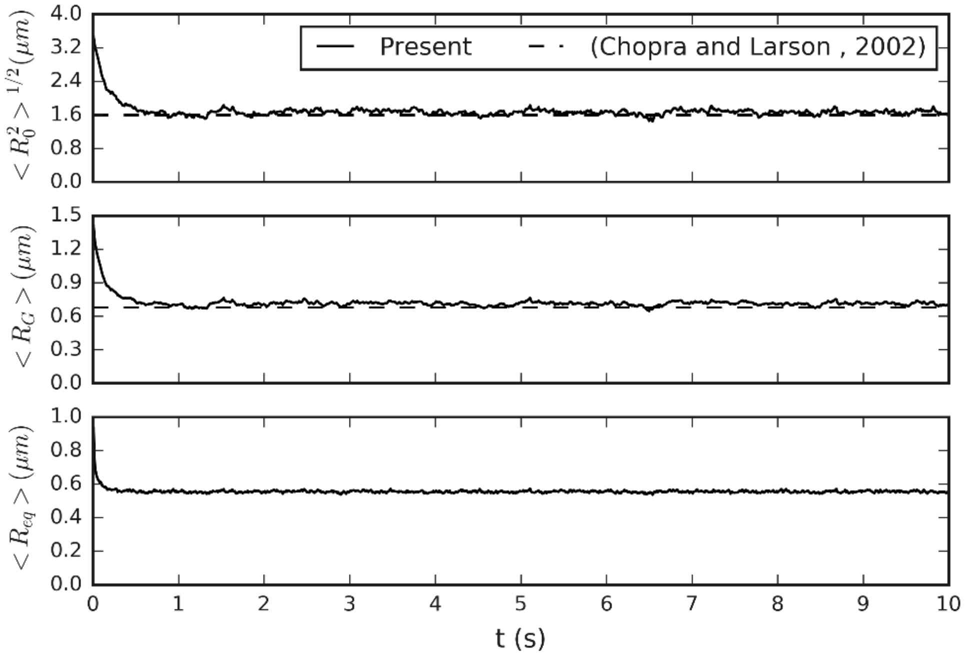

Validation data from M. Chopra and R. G. Larson, *J. Rheol.*, 2002, 46, 831–862

End-to-end distance vector $$< R_0^2 >^{\frac{1}{2}} = \sqrt{\frac{\sum_p \left(\boldsymbol{X}_{N_B,p} - \boldsymbol{X}_{1,p}\right)^2}{N_P}}$$

Radius of gyration $$< R_G^2 >^{\frac{1}{2}} = \sqrt{\frac{\sum_p \frac{\sum_b \left(\boldsymbol{X}_{b,p} - \boldsymbol{X}_{COM,p}\right)^2}{N_B - 1}}{N_P}}$$

Equilibrium stretch $$< R_{eq}^2 >^{\frac{1}{2}} = \sqrt{\frac{\sum_p \frac{\sum_r \boldsymbol{R}^2}{N_B - 1}}{N_P}}$$

Ensemble of polymers under shear flow regime

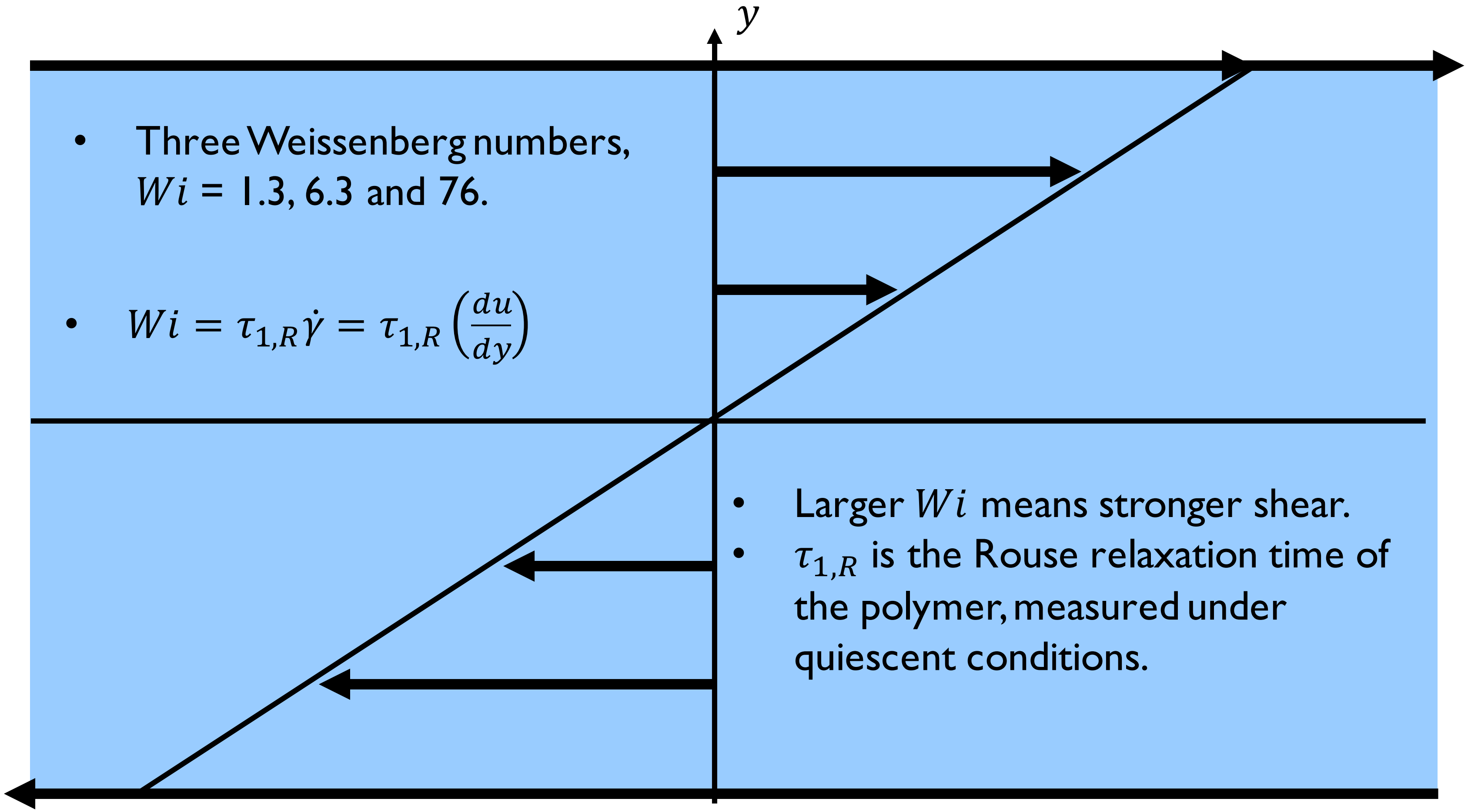

- Three Weissenberg numbers, Wi = 1.3, 6.3 and 76.
- $Wi = \tau_{1,R}\dot{\gamma} = \tau_{1,R}\left(\frac{du}{dy}\right)$

- Larger Wi means stronger shear.
- $\tau_{1,R}$ is the Rouse relaxation time of the polymer, measured under quiescent conditions.

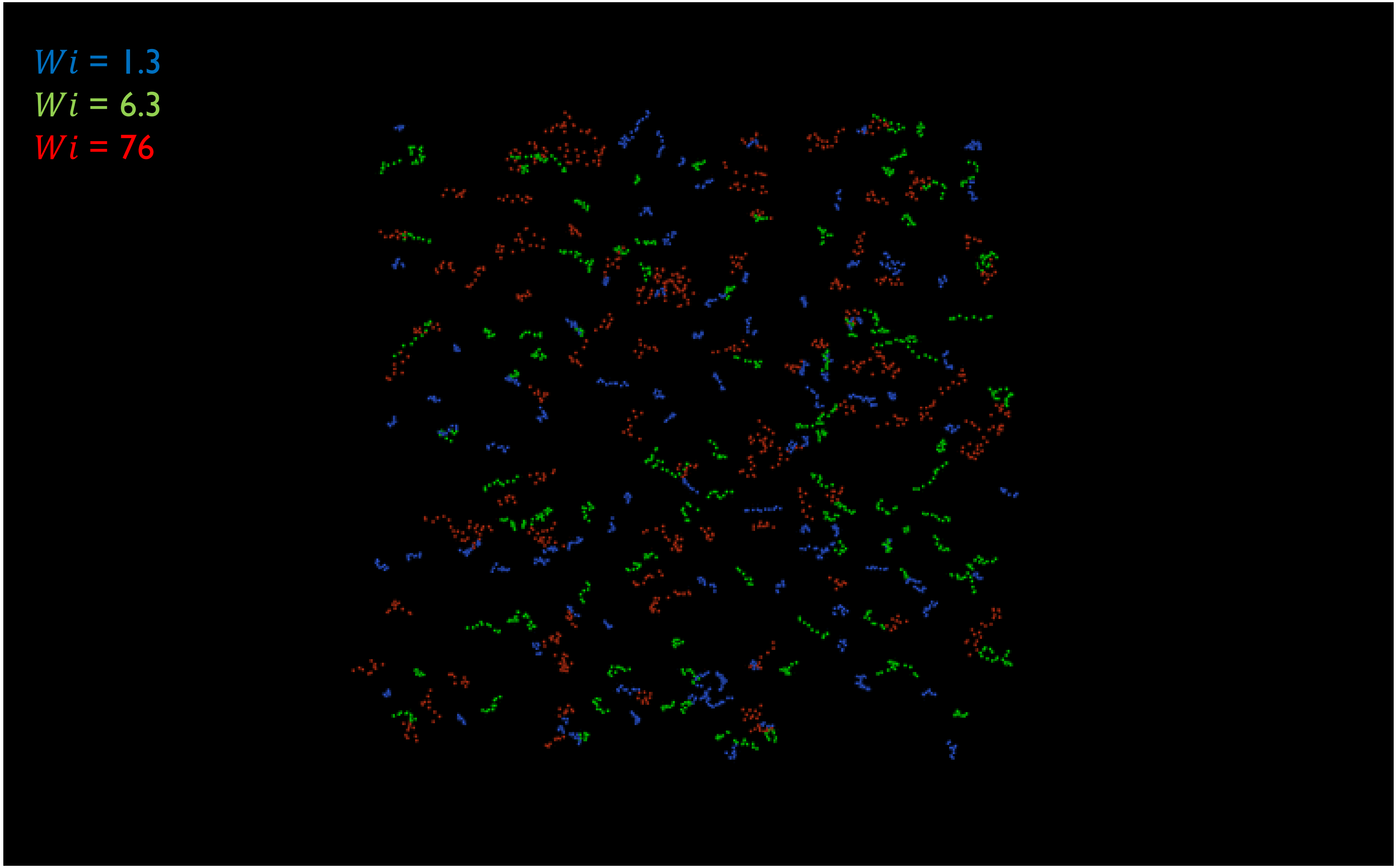
Wi = 1.3
Wi = 6.3
Wi = 76

Ensemble of polymers under shear flow regime - results

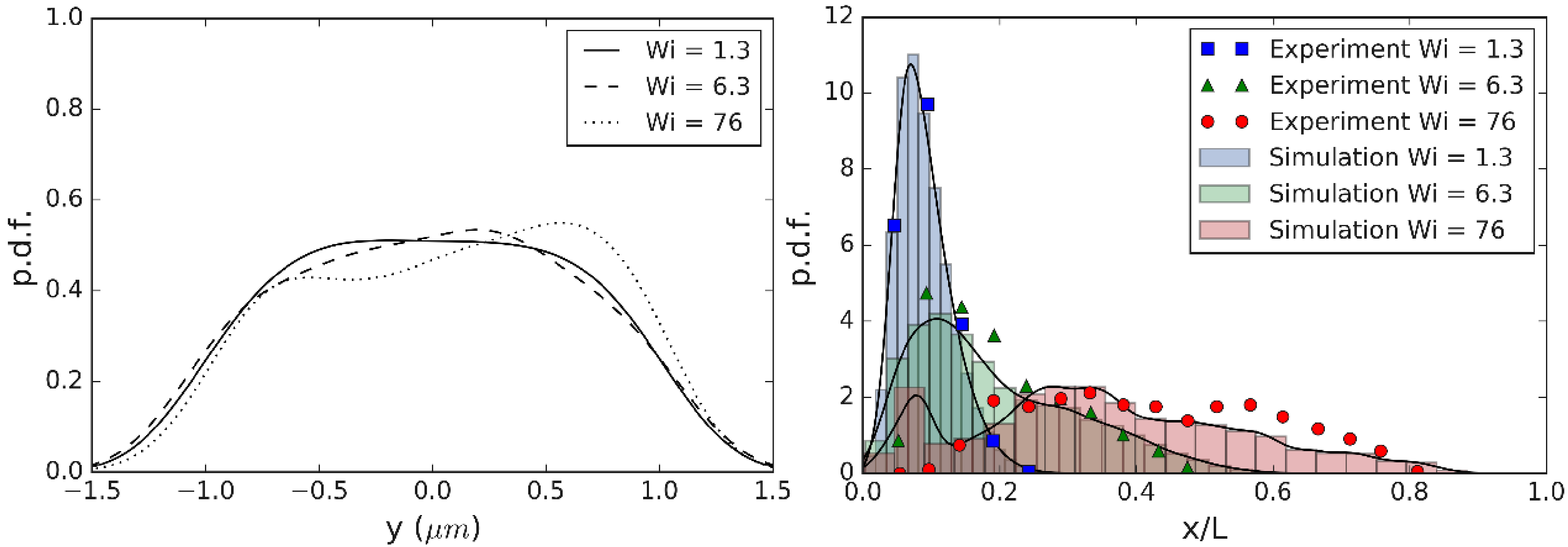

Shear flow simulation for $Wi = 1.3, 6.3$ and 76. Probability distribution functions of bead position within the domain (left) and mean polymer extension (right).

Polymer-fluid interaction

- Stress tensor in Navier-Stokes equations is altered to account for additional contribution from polymers.

$$\frac{\partial u_i}{\partial t} + u_j \frac{\partial u_i}{\partial x_j} = -\frac{1}{\rho_F}\frac{\partial P}{\partial x_i} + \frac{1}{\rho_F}(\tau_{ij}^s + \tau_{ij}^P)$$

$$\tau_{ij}^P = \frac{\mu_P}{\lambda_P}(f(r)c_{ij} - \delta_{ij})$$

$$f(r) = \frac{R_0^2 - 3}{R_0^2 - R^2}$$

$$c_{ij} = 3 < R_i R_j > \frac{1}{< R^2 >_{eq}}$$

R: Spring extension

R_0: Maximum spring extension
$< R^2 >$: Root-mean-square extension for full chain.

μ_P: Polymeric solution viscosity

Polymer-laden turbulent flow

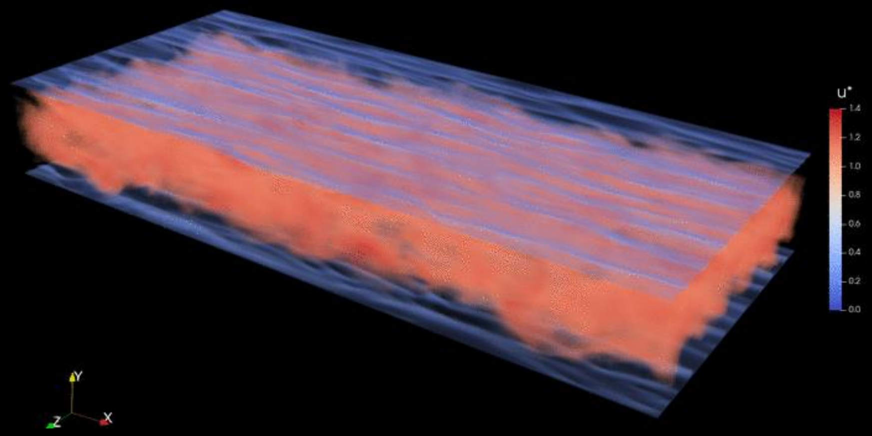

- Ratio of solvent to mixture viscosity, $\beta = 0.9$
- $Re_\tau = 180$

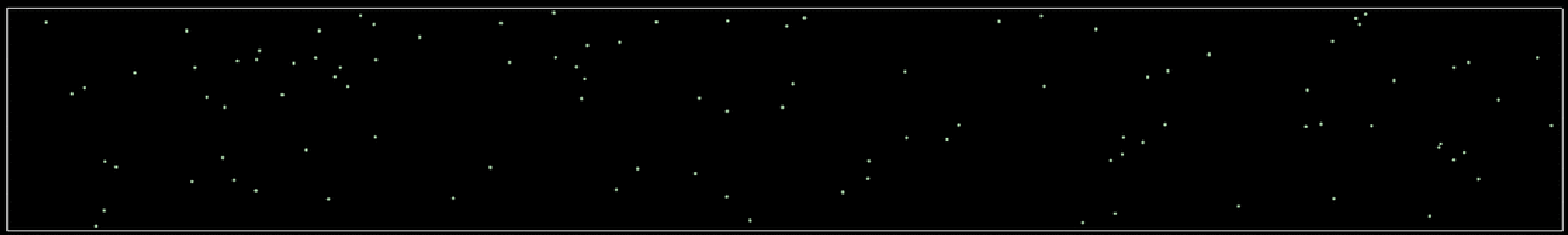

Polymer-laden turbulent flows

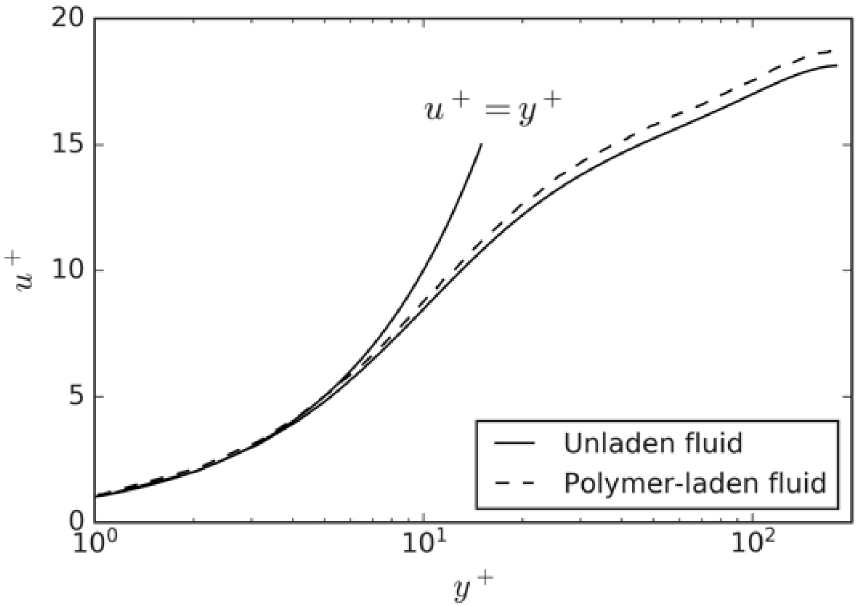

FIG. 3. Mean streamwise velocity normalized by shear velocity, u_τ, for turbulent channel flow at Re_τ=180.

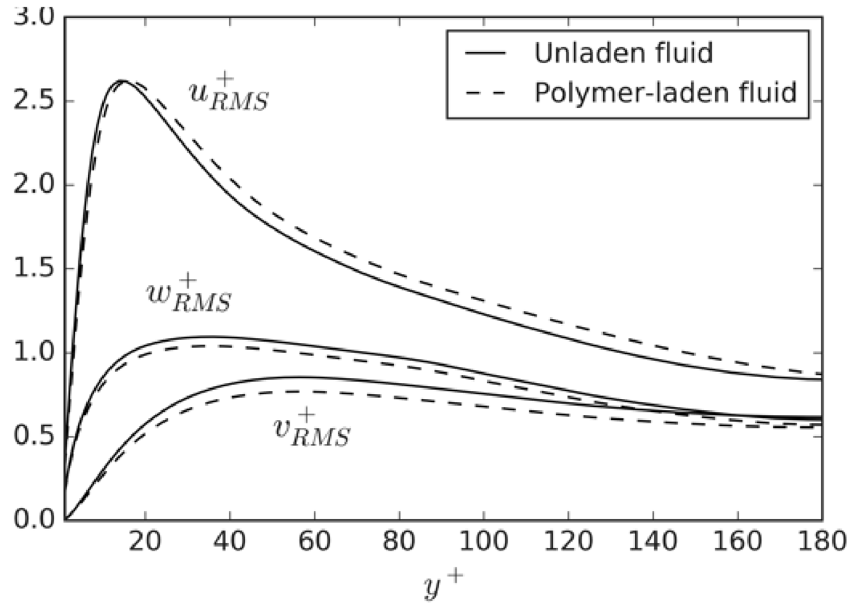

FIG. 4. Root-mean-square of velocity fluctuations normalized by shear velocity, u_τ, for turbulent channel flow at Re_τ=180.

Polymer-laden turbulent flows

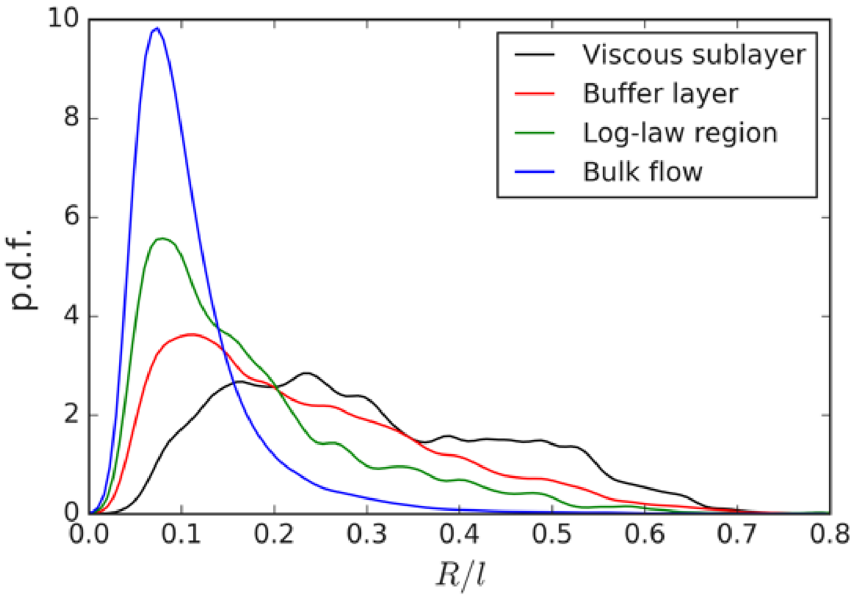

FIG. 5. Probability density distribution functions of mean polymer extension in turbulent channel flow simulation. Comparison of polymers located within individual flow regions.

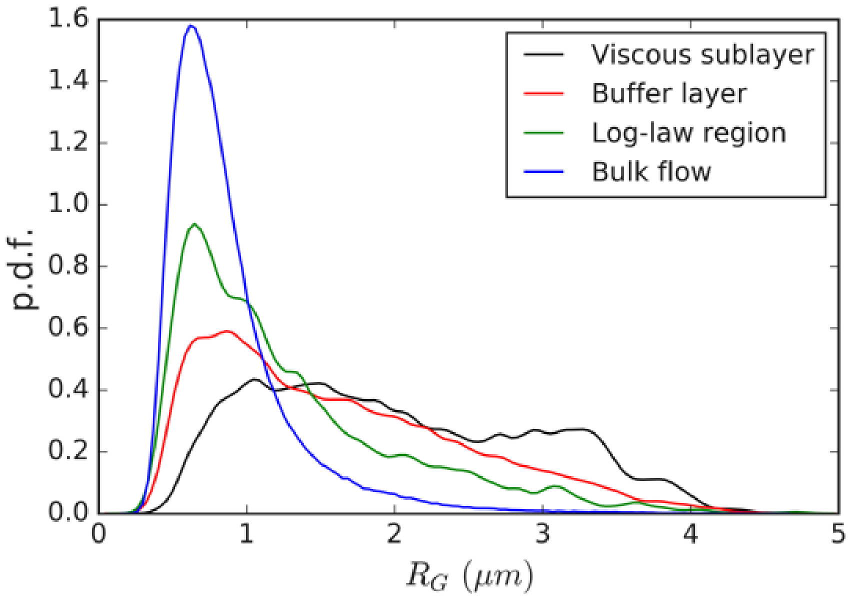

FIG. 6. Probability density distribution functions of mean polymer radius of gyration in turbulent channel flow simulation. Comparison of polymers located within individual flow regions.

Polymer-particle interaction

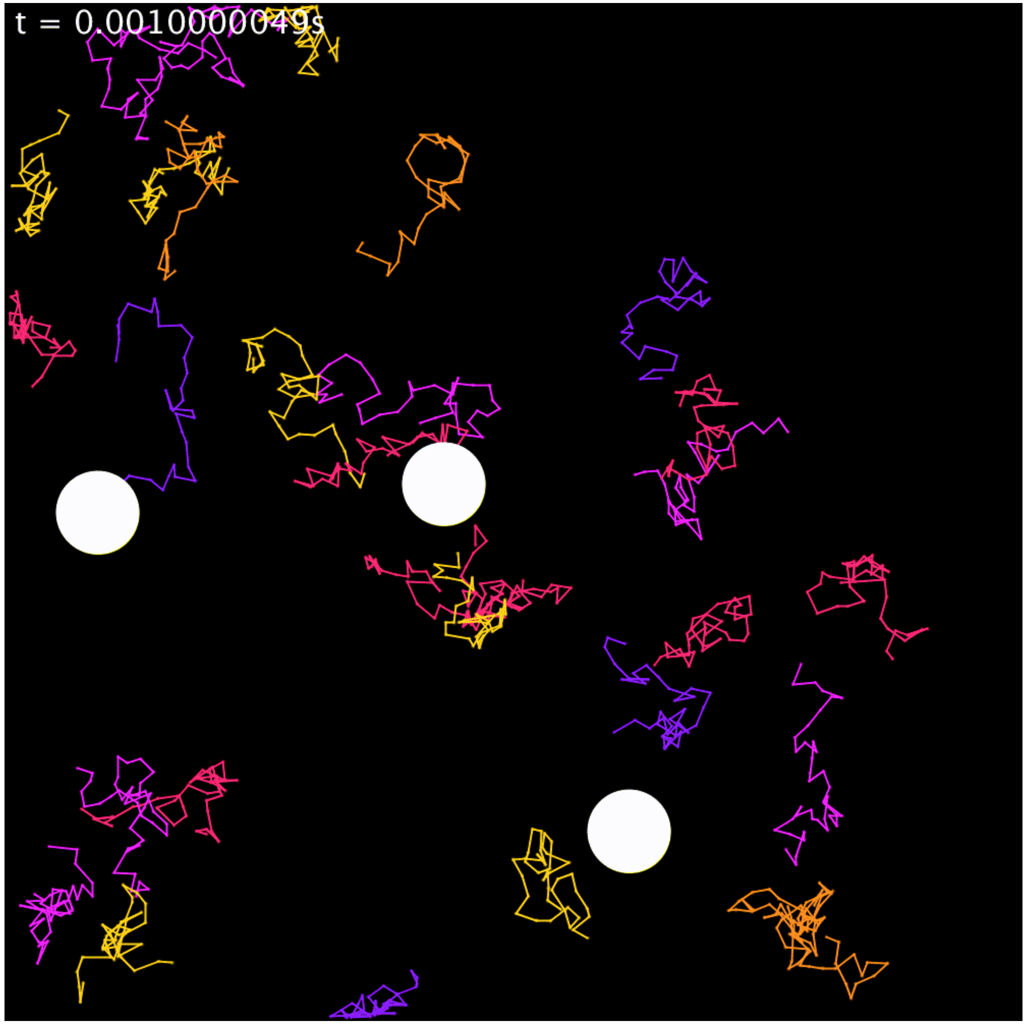

- Adsorption mechanism activates upon collision of bead with particle.
- Bead-spring force is two-way coupled with particle, with restoring force also exerted on particles.

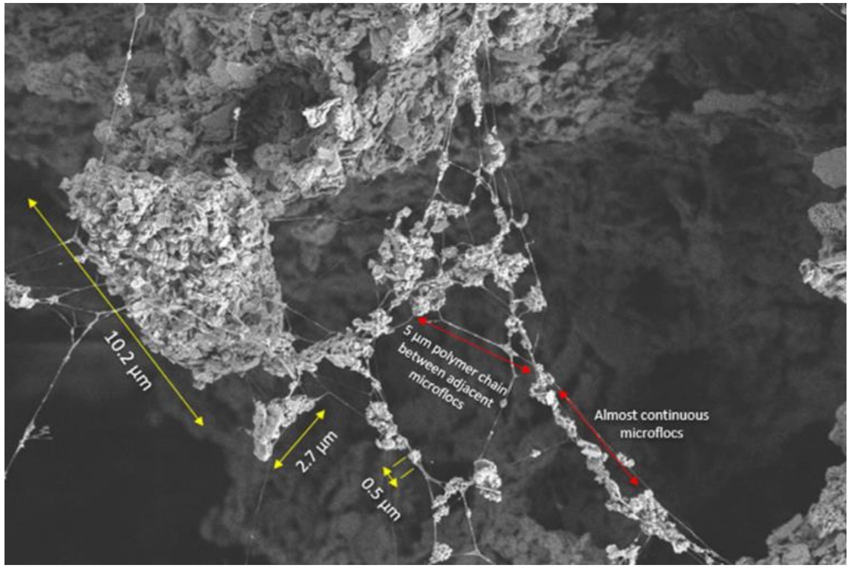

Microstructure of kaolinite floc as revealed by cryo-SEM - Sharma, S., Lin, C. L., & Miller, J. D. (2017). Multi-scale features including water content of polymer induced kaolinite floc structures. Minerals Engineering, 101, 20-29.

Conclusions & further work

- FENE bead-spring polymer model has been developed and implemented in Nek5000, an open-source spectral-element based solver.
- After having validated the polymer dynamics in a simple quiescent case and a shear flow, a turbulent channel flow simulation was performed at $Re_\tau = 180$ which predicts mean and rms velocity fluctuations typical of a drag-reduced flow.
- We also observe how the various regions of the channel affect the deformation of the polymer chain such that polymers in the wall-region are more stretched and possess larger radii of gyration than their bulk flow counterparts.
- Polymer-particle interaction mechanism has been implemented and tested, with preliminary simulations exhibiting similar behaviour to that shown in experiments.
- This mechanism is now being used in a channel flow to determine the effects of polymer additives on flow mechanisms such as dispersion, deposition and agglomeration.

Other work on behavioural modification

Pending submission:

Mortimer, L. F. and Fairweather, M., TBC. Development of behavioural modification techniques through simulation of binary particle agglomeration events in isotropic turbulence.

Published:

Mortimer, L. F. and Fairweather, M., 2020. Density ratio effects on the topology of coherent turbulent structures in two-way coupled particle-laden channel flows. *Physics of Fluids*, *32*(10), p.103302. doi: 10.1063/5.0017458

Mortimer L. F., Njobuenwu D. O. , Fairweather M. 2020. Agglomeration dynamics in liquid–solid particle-laden turbulent channel flows using an energy-based deterministic approach. *Physics of Fluids.* 32.4 doi: 10.1063/5.0001596

Mortimer L. F., Njobuenwu D. O. , Fairweather M. 2019. Near-wall dynamics of inertial particles in dilute turbulent channel flows. *Physics of Fluids.* 063302-1-063302-19 31.6 doi:10.1063/1.5093391

Acknowledgements

This work is supported by a UK Engineering and Physical Sciences Research Council grant at the University of Leeds from the TRANSCEND (Transformative Science and Engineering for Nuclear Decommissioning) project.

EPSRC
Engineering and Physical Sciences
Research Council

TRANSCEND

Thank you for your attention!

Transformative Science and Engineering for Nuclear Decommissioning

Thank you

&

Questions?

Dr. Lee Mortimer
PhD, MPhys
Research Fellow
Office 2.22 Chemical and Process Engineering Building
School of Chemical and Process Engineering
University of Leeds
l.f.mortimer@leeds.ac.uk

Analysis of a Titanosilicate glass series – at least, what the pandemic has permitted

Lucas-Jay Woodbridge, University of Sheffield

Transcend theme meeting, integrated waste management

Date: 02/12/20
Location: Mainly Oregon, Iowa and the Carolinas

Analysis of a Titanosilicate glass series – at least, what the pandemic has permitted

Lucas-Jay Woodbridge*

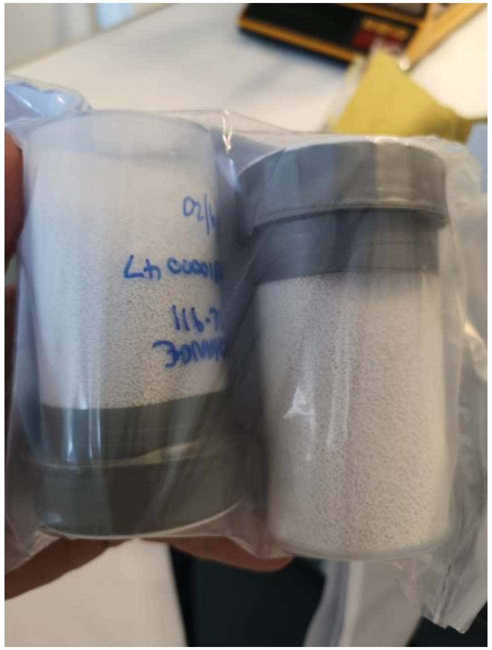

Ionsiv IE-911 received from NIS ltd (Tony Kay)

Powered respirator – image from arco.co.uk

*lwoodbridge1@Sheffield.ac.uk

Re-visiting the glasses

- Why this chemistry
- Vitrification[1]
- Glass success

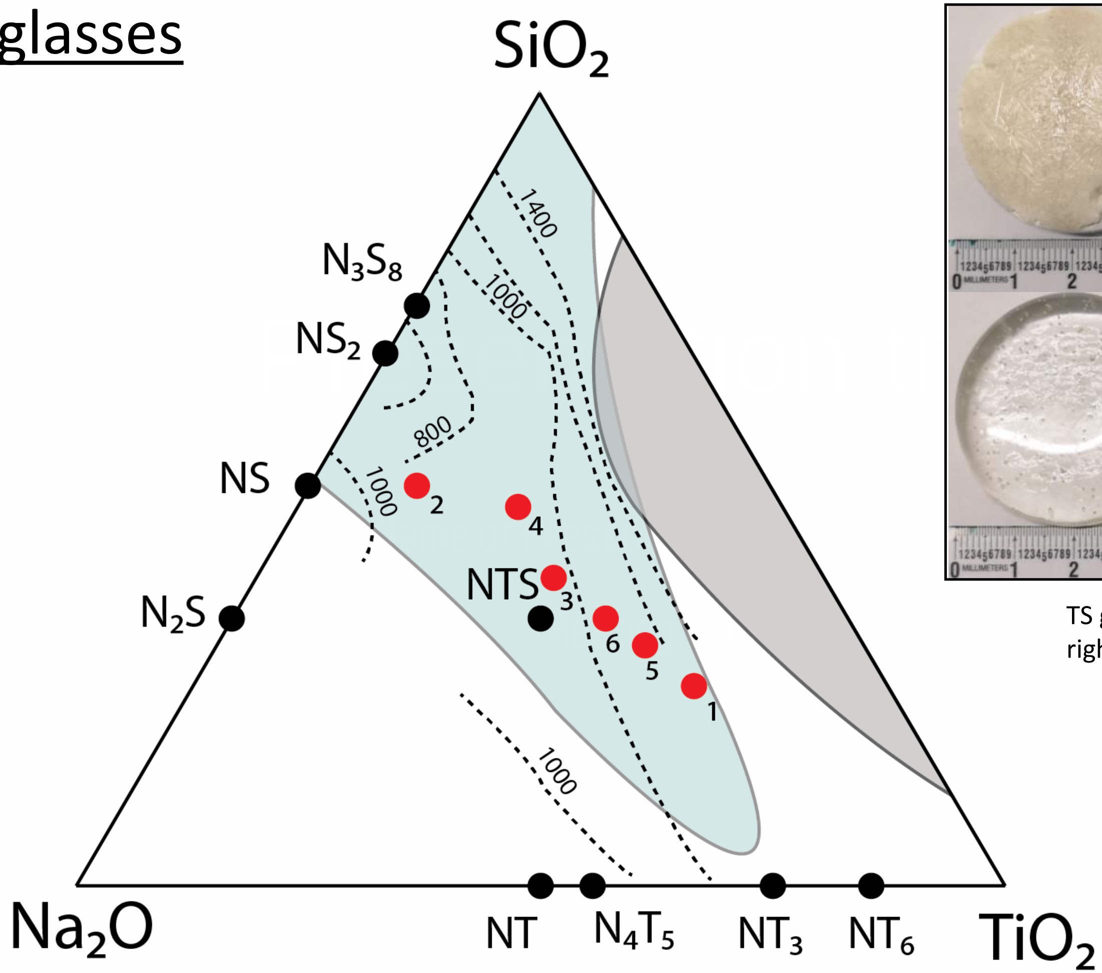

TS glass series stoichiometry plotted on ternary phase diagram[1]

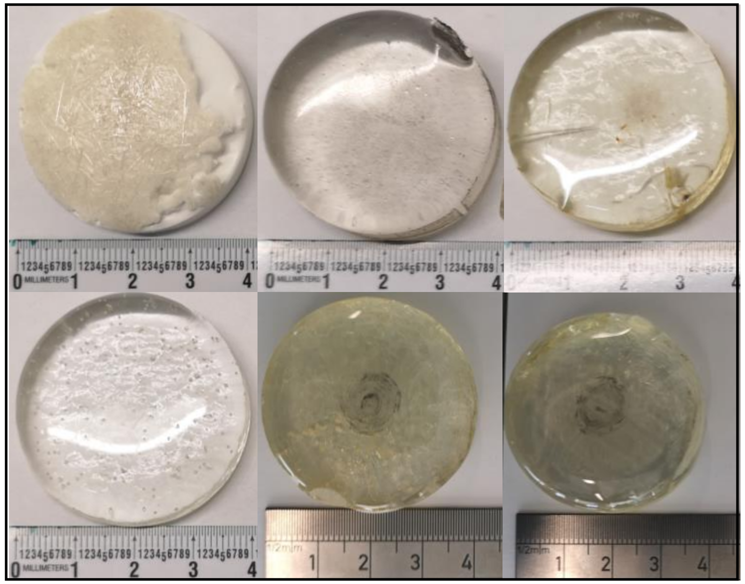
TS glass series 1-6 (top left to bottom right)

The original material

- Framework Titanosilicate[2]
- Ionsiv-IE911[3]

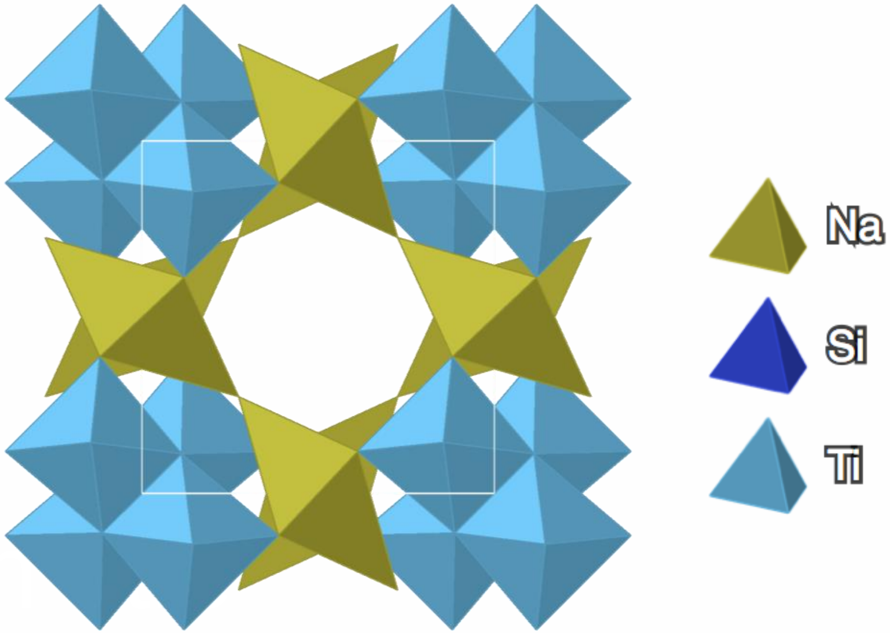

C-axis view of Ionsiv IE-911[4]

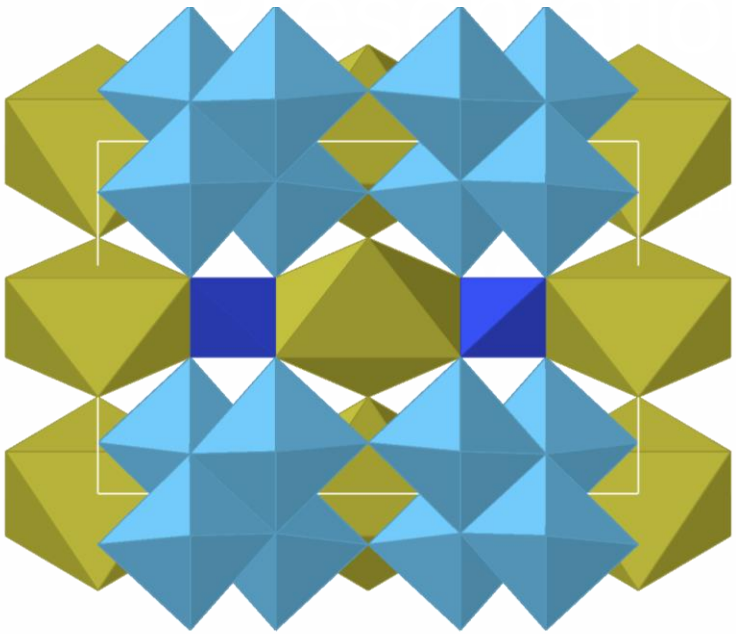

B-axis view of Ionsiv IE-911[4]

Ion exchange mechanism

- Ion exchange [3,5,6]
- Protonation step[5]
- Final uptake[5]

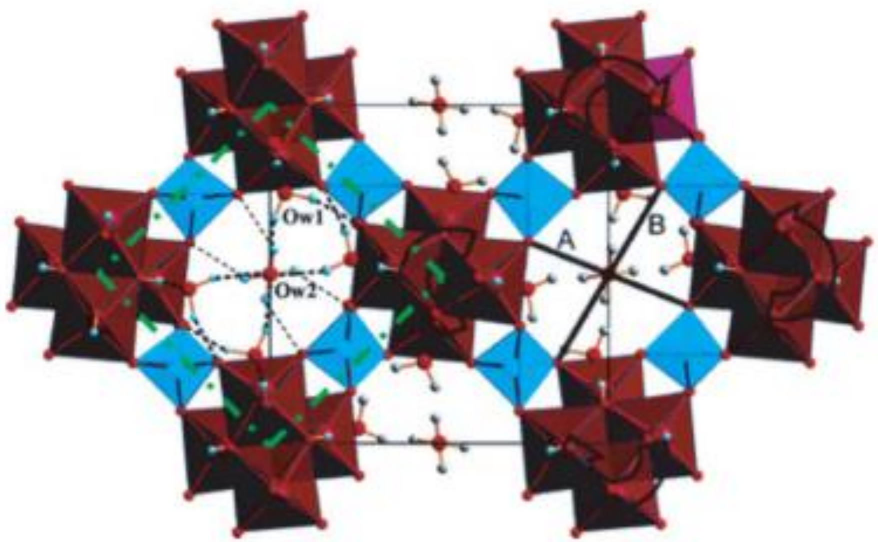

Protonated form of a framework titanosilicate[5]

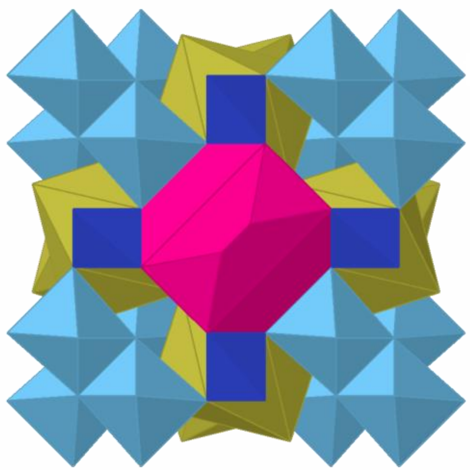

C-axis view of Ionsiv IE-911 with Cs in tunnel structure[4]

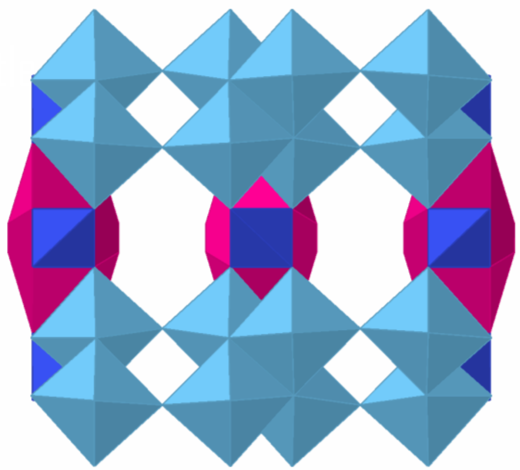

B-axis view of Ionsiv IE-911 with Cs in tunnel structure[4]

Transformative Science and Engineering for Nuclear Decommissioning

XRD of glasses

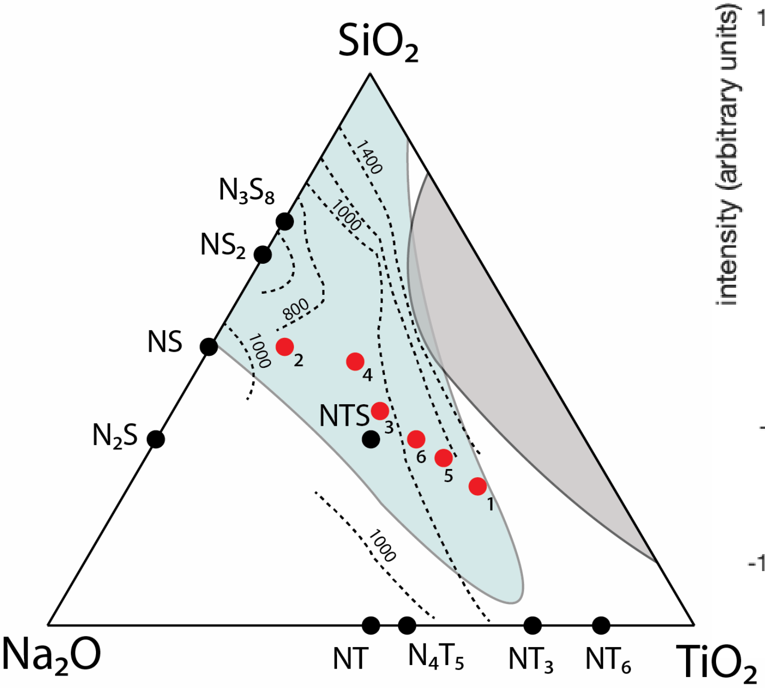

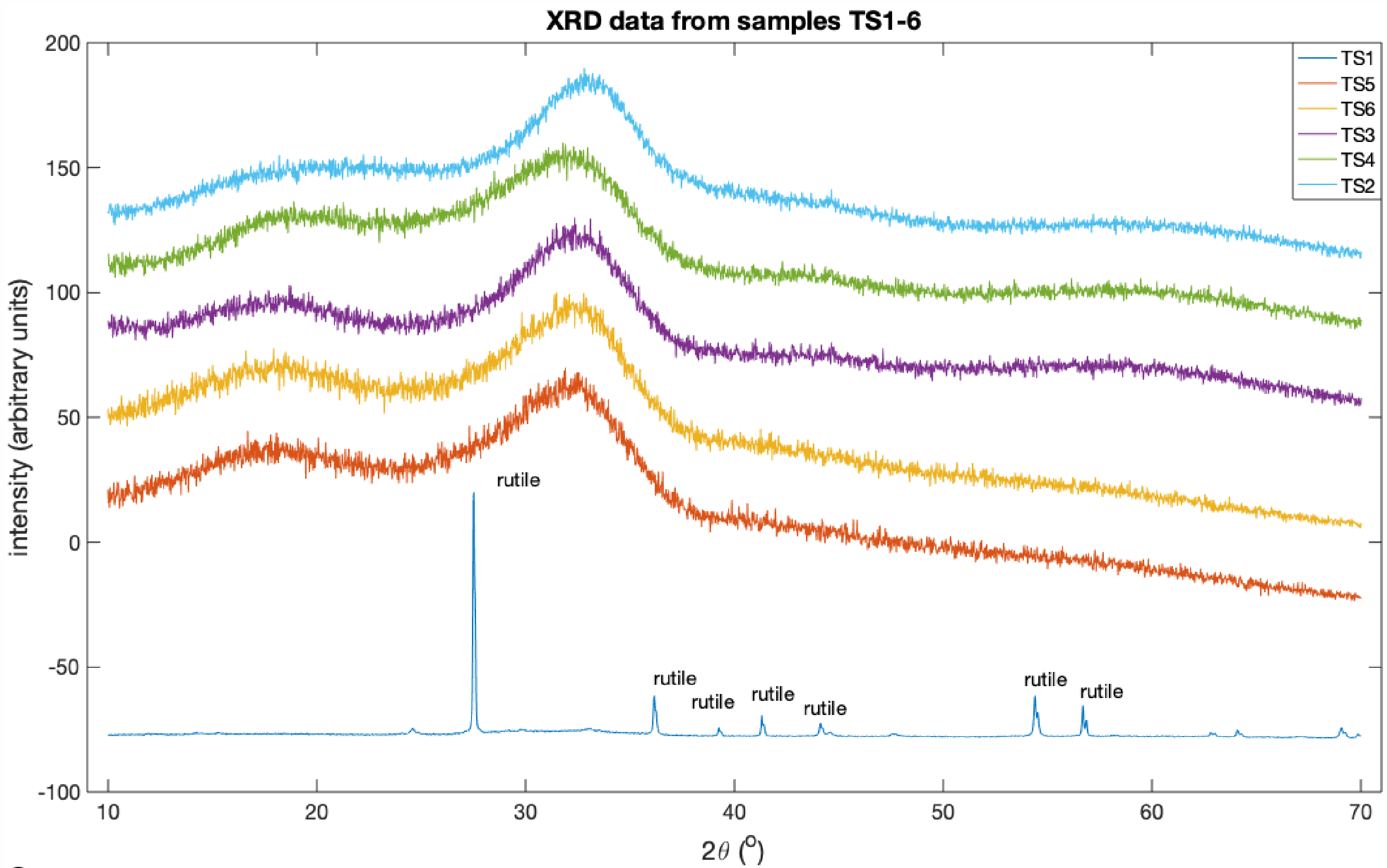

Thermal analysis of glasses

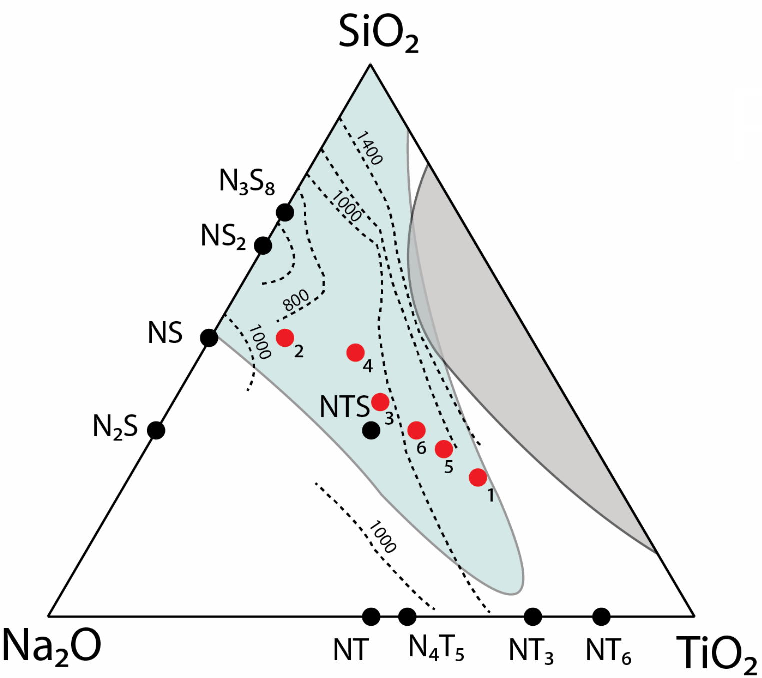

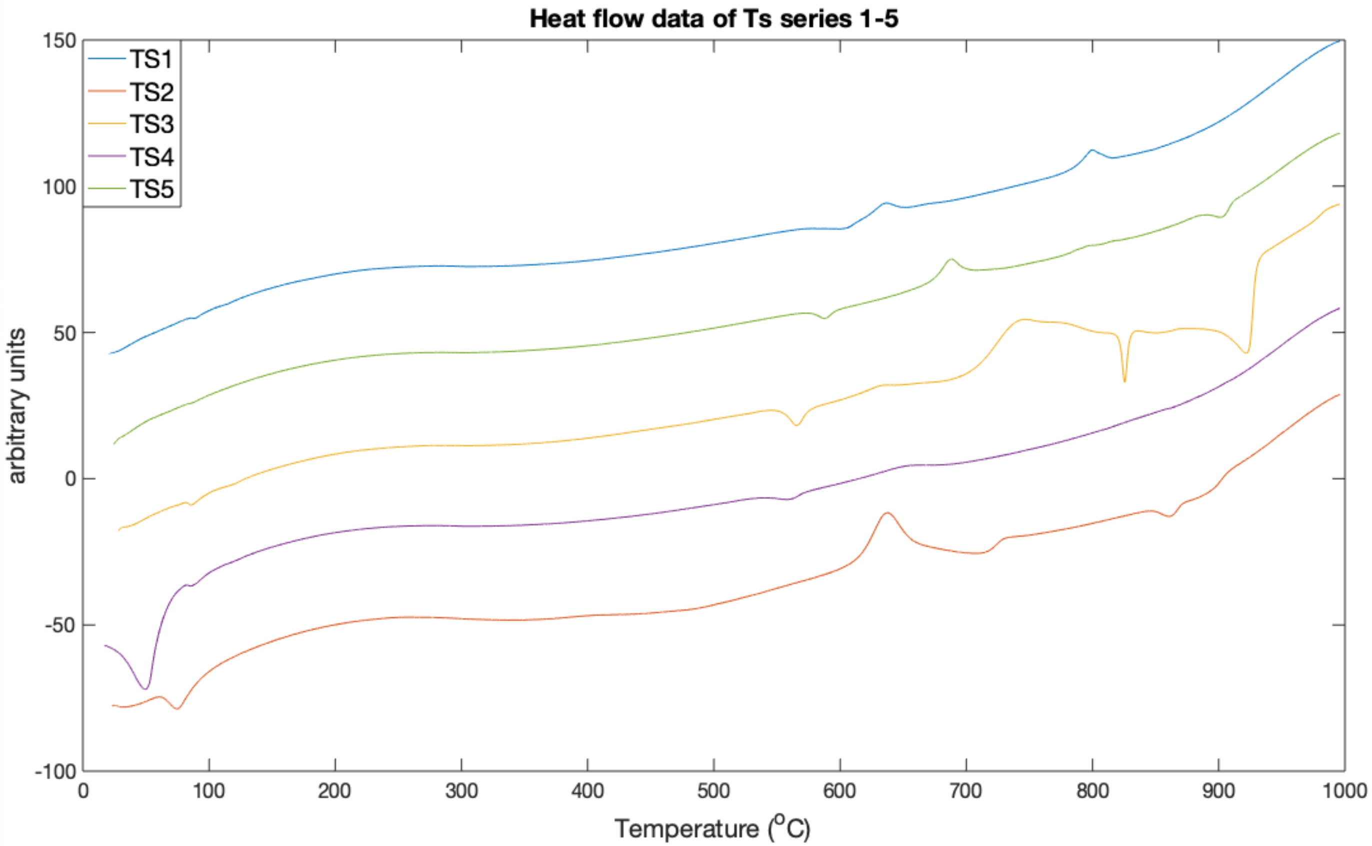

Thermal analysis of glasses

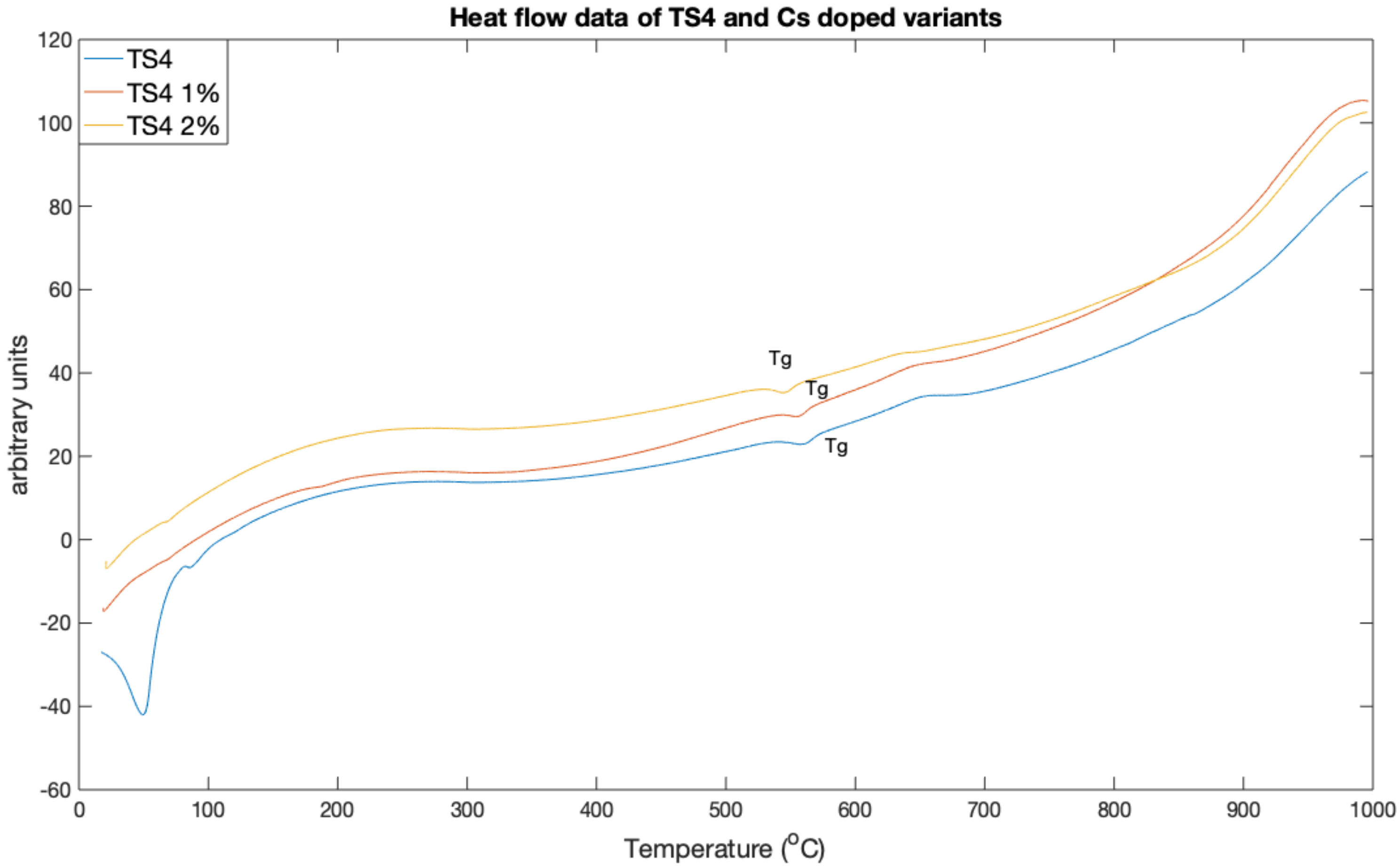

Plan going forward

- Melts
- Raman
- Verify Thermal data
- XAFS, XANES
- XRF
- Load Ionsiv and repeat

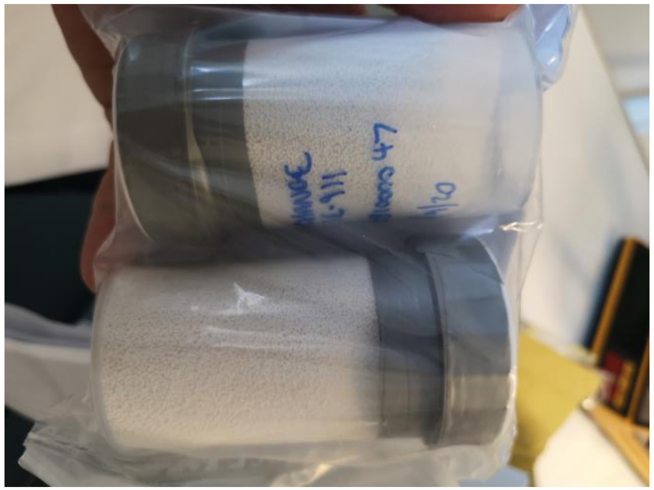

TRANSCEND

Transformative Science and Engineering for Nuclear Decommissioning

Acknowledgements

"This research utilised the HADES / MIDAS facility at The University of Sheffield established with financial support from EPSRC and BEIS, under grant EP/T011424/1."

References

1) Glass formation in silicates: Insights from composition – Pascal Richet, Mathieu Roskosz & Jacques Roux – 2006
2) Review Titanosilicates in cation adsorption and cation exchange-A review - Oleksiienko, Olga, Wolkersdorfer, Christian, Sillanpää, Mika - 2017
3) Optimization of Nb-substitution and Cs + /Sr +2 ion exchange in crystalline silicotitanates (CST) - S. Chitra, R. Sudha, S. Kalavathi, A. G. S. Mani, S. V. S. Rao, P. K. Sinha – 2013
4) Tripathi, A., Medvedev, D. G., Nyman, M. & Clearfield, A. Selectivity for Cs and Sr in Nb-substituted titanosilicate with sitinakite topology. in *Journal of Solid State Chemistry* vol. 175 72–83 (Academic Press Inc., 2003).
5) The origin of ion exchange selectivity in a porous framework titanium silicate - Celestian, Aaron J., Clearfield, Abraham – 2007
6) Evaluation of synthetic inorganic ion exchangers for cesium and strontium removal from contaminated groundwater and wastewater - Anatoly I. Bortun , Lyudmila N. Bortun & Abraham Clearfield - 1997

Transformative Science and Engineering for Nuclear Decommissioning

Thank you

lwoodbridge1@Sheffield.ac.uk

Transformative Science and Engineering for Nuclear Decommissioning

Generation and Transport of Radiolytic Hydrogen in Hydroxide Sludges

Mel O'Leary, DCF, The University of Manchester

NDA Transcend Conference

Energy
For a Low Carbon Future

Introduction

Experimental Setup

Transport Measurements

Bubbles

Conclusions

Mel O'Leary Email: mel.oleary@manchester.ac.uk

Transformative Science and Engineering for Nuclear Decommissioning

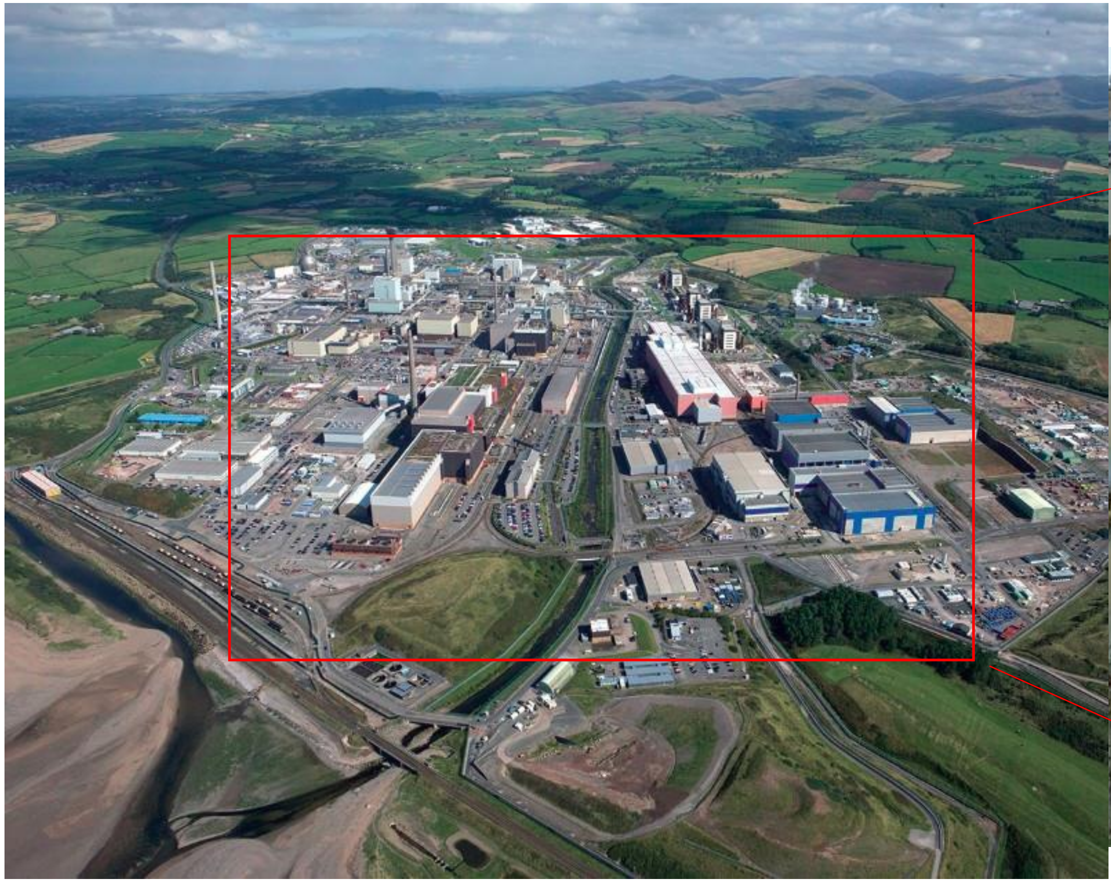

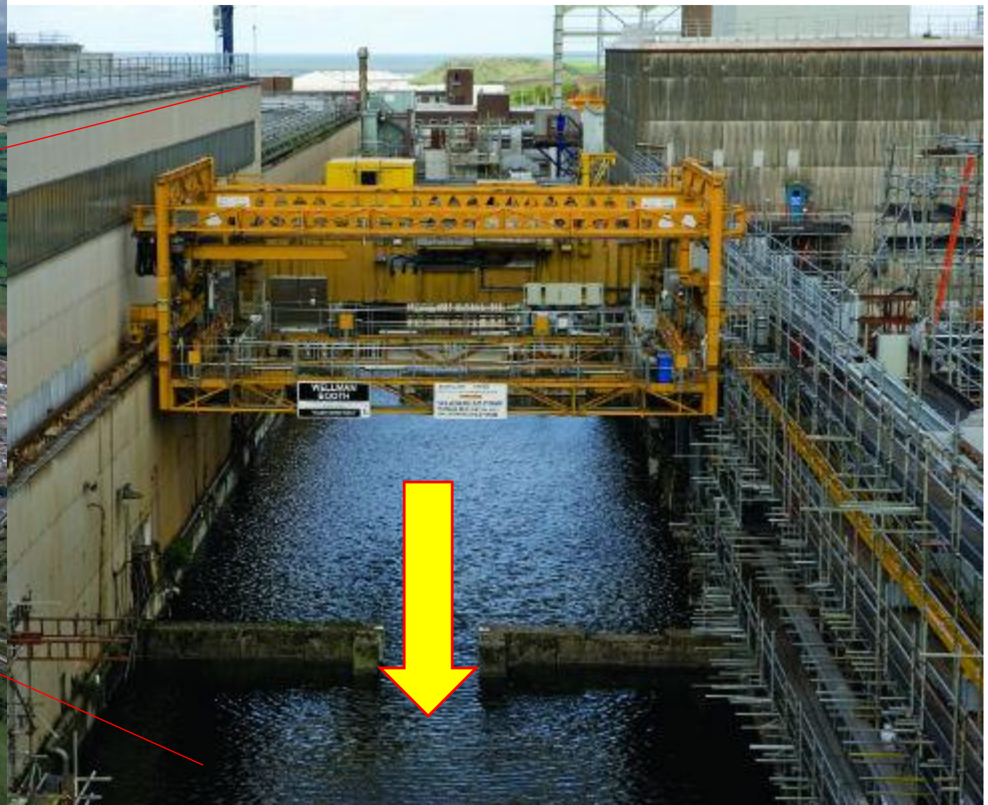

Mel O'Leary Email: mel.oleary@manchester.ac.uk

Experimental Setup

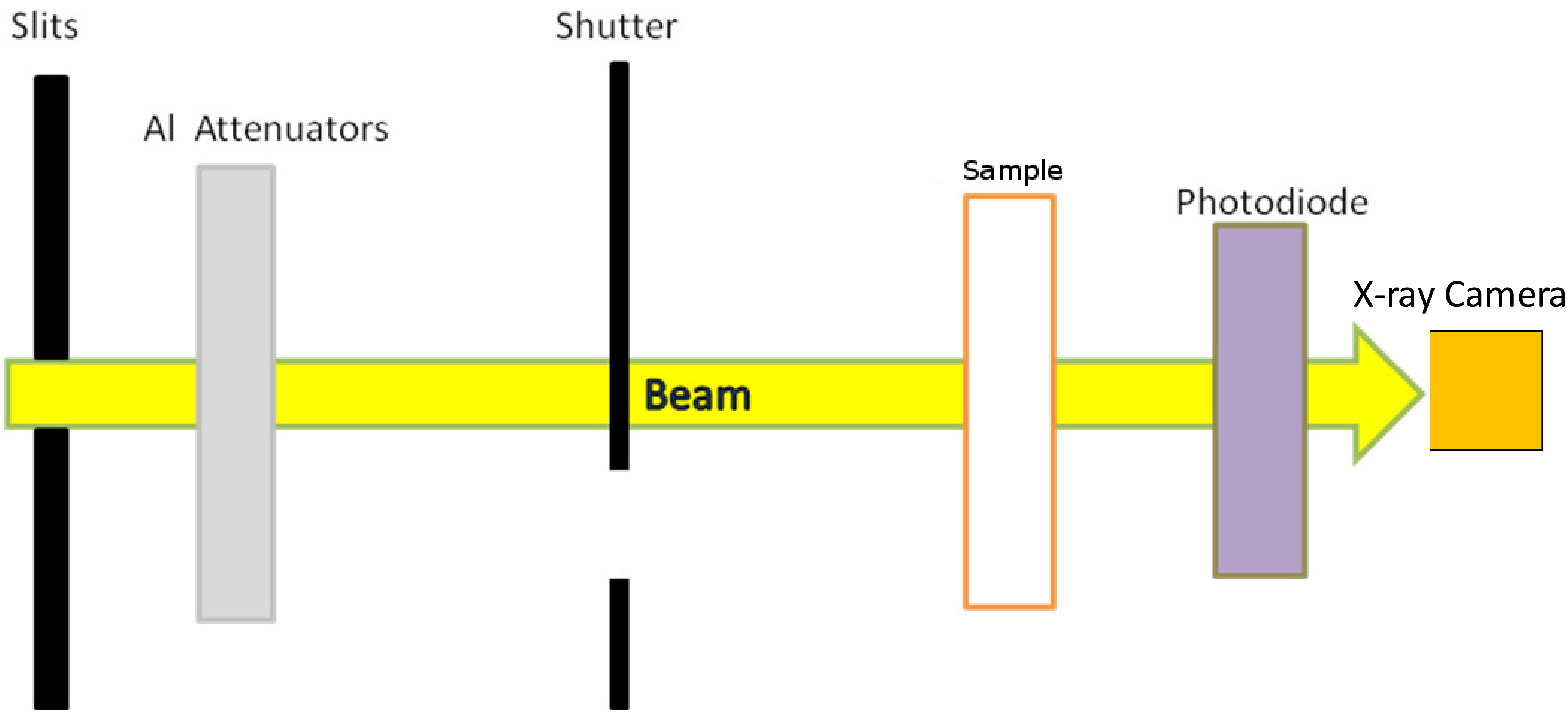

Mel O'Leary Email: mel.oleary@manchester.ac.uk

Irradiation

diamond

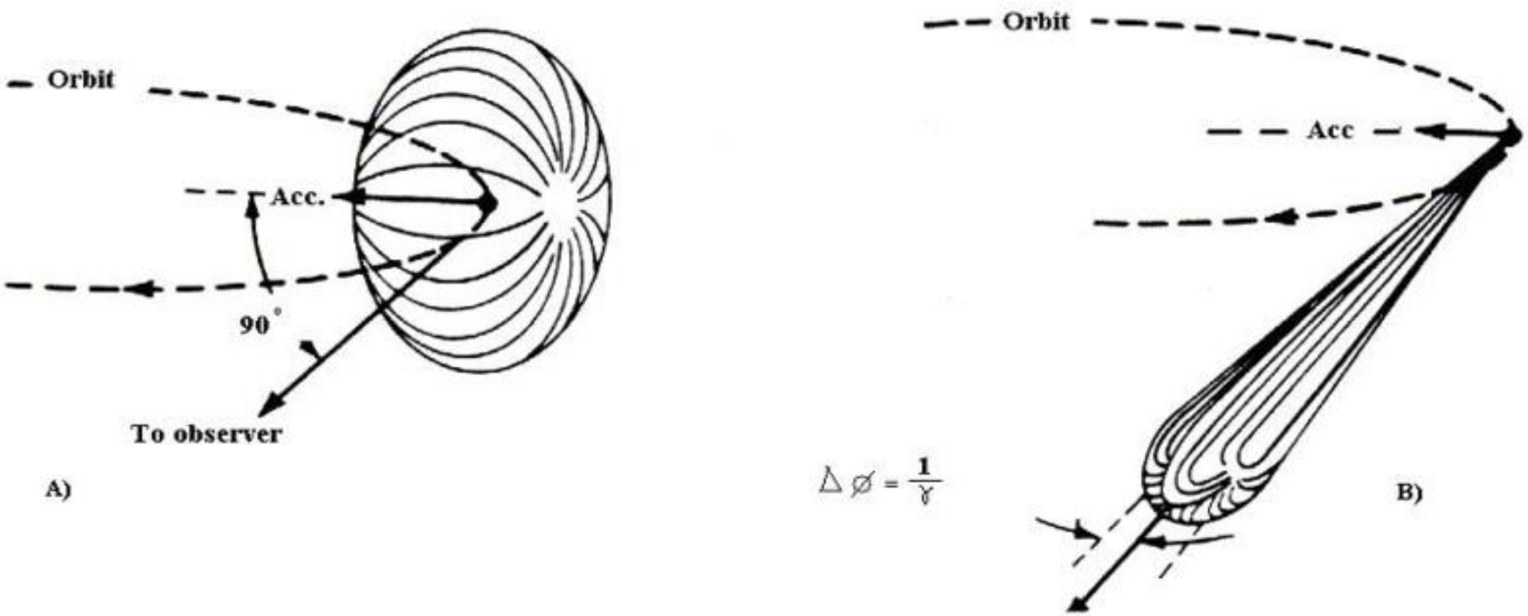

Highly collimated intense beam

Mel O'Leary Email: mel.oleary@manchester.ac.uk

Transformative Science and Engineering for Nuclear Decommissioning

Irradiation

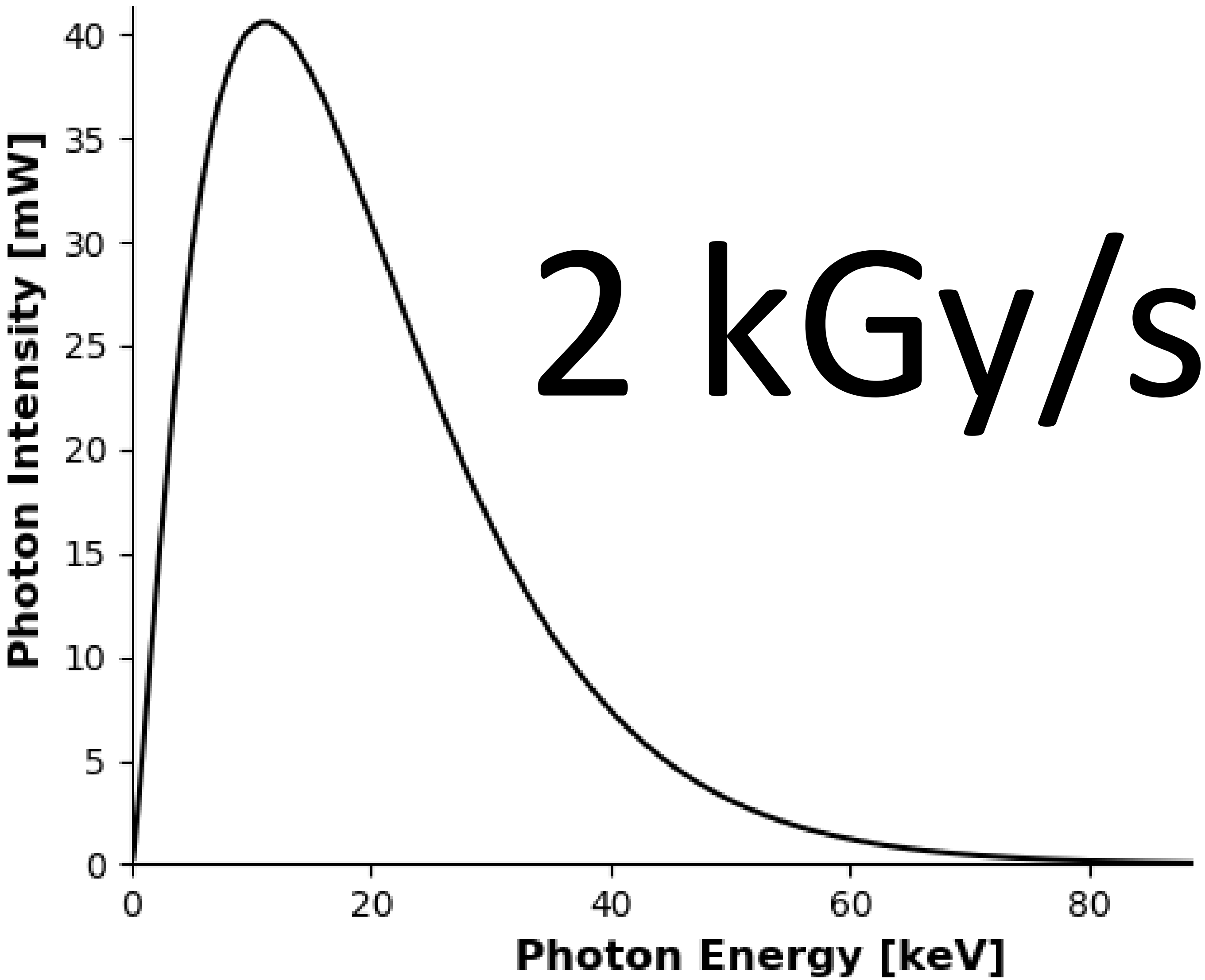

2 kGy/s

Mel O'Leary Email: mel.oleary@manchester.ac.uk

Irradiation

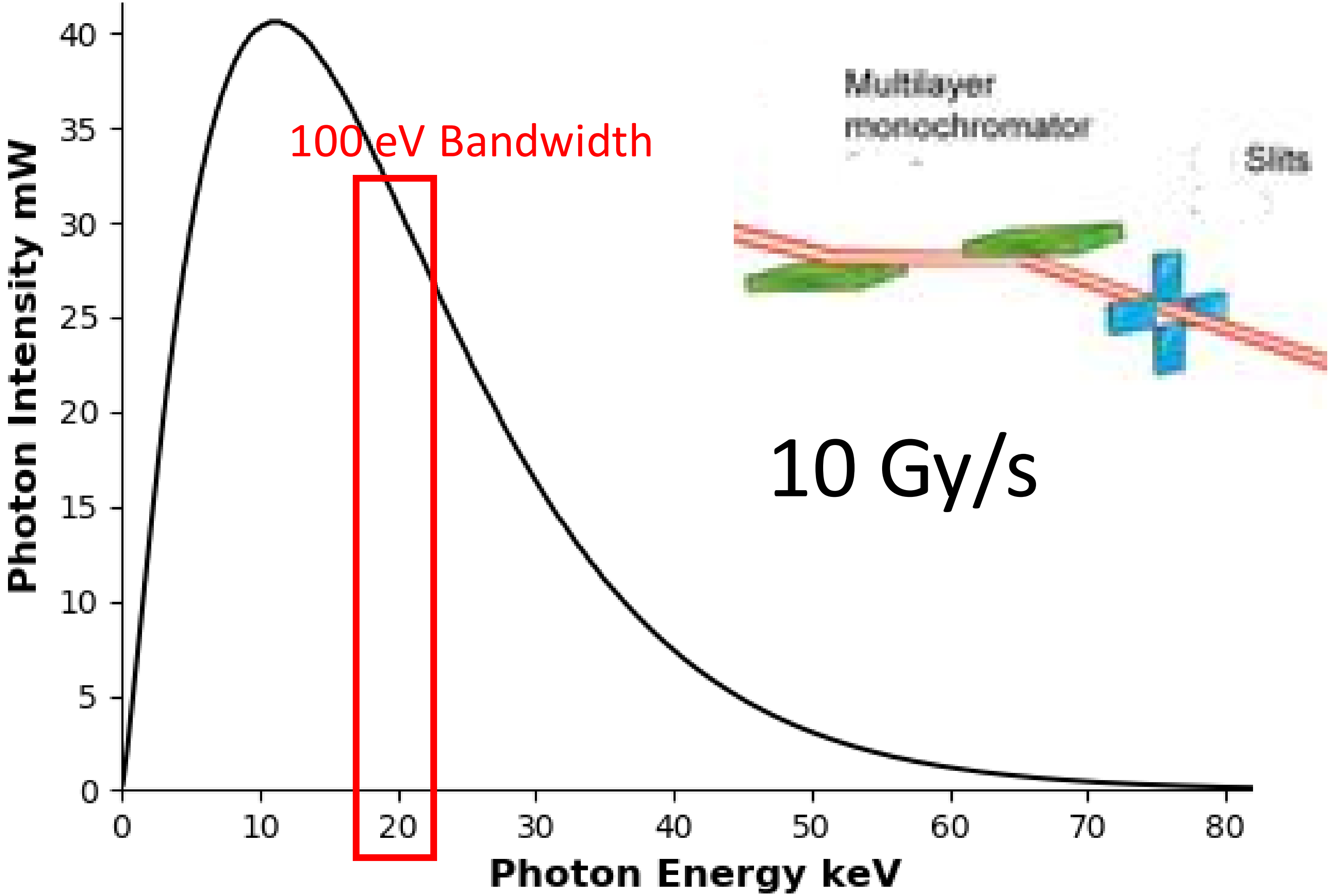

10 Gy/s

Mel O'Leary Email: mel.oleary@manchester.ac.uk

Samples

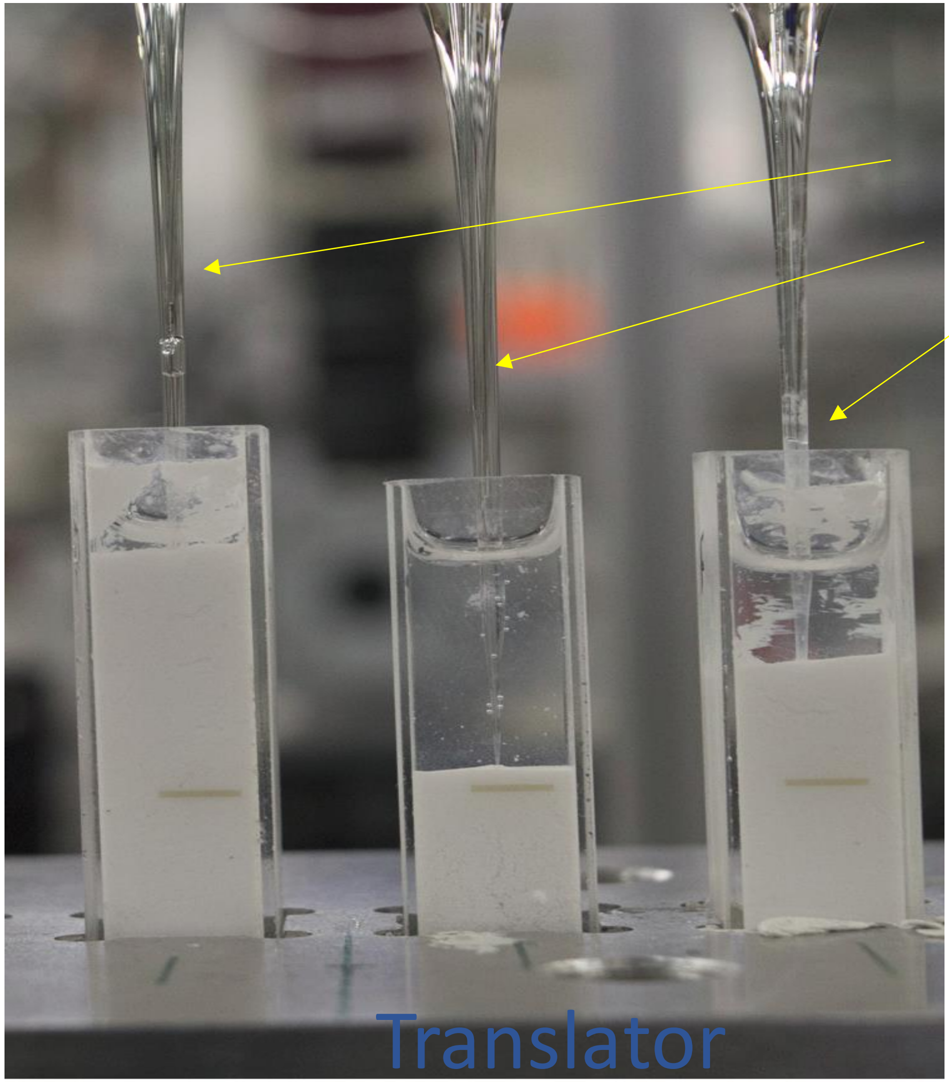

Probes

12 samples in parallel

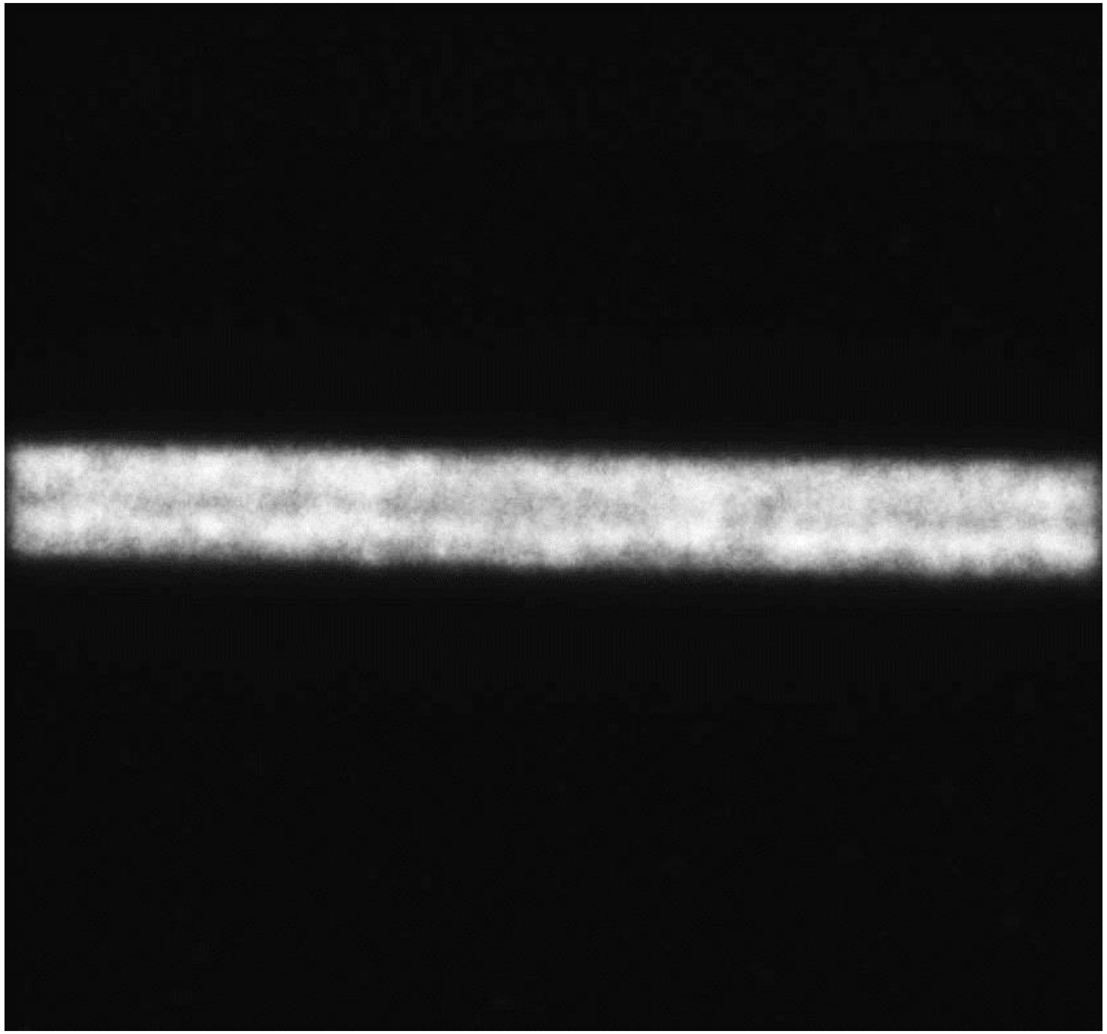

Mel O'Leary Email: mel.oleary@manchester.ac.uk

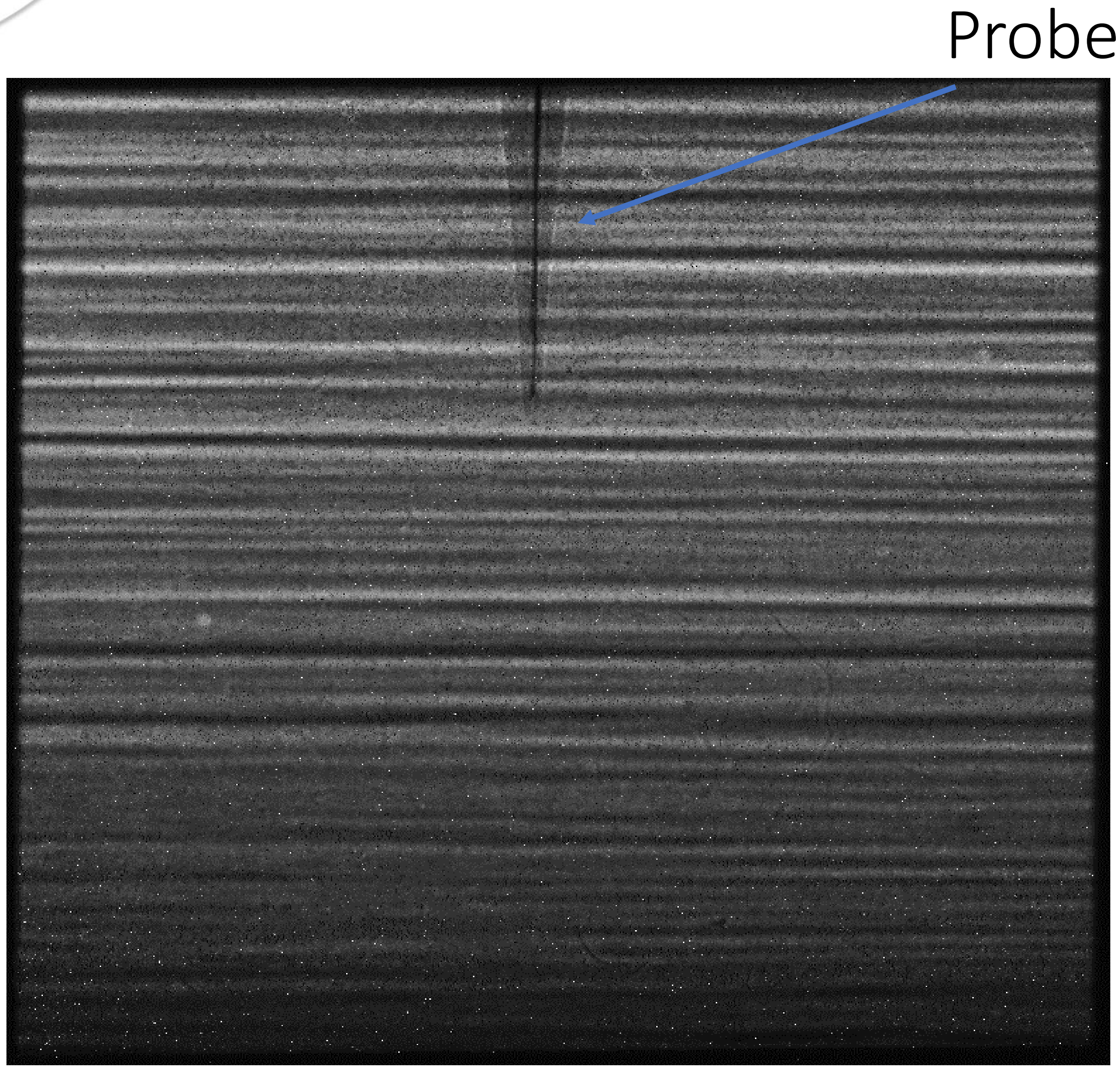

Mel O'Leary Email: mel.oleary@manchester.ac.uk

Dosimetry

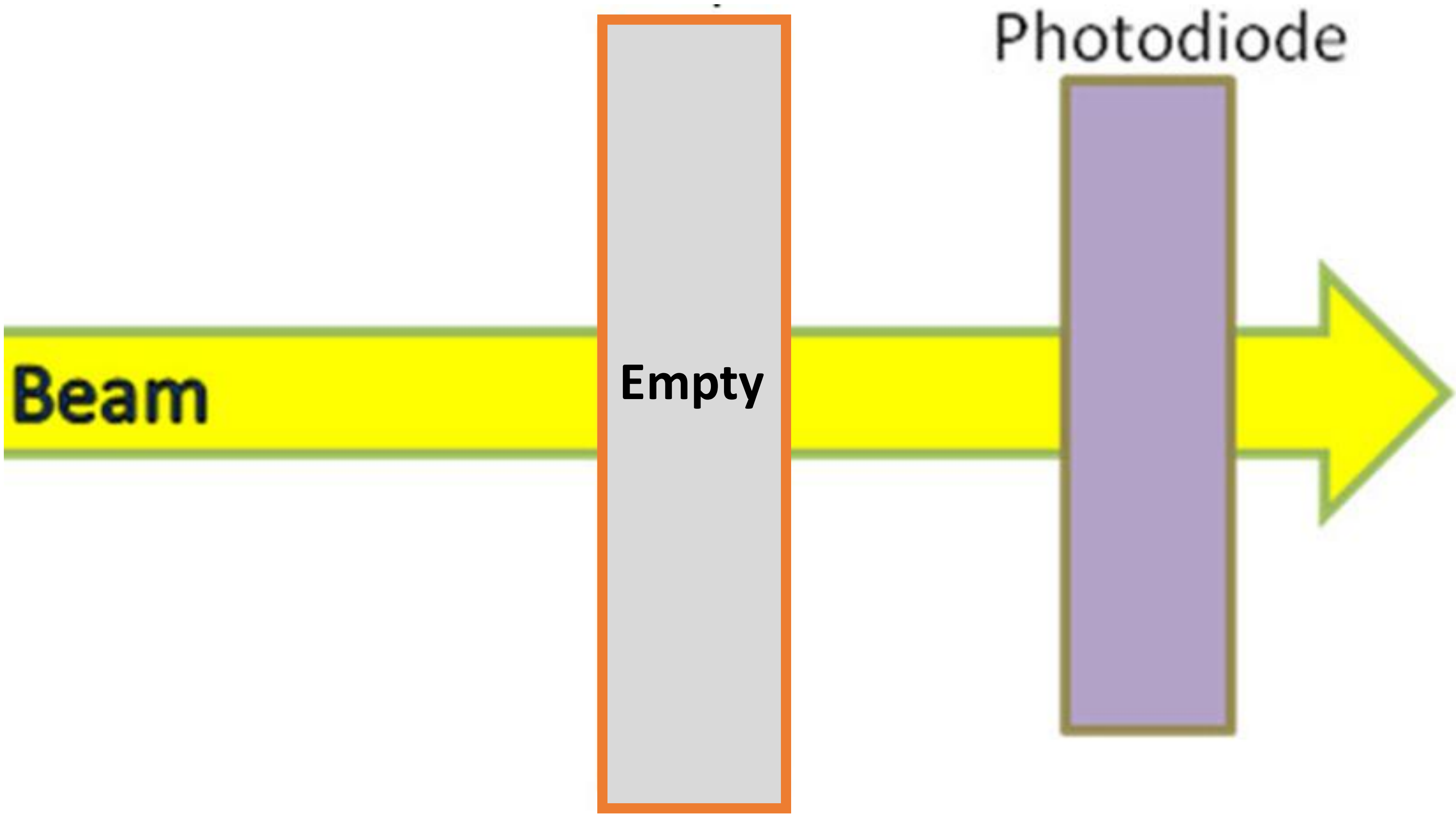

Dosimetry

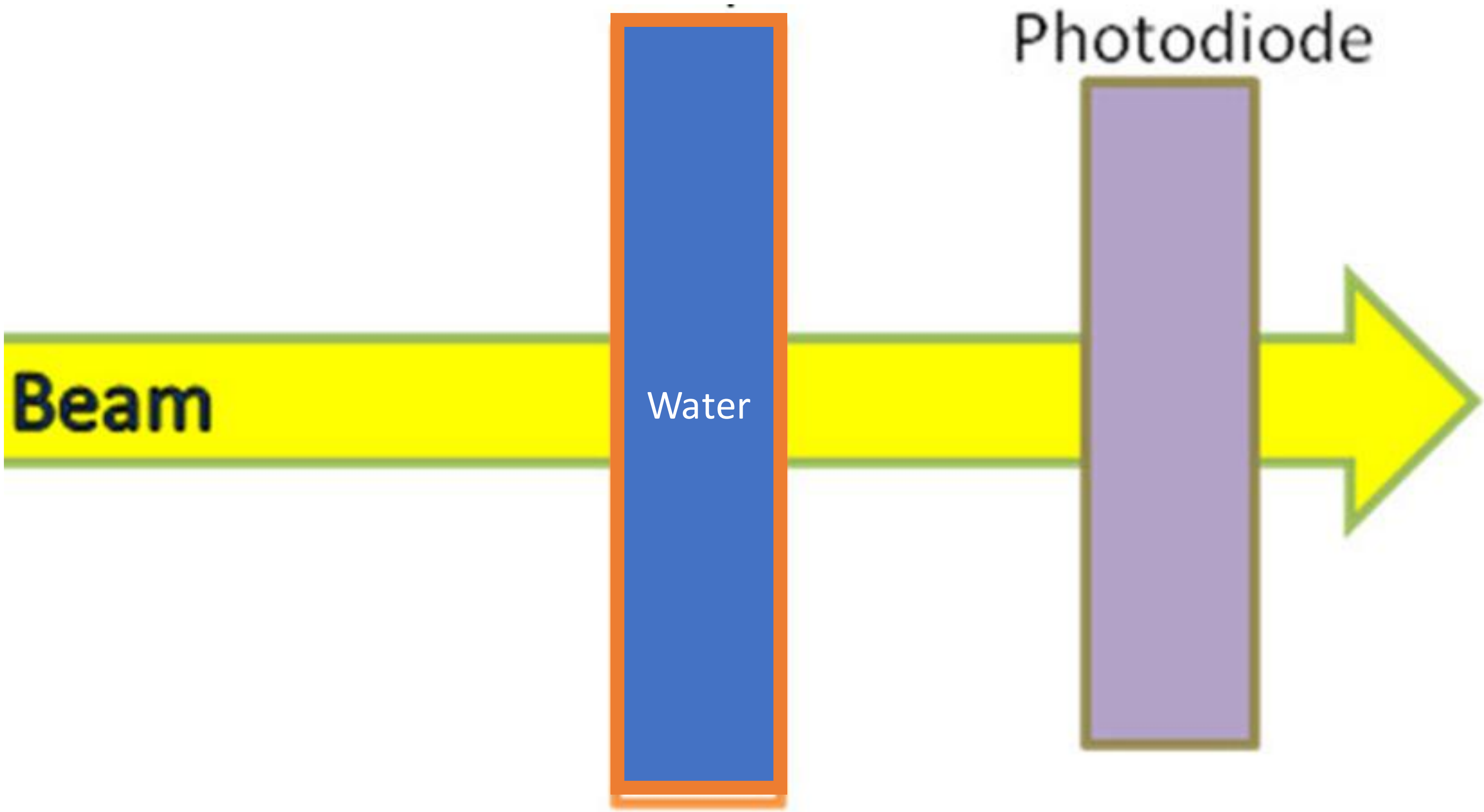

Mel O'Leary Email: mel.oleary@manchester.ac.uk

Dosimetry

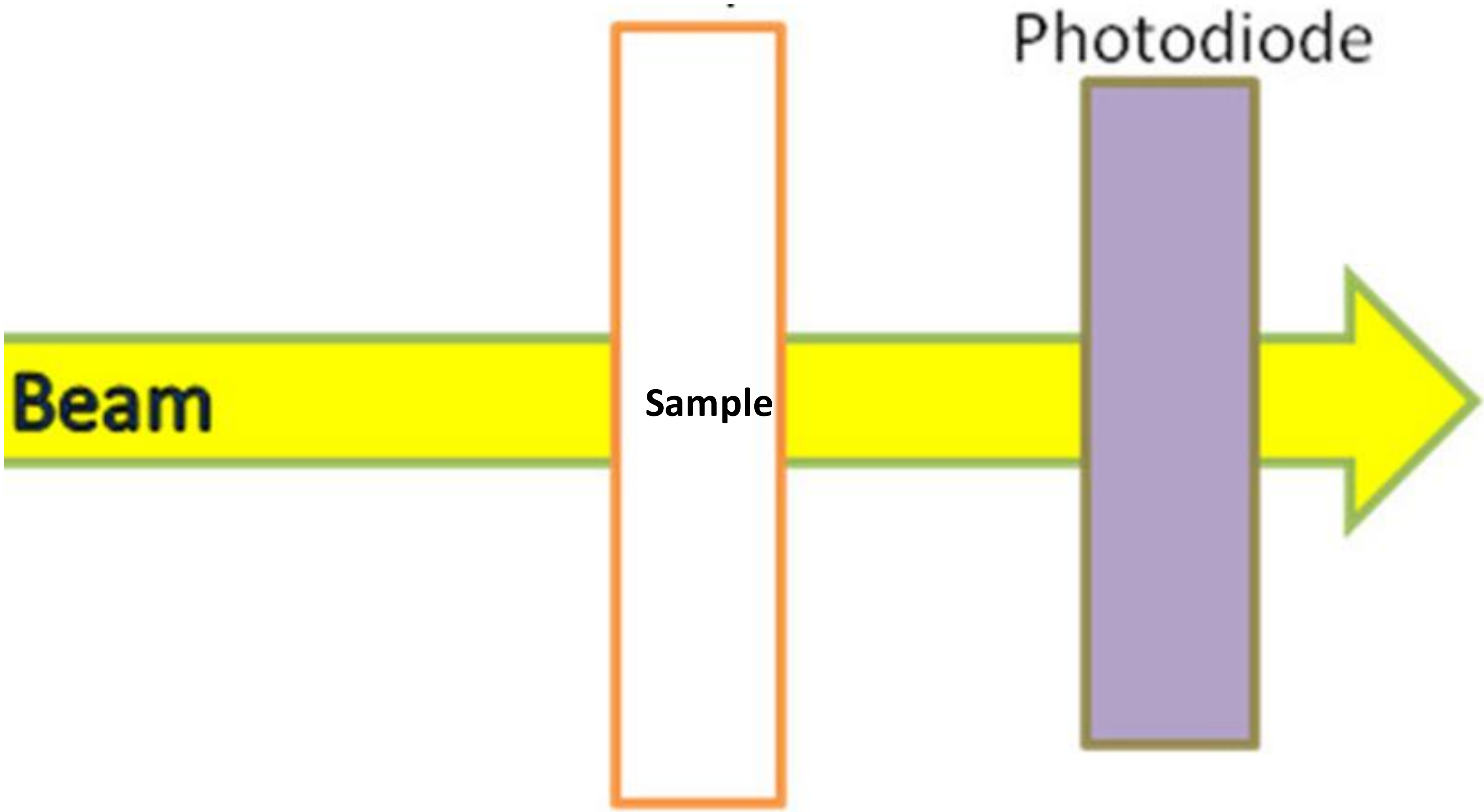

Introduction

Experimental Setup

Transport Measurements

Bubbles

Conclusions

Mel O'Leary Email: mel.oleary@manchester.ac.uk

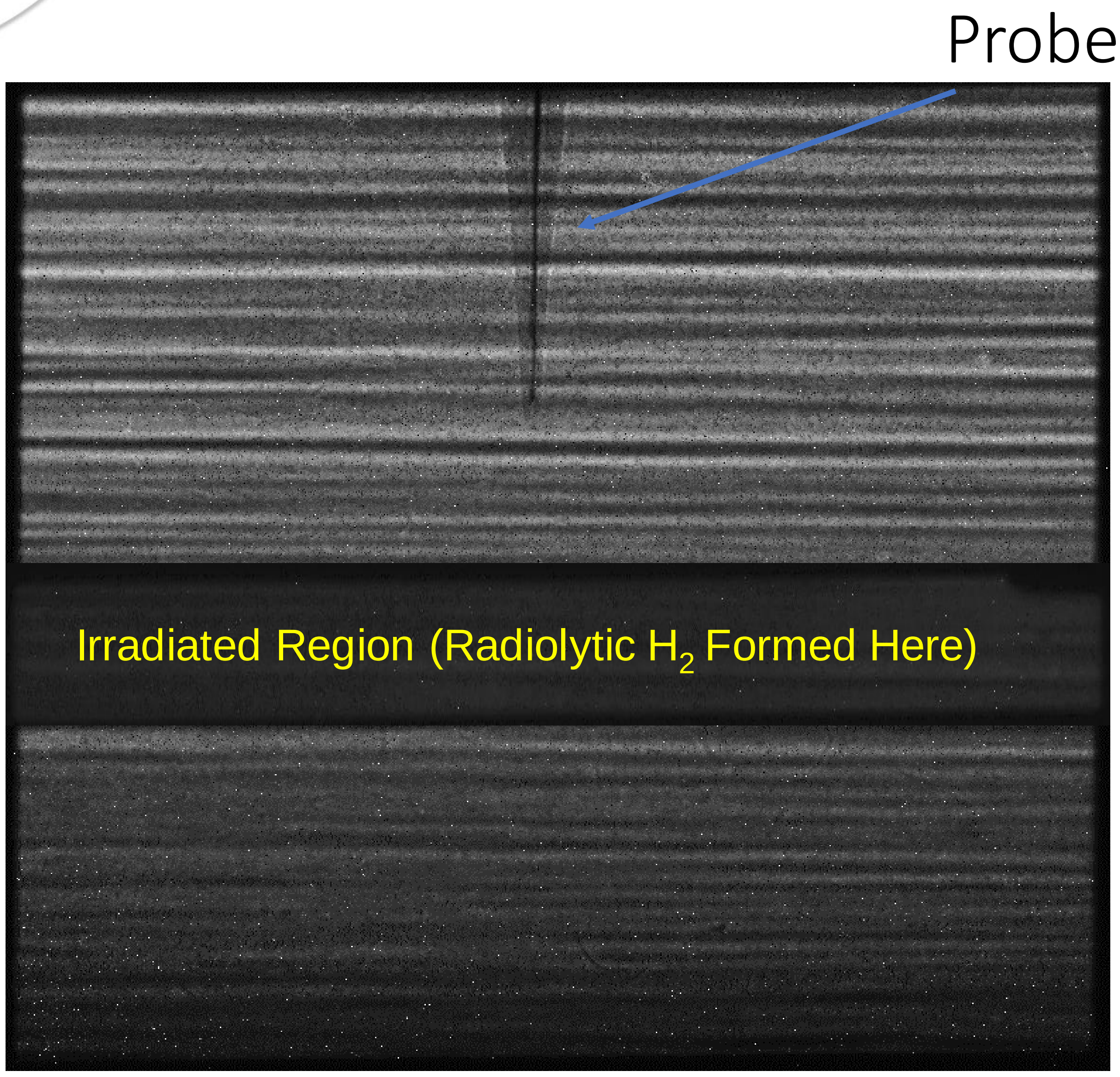

Mel O'Leary Email: mel.oleary@manchester.ac.uk

Diffusion

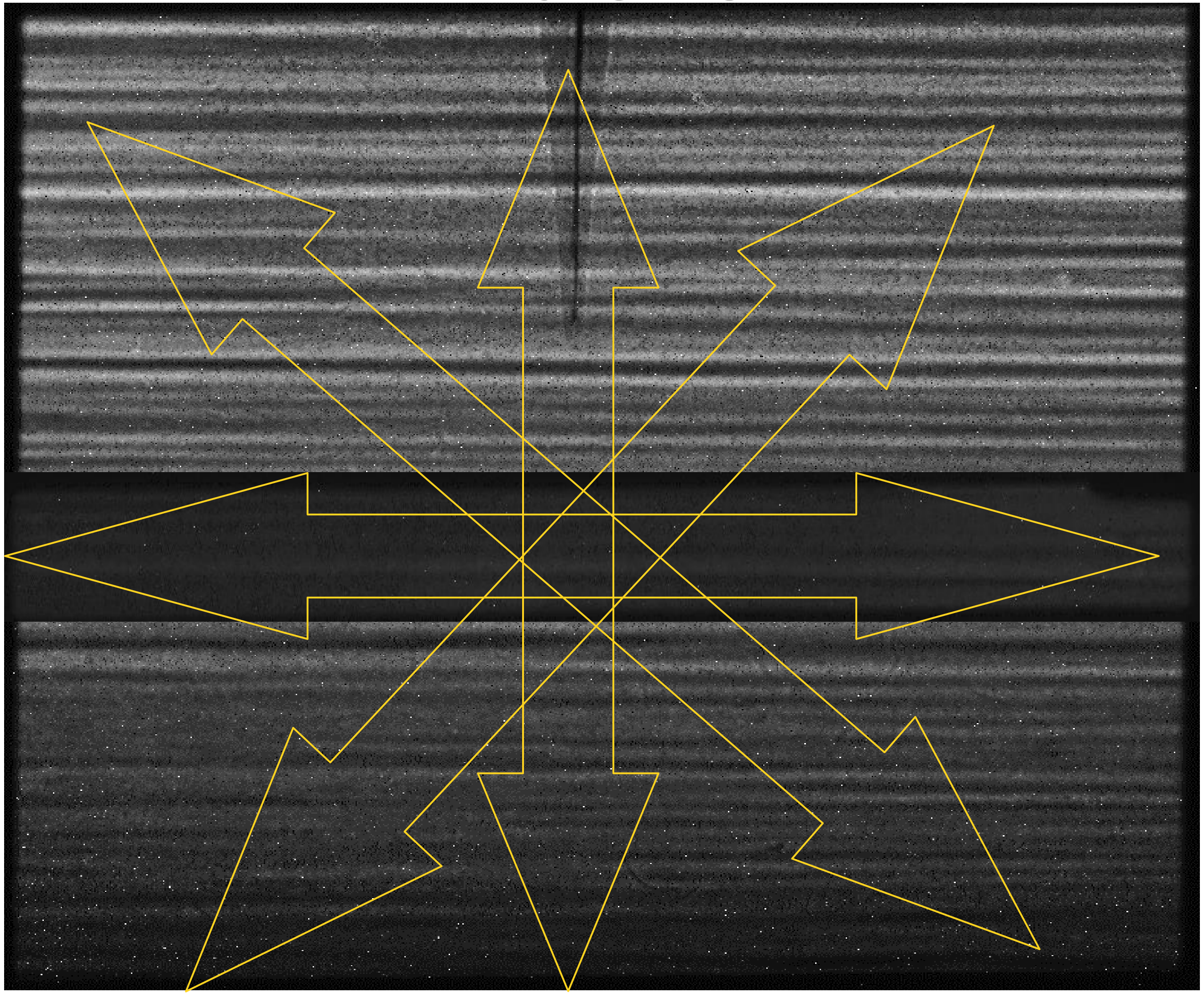

Mel O’Leary Email: mel.oleary@manchester.ac.uk

1D Diffusion

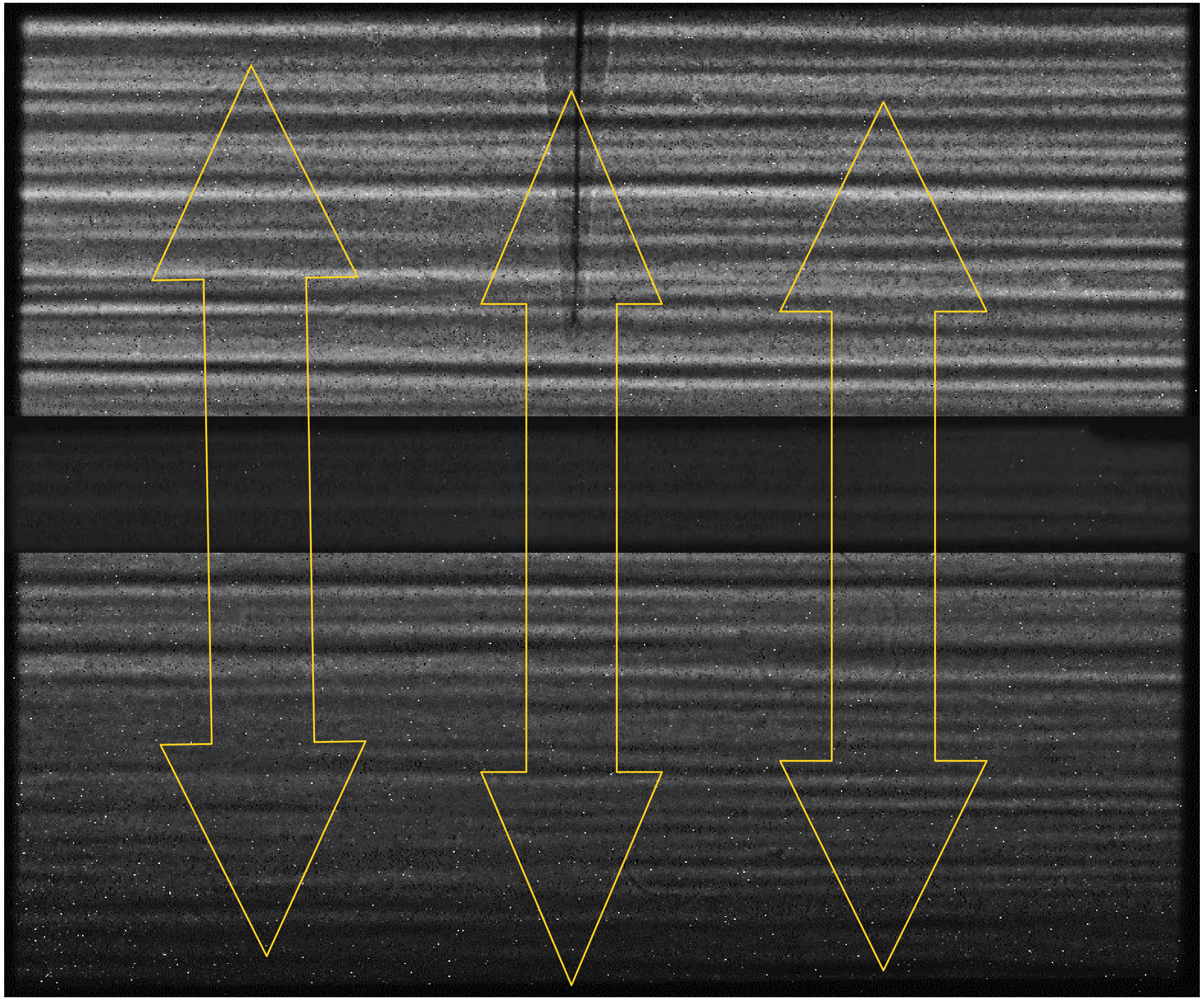

Mel O'Leary Email: mel.oleary@manchester.ac.uk

Fit to Data

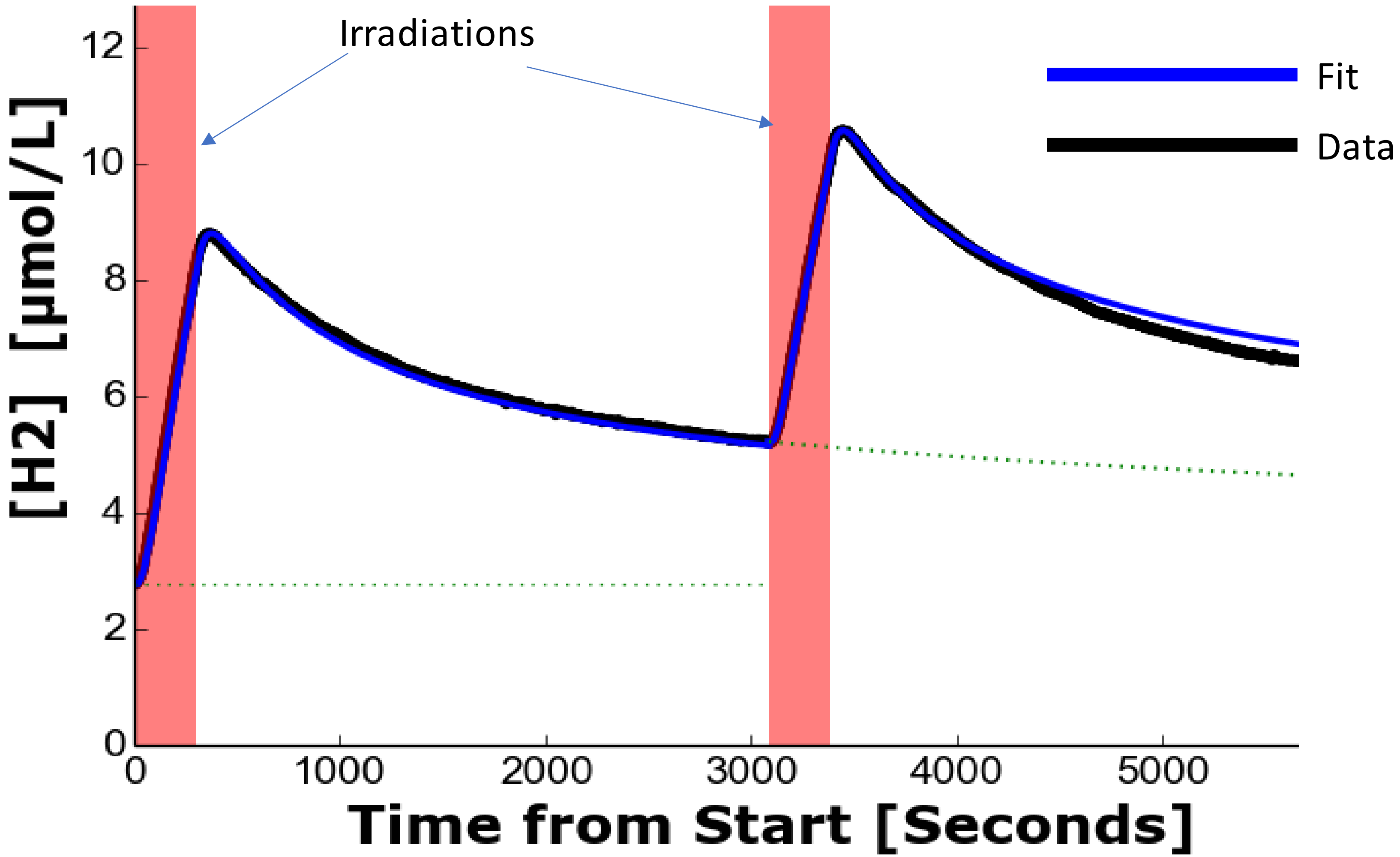

Mel O'Leary Email: mel.oleary@manchester.ac.uk

Parameters from Fit

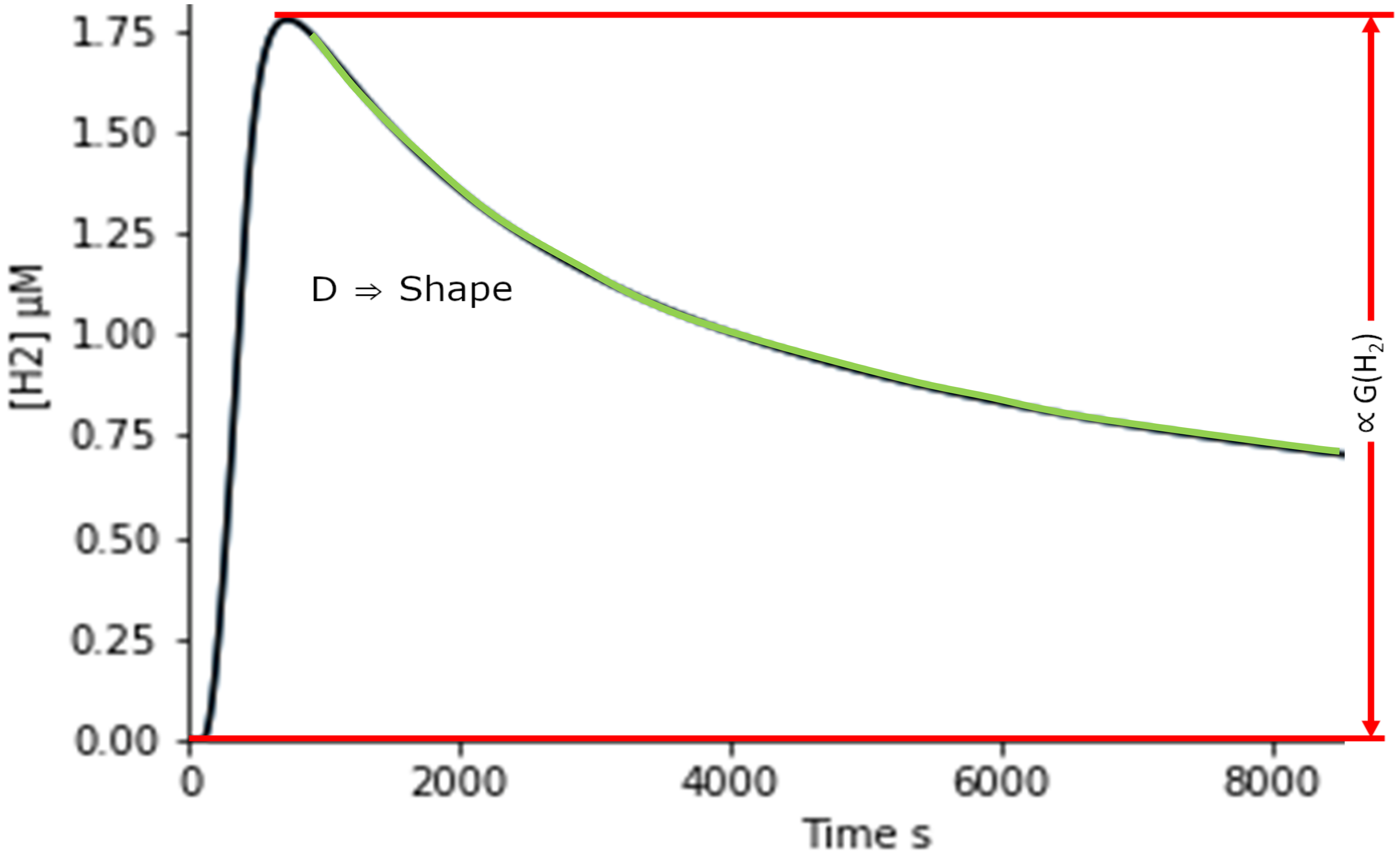

Mel O’Leary Email: mel.oleary@manchester.ac.uk

Diffusion Coefficients

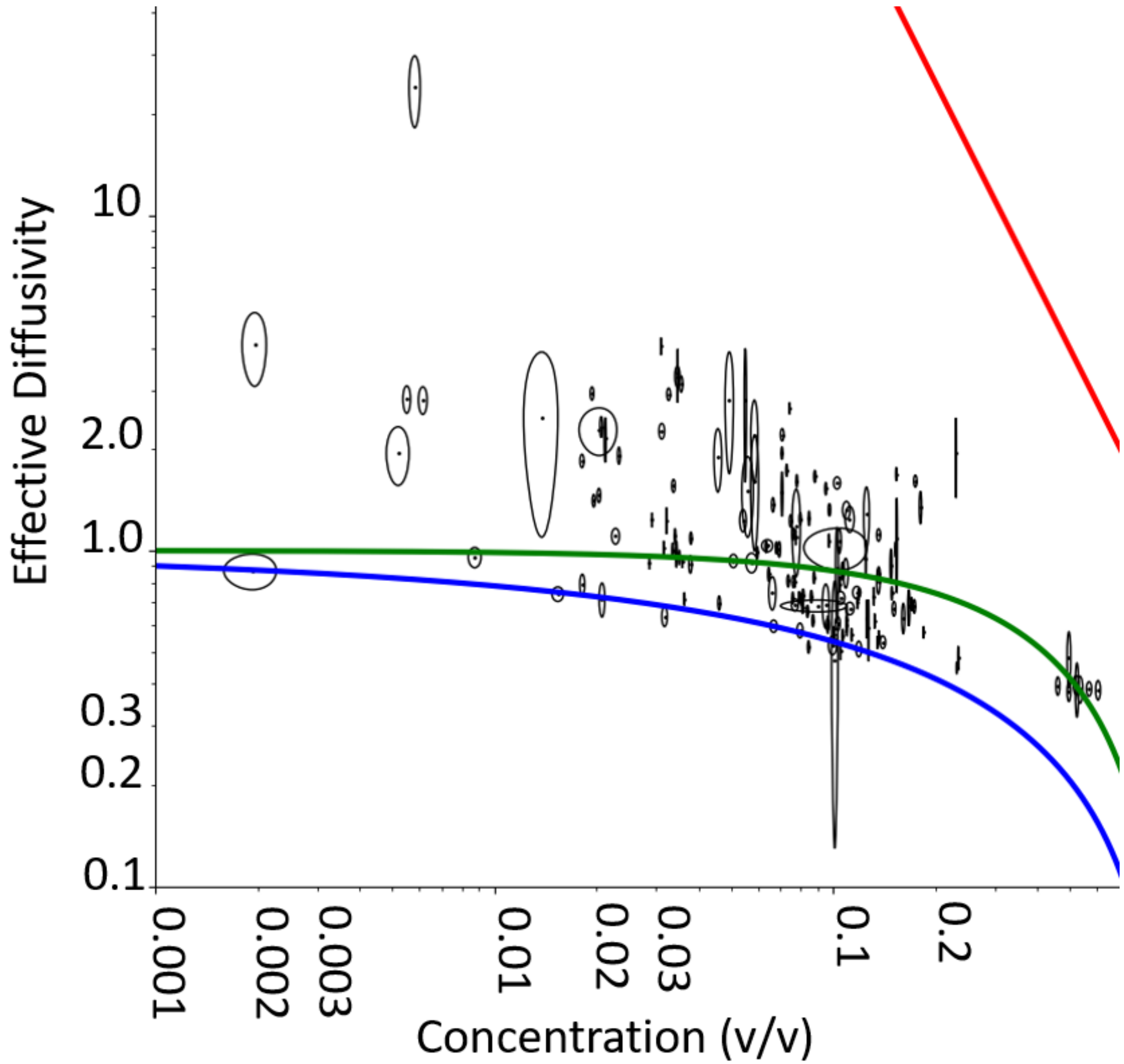

Mel O’Leary Email: mel.oleary@manchester.ac.uk

Radiolytic Yield

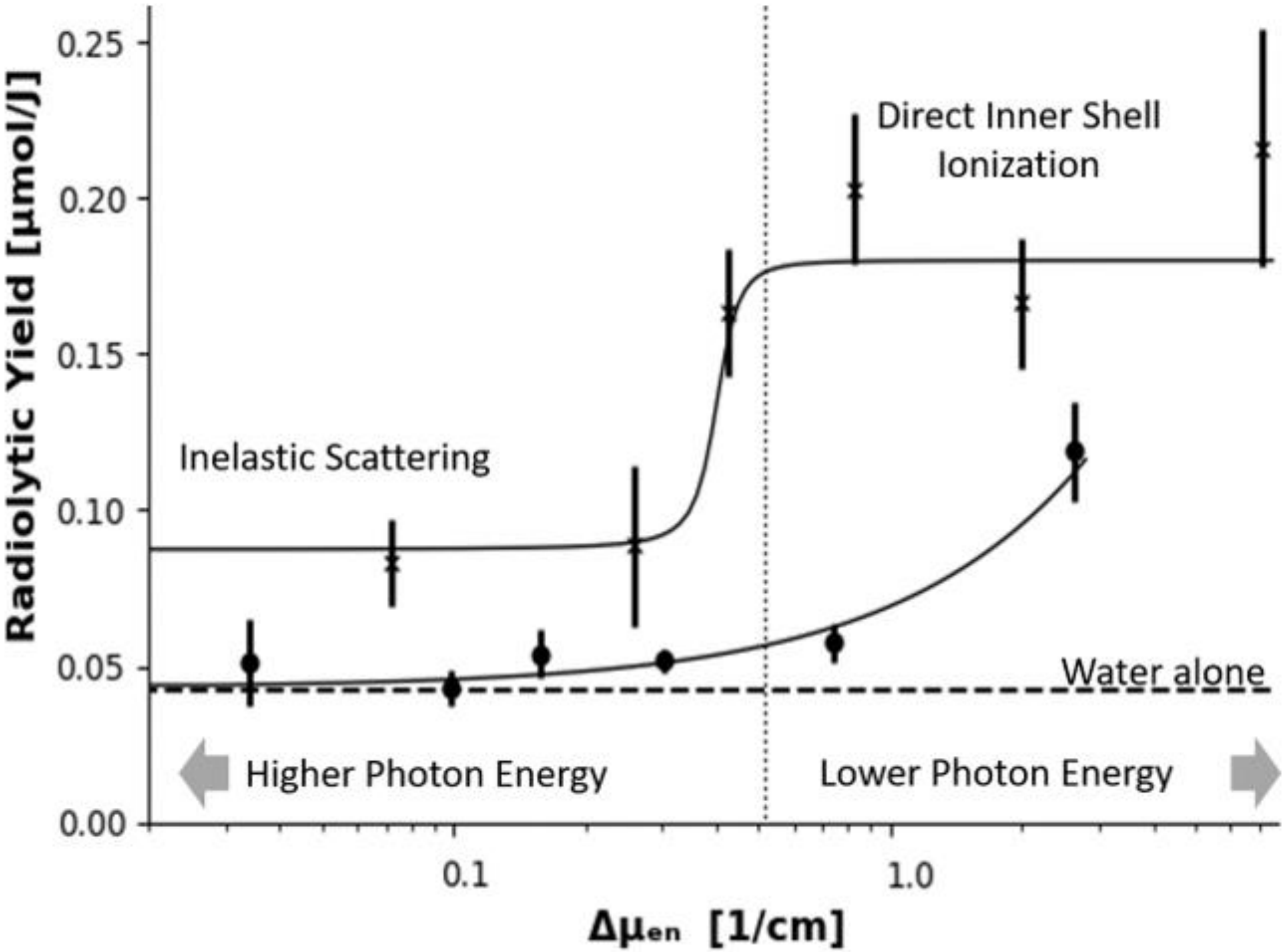

Mel O'Leary Email: mel.oleary@manchester.ac.uk

Introduction

Experimental Setup

Transport Measurements

Bubbles

Conclusions

Mel O'Leary Email: mel.oleary@manchester.ac.uk

Bubbles

Irradiation

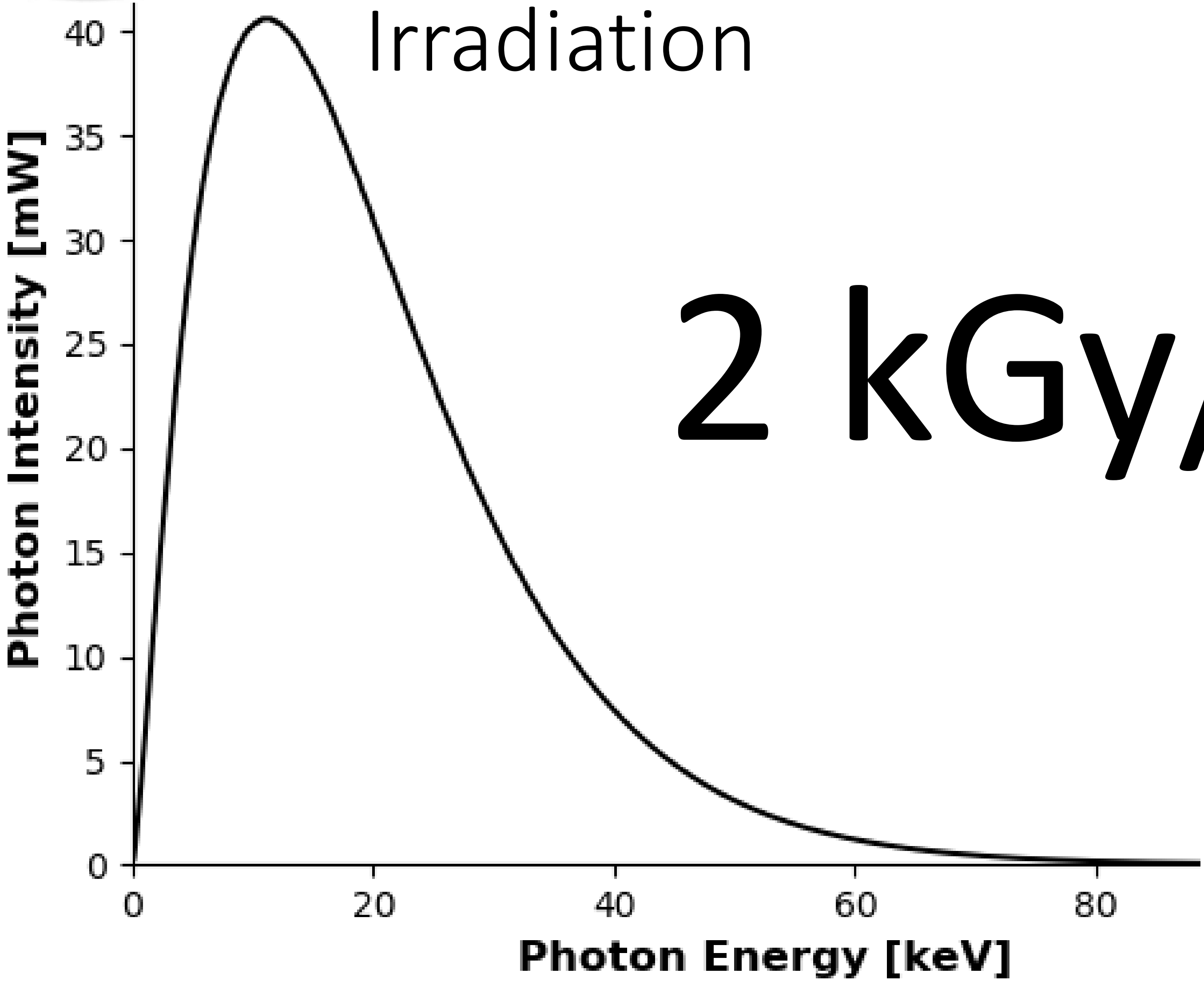

2 kGy/s

Mel O'Leary Email: mel.oleary@manchester.ac.uk

Bubbles

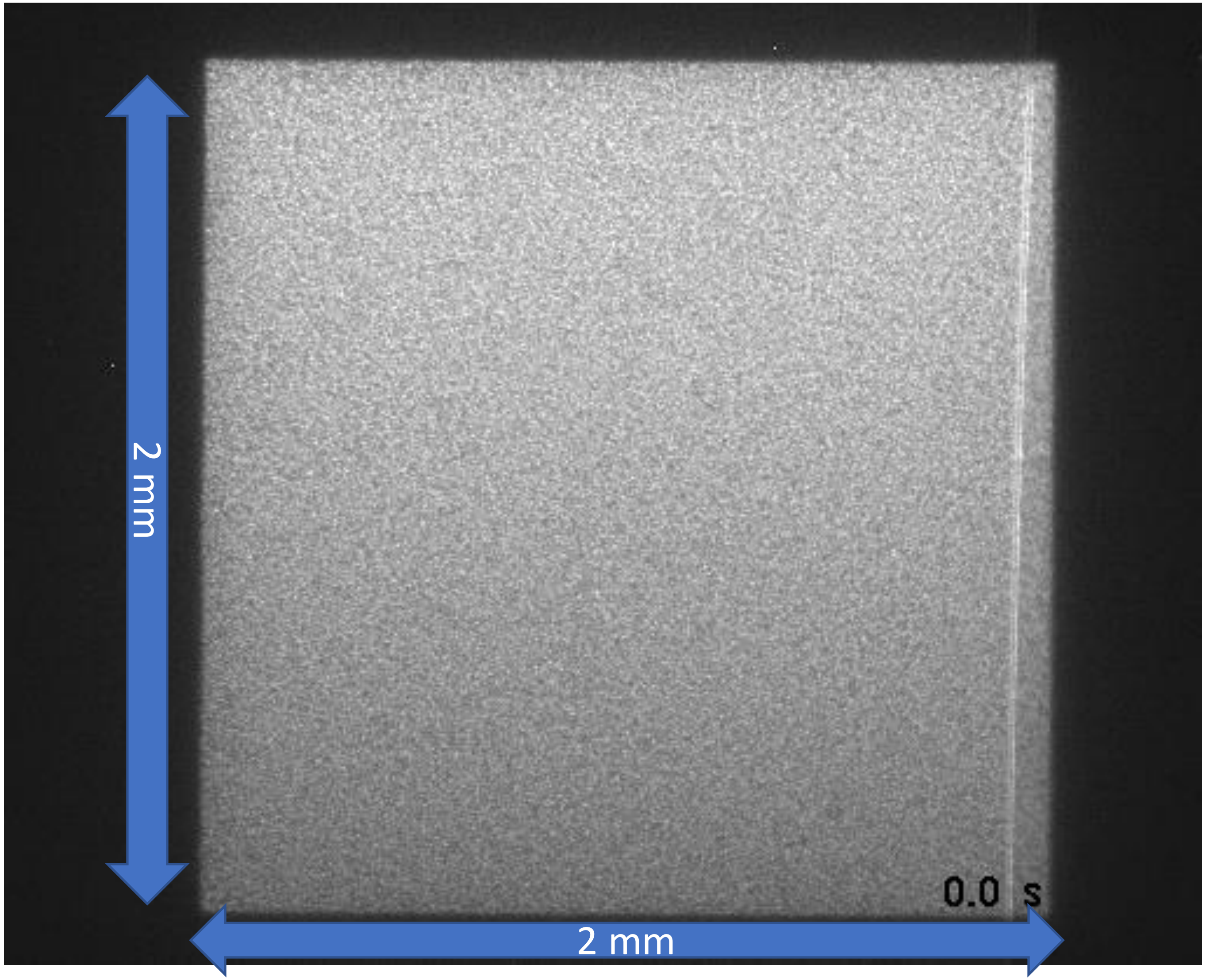

Mel O'Leary Email: mel.oleary@manchester.ac.uk

Bubbles

Model

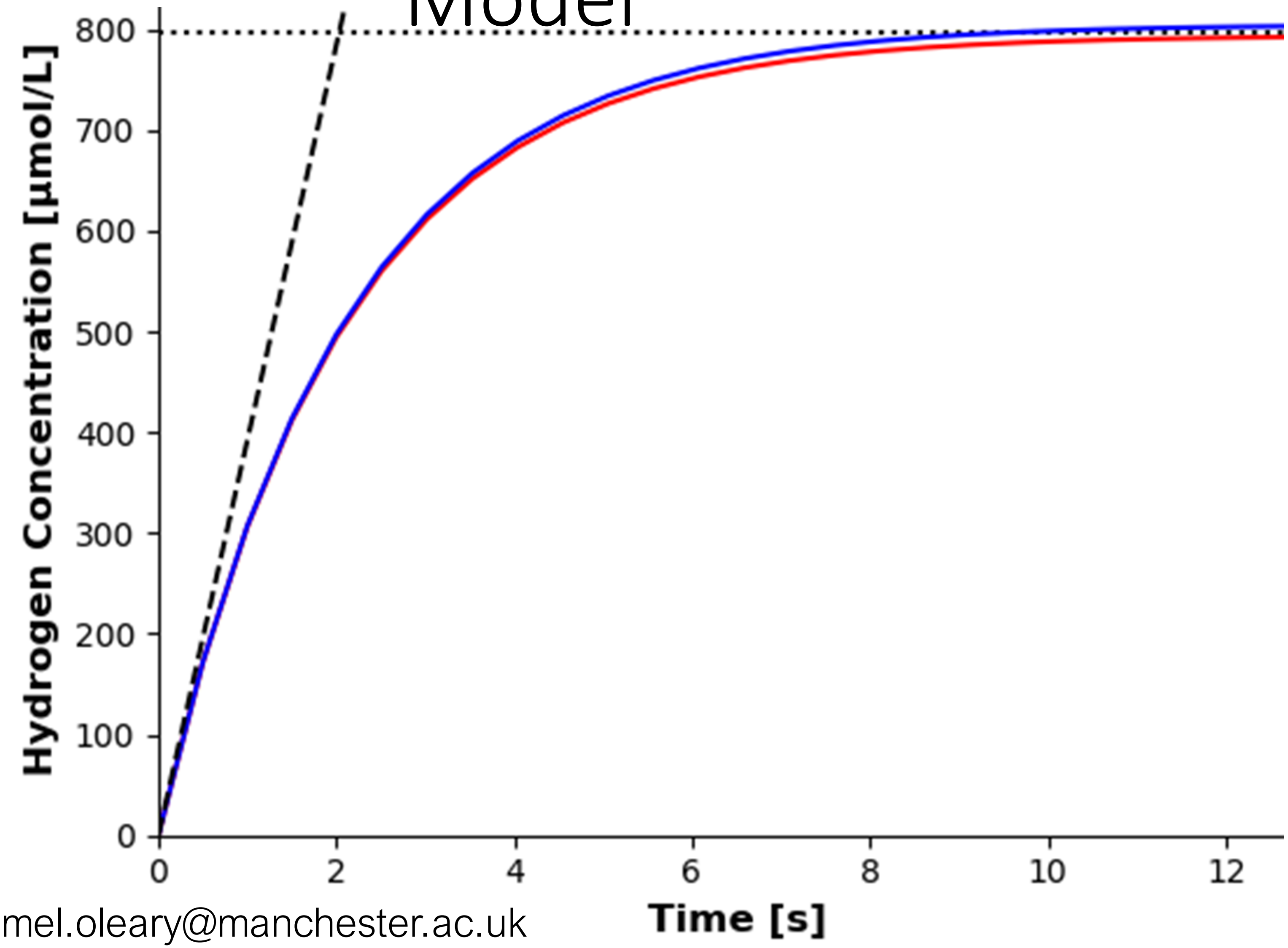

Mel O'Leary Email: mel.oleary@manchester.ac.uk

Bubble Formation

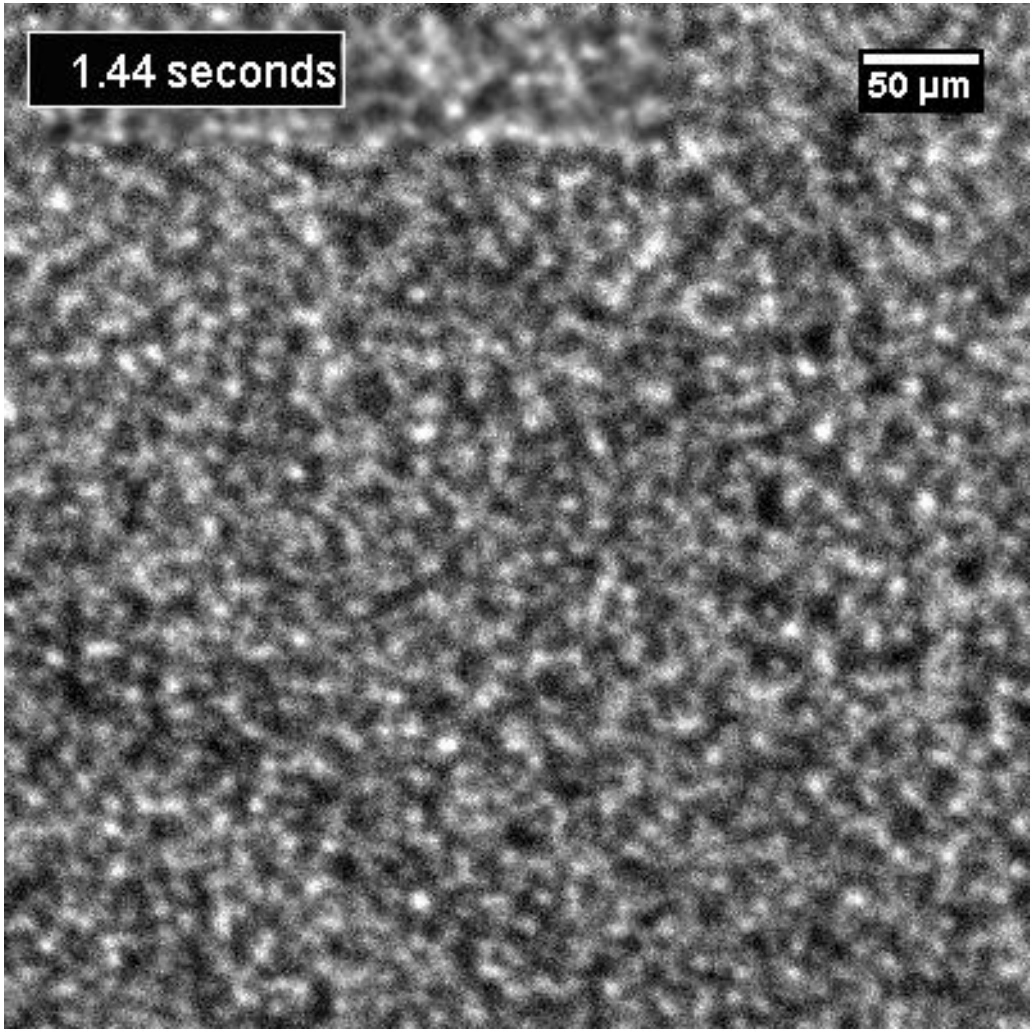

Mel O'Leary Email: mel.oleary@manchester.ac.uk

Introduction
Experimental Setup
Transport Measurements
Bubbles
Conclusions

Mel O’Leary Email: mel.oleary@manchester.ac.uk

Thank you

Mel O’Leary
Email: mel.oleary@manchester.ac.uk

TRANSCEND

Transformative Science and Engineering for Nuclear Decommissioning

Optimising Magnesium-Silicate-Hydrate Cement Made From Brucite

Mercedes Baxter Chinery, Imperial College London

Energy

For a Low Carbon Future

Background

- Sludges from Sellafield ponds need to be turned into a waste form
- Known to be rich in $Mg(OH)_2$
- A novel cement based on MgO and SiO_2 sets as strong as OPC
- Opportunity to use the waste as an encapsulating cement

Earlier Results

- Reproduced initial system
- Optimised by Zhang (DIAMOND, 2012)
- Compressive strength as expected
- Good dimensional stability

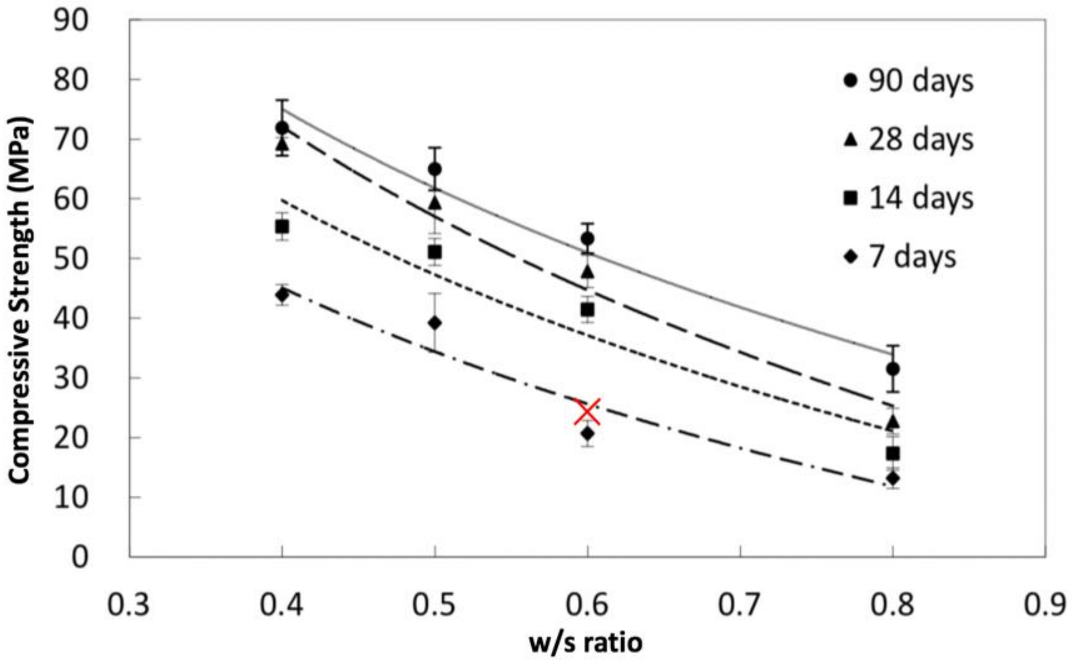

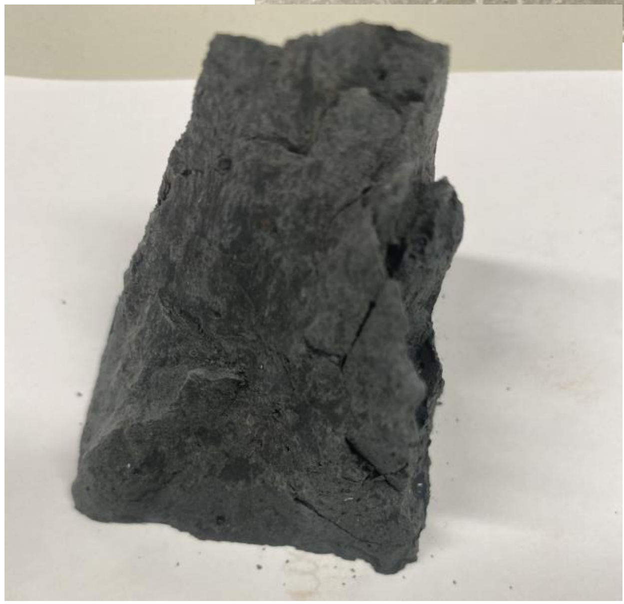

Current Work

- Investigating how replacing the MgO with $Mg(OH)_2$ affects
  - fluidity
  - setting
  - properties of the cement

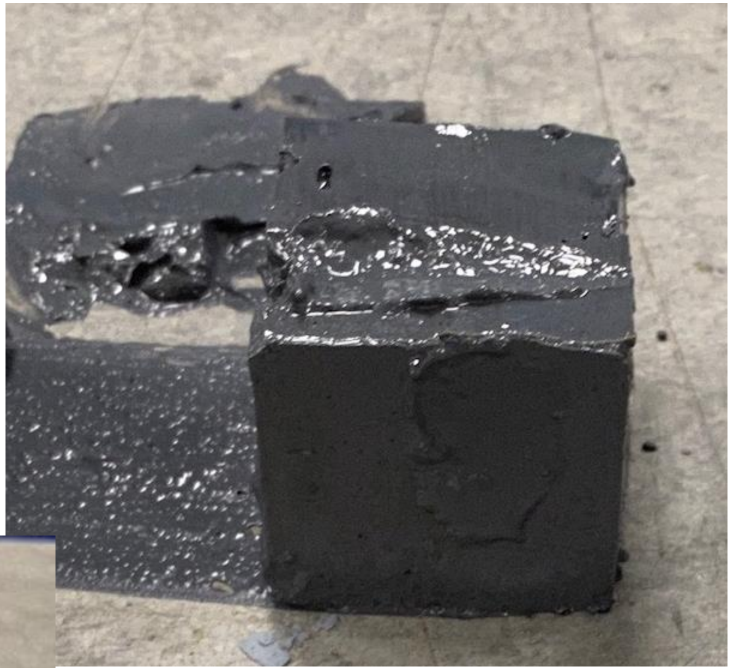

Current Work

- Setting and measuring strength for properties
- Adapting water content and dispersants to improve fluidity
- ICP to investigate reactants available

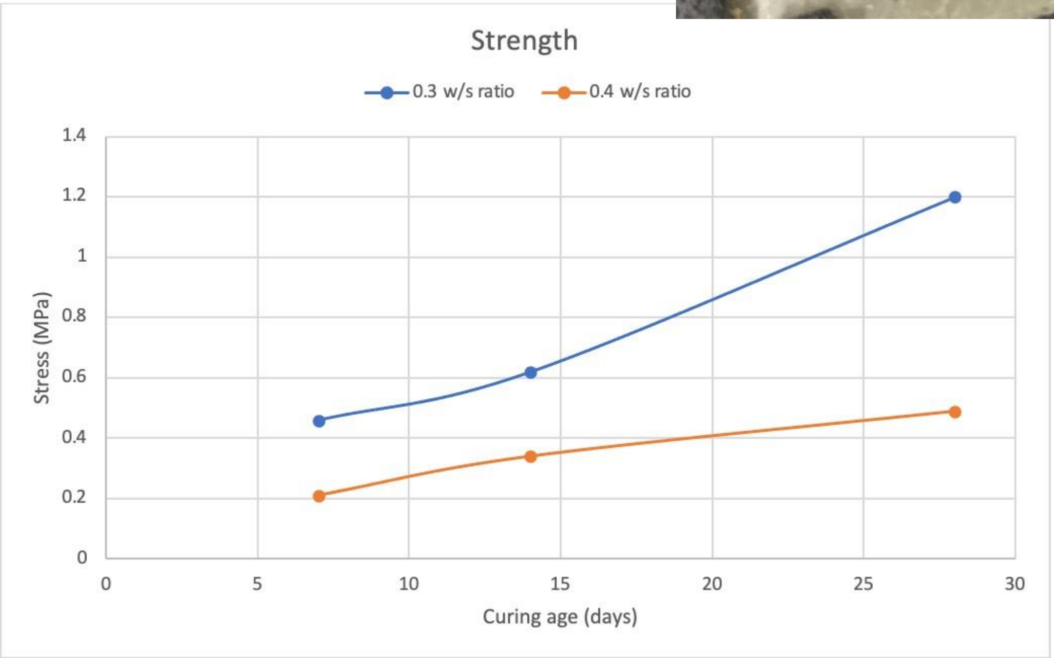

Future Outlook

- Trials with artificial sludge from Sellafield
- Understand the durability properties of the cement

Transformative Science and Engineering for Nuclear Decommissioning

Thank you

m.baxter-chinery19@imperial.ac.uk

TRANSCEND

Transformative Science and Engineering for Nuclear Decommissioning

Radiation effects on nuclear waste forms: How does the degree of crystallinity in a glass-ceramic affect radiation tolerance?

Tamás Zagyva – The University of Manchester, Dalton Cumbrian Facility

Theme 1 Integrated Waste Management

2nd December 2020
Online

MANCHESTER 1824
The University of Manchester
Dalton Nuclear Institute

NATIONAL NUCLEAR LABORATORY

Energy
For a Low Carbon Future

Transformative Science and Engineering for Nuclear Decommissioning

Stored highly active materials with high MoO_3 content

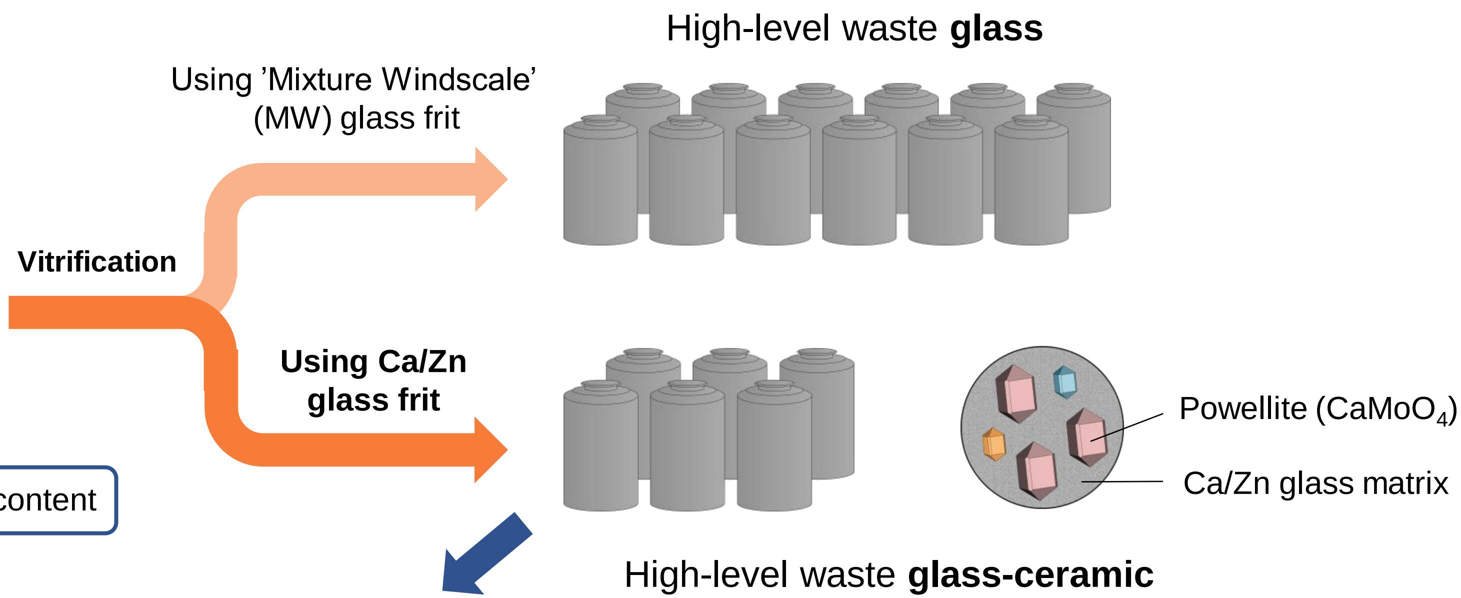

~ 300 less product canisters which offers ~ £55 million savings to the UK taxpayers [1].

Vitrification test rig (VTR) samples:

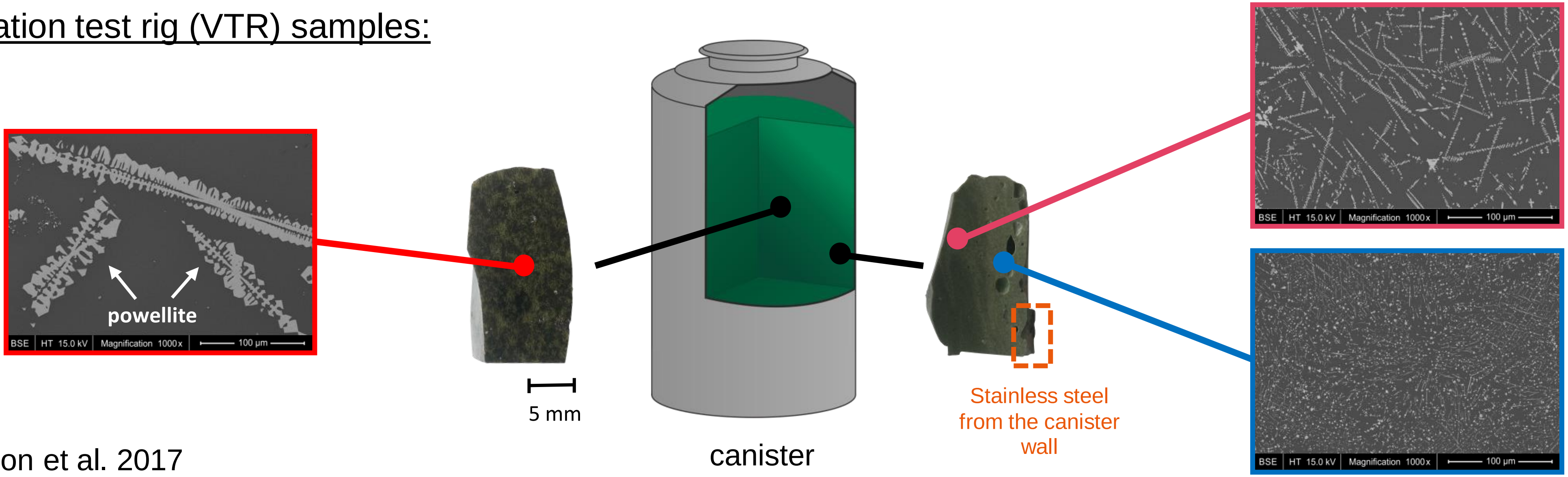

[1] Paterson et al. 2017

PhD topic

Radiation effects on nuclear waste forms: How does the degree of crystallinity in a glass-ceramic affect radiation tolerance?

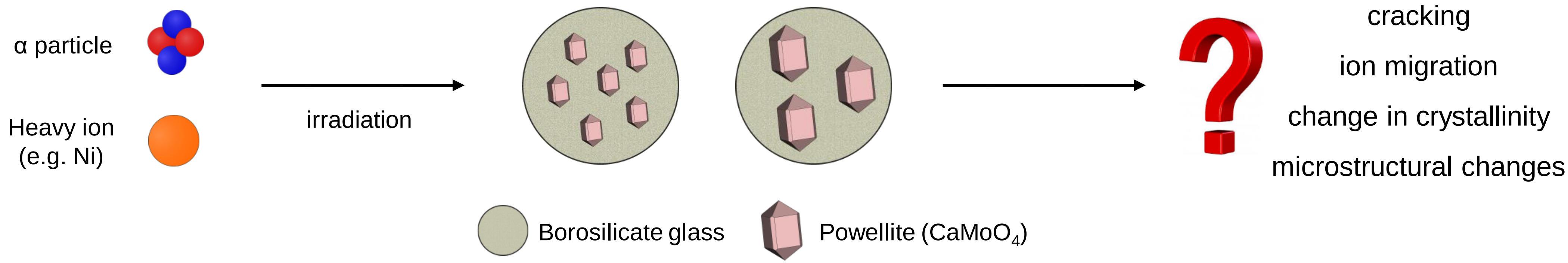

Vitrification test rig (VTR) samples:

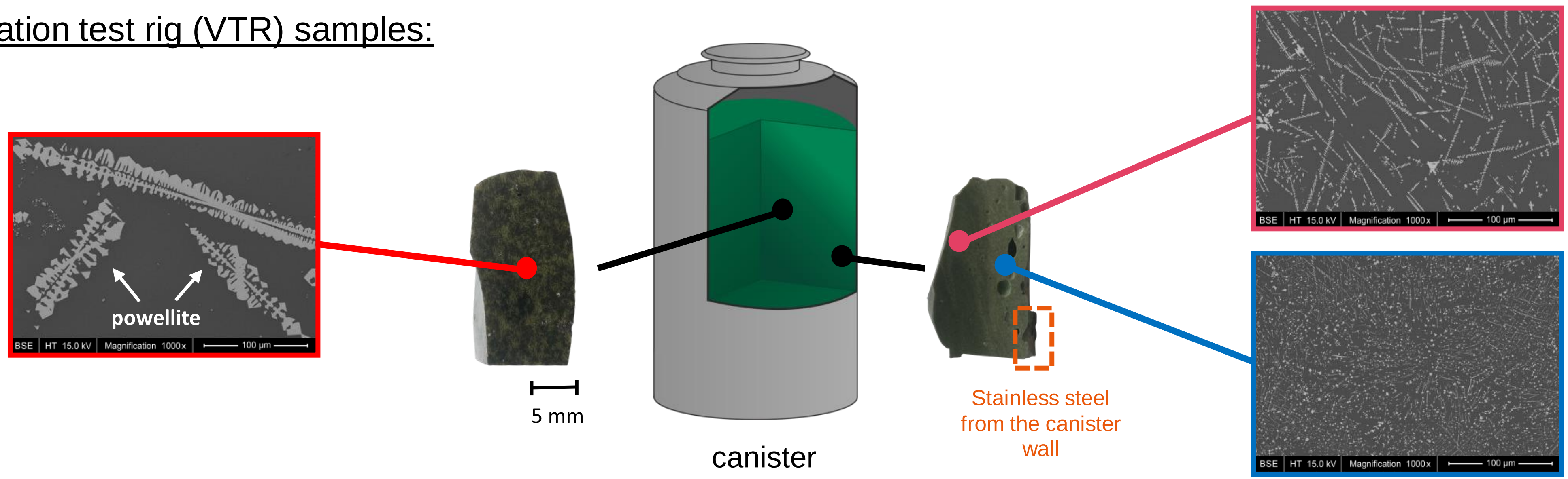

PhD topic

Radiation effects on nuclear waste forms: How does the degree of crystallinity in a glass-ceramic affect radiation tolerance?

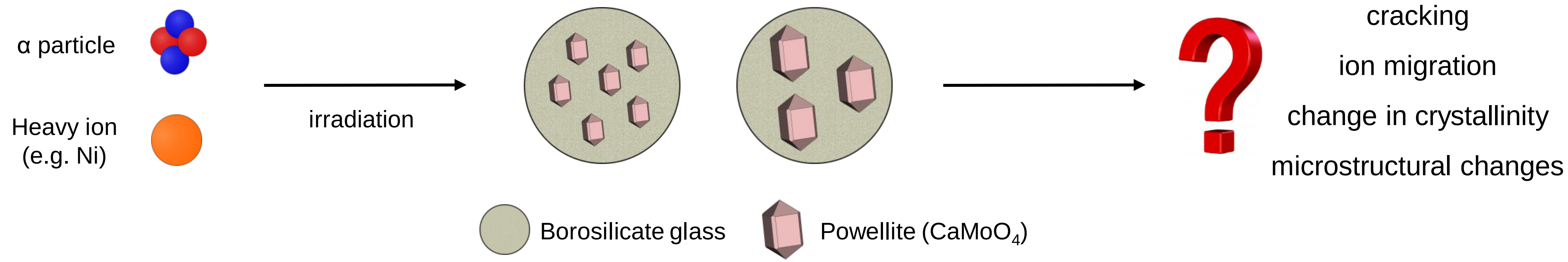

Materials:

VTR samples

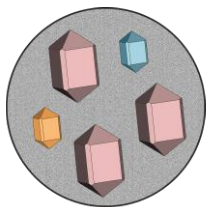

NATIONAL NUCLEAR LABORATORY

complex glass-ceramics with several crystalline phases

Simple Ca/Zn GC samples

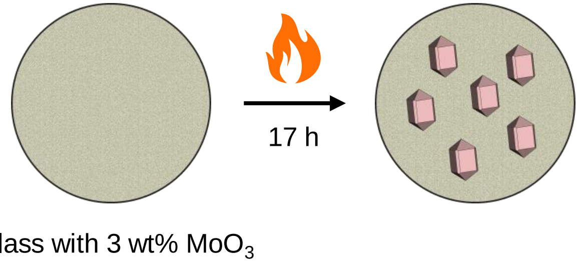

simple glass-ceramics with only powellite crystals

Crystalline phases in the VTR samples:

- – powellite
- – cerium zirconium oxide
- – zircon
- – zinc chromite
- – ruthenium oxide
- – barium molybdate

NATIONAL NUCLEAR LABORATORY

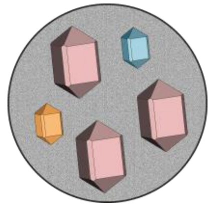

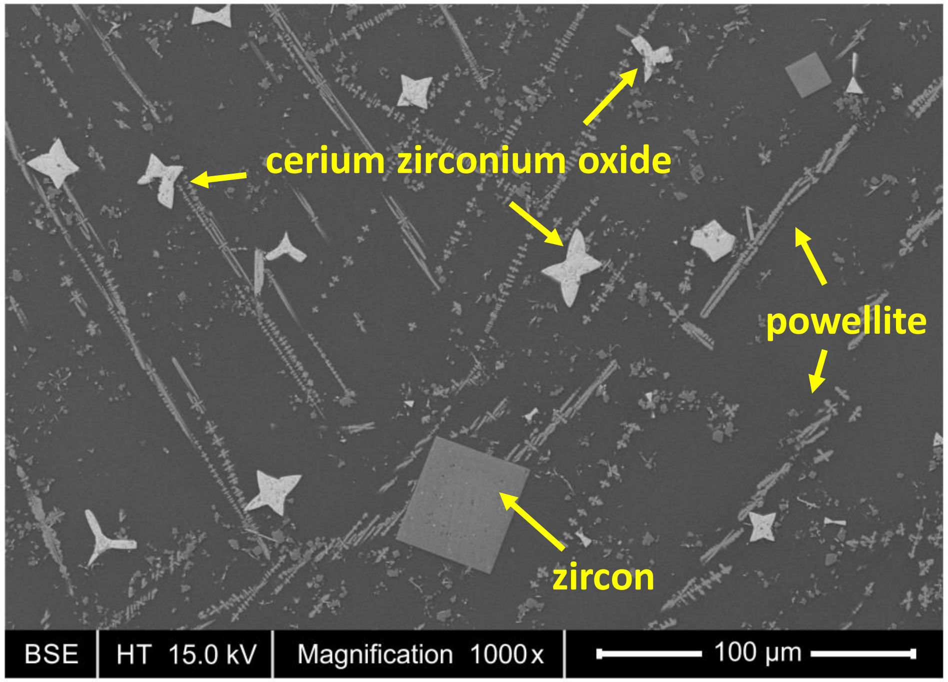

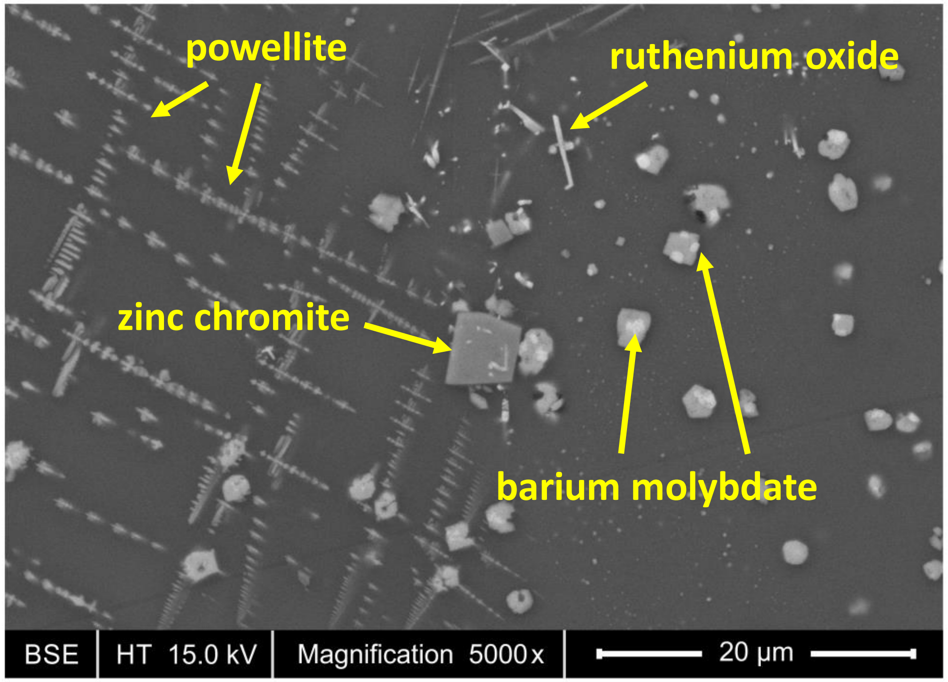

Transformative Science and Engineering for Nuclear Decommissioning

VTR samples | Simple Ca/Zn GC samples | Irradiation experiments

VTR sample containing <u>large powellite crystals</u>

– horizontal cracks

– formed probably at a late stage (during cooling)

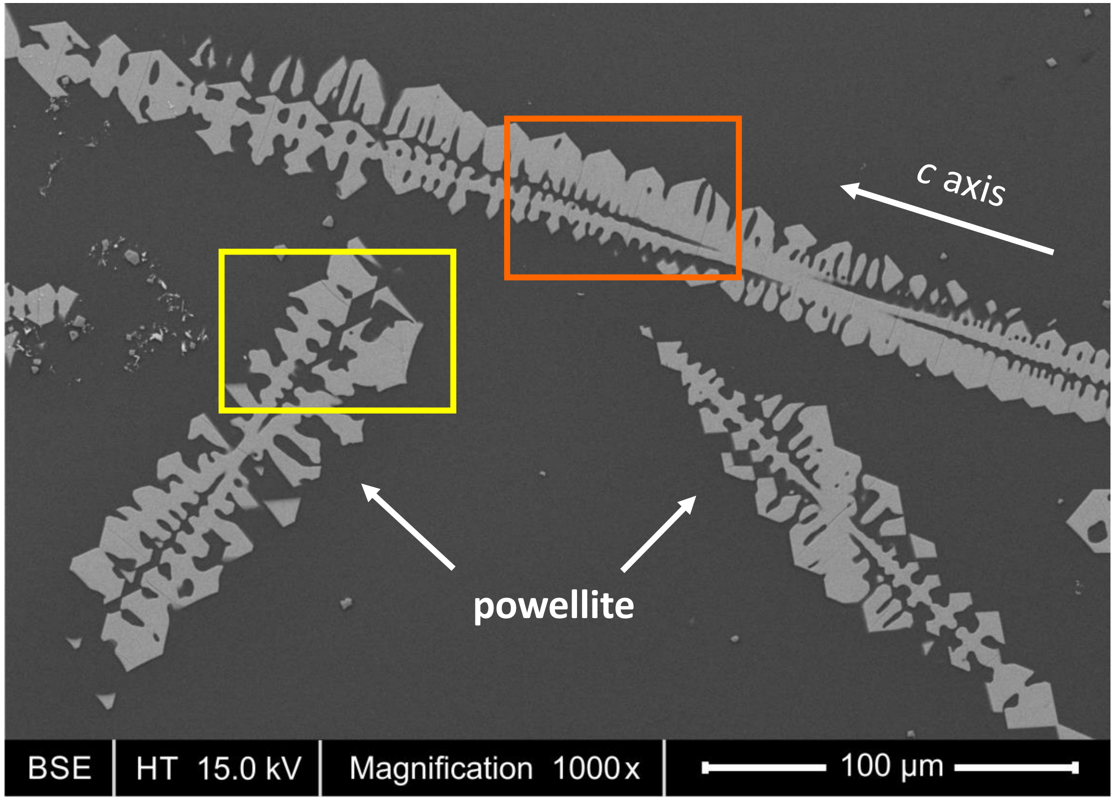

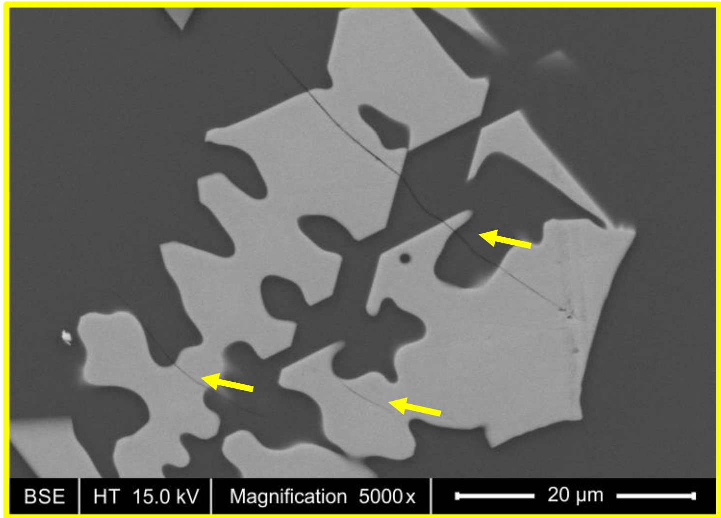

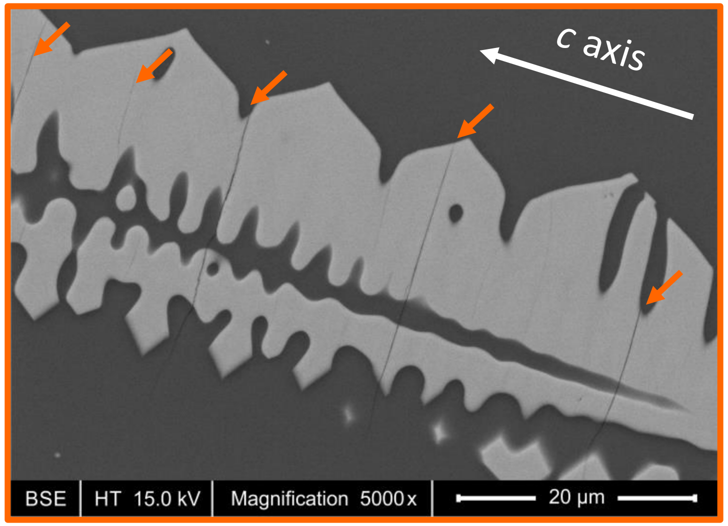

VTR sample containing large zircon crystals

– cracks mostly around the crystals

– formed probably at a late stage (during cooling)

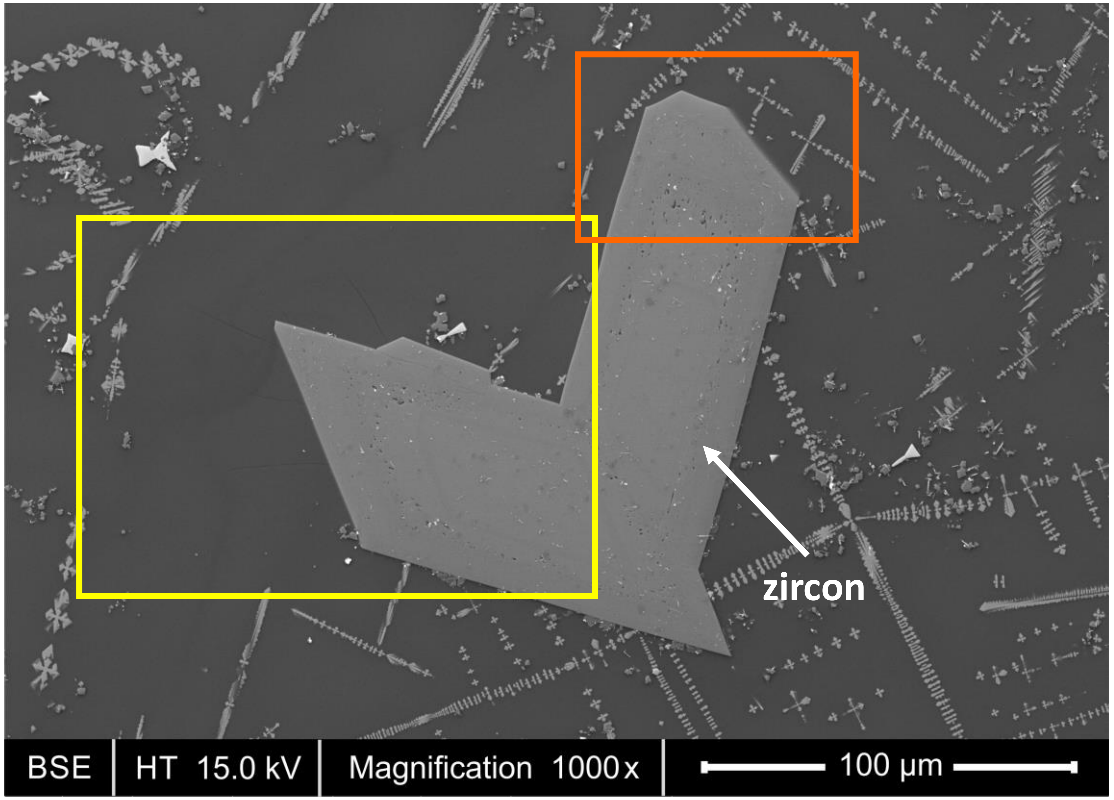

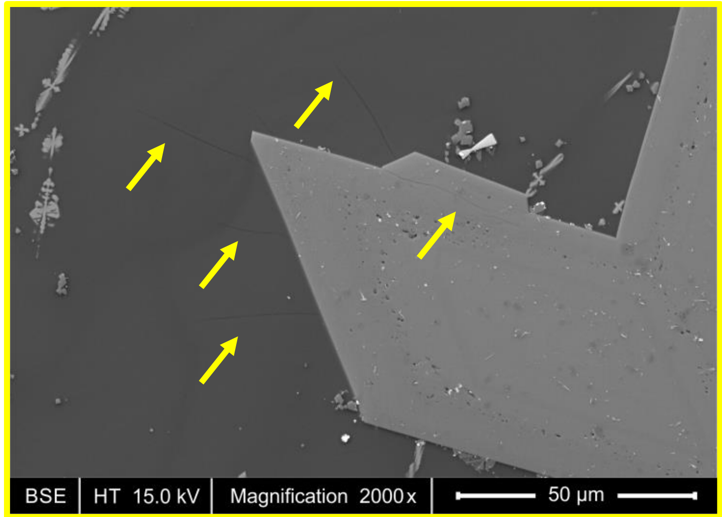

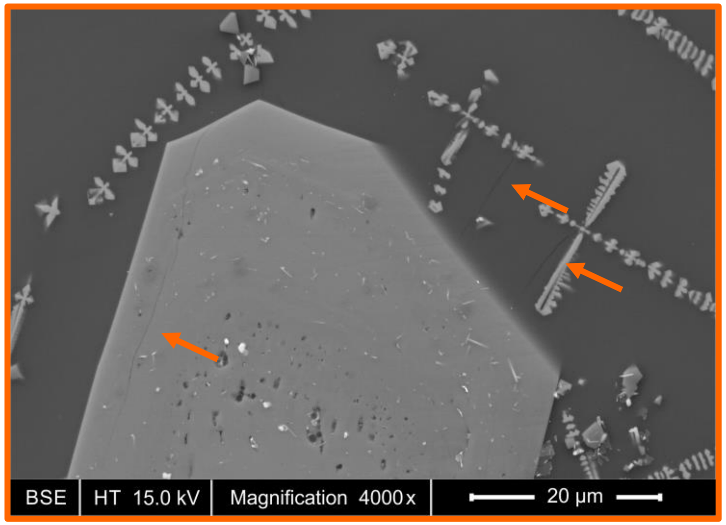

VTR samples

Simple Ca/Zn GC samples

Irradiation experiments

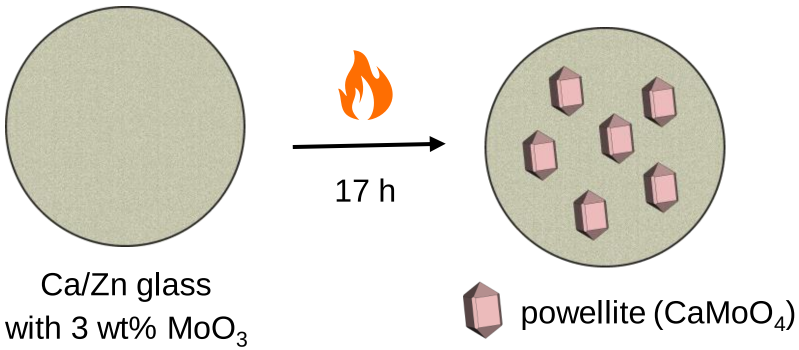

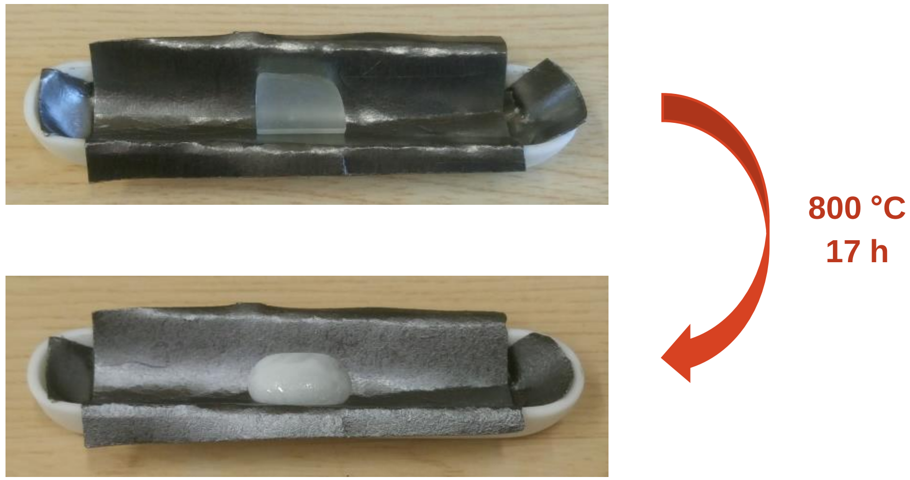

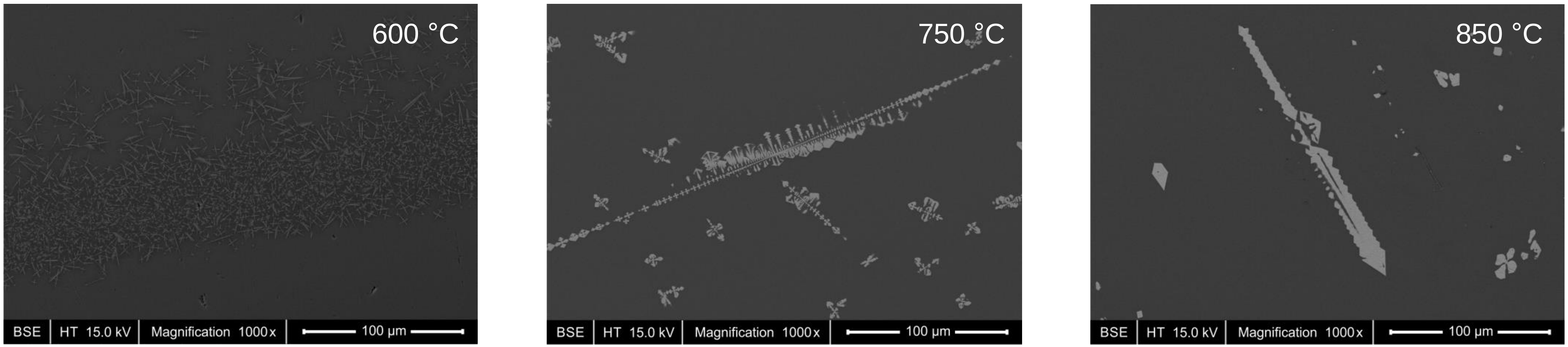

VTR samples

Simple Ca/Zn GC samples

Irradiation experiments

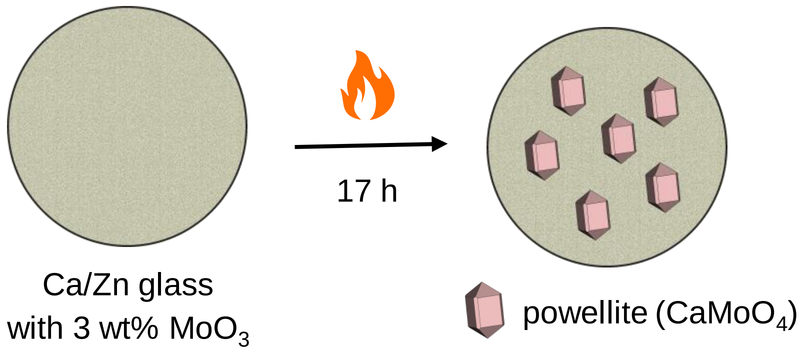

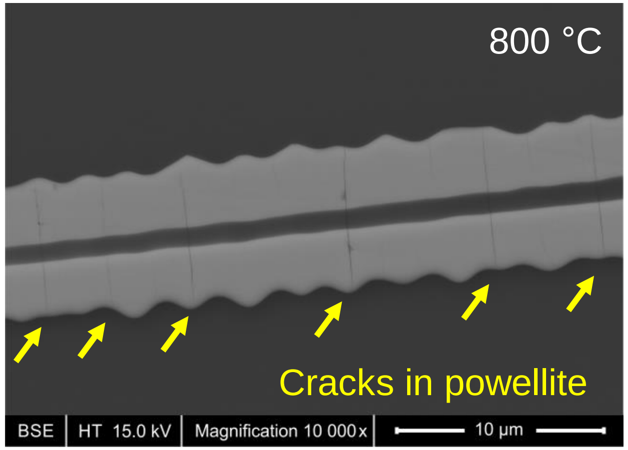

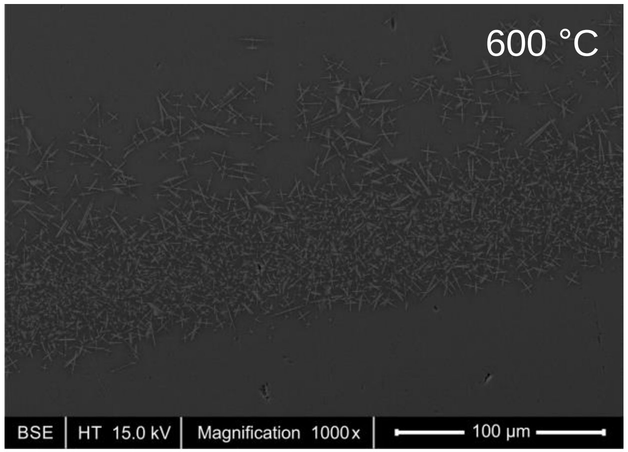

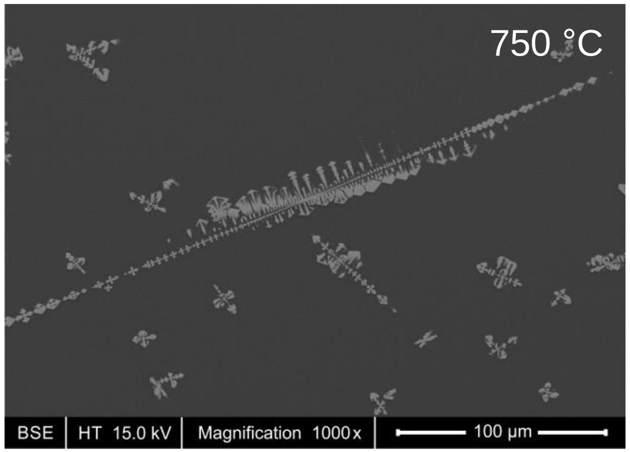

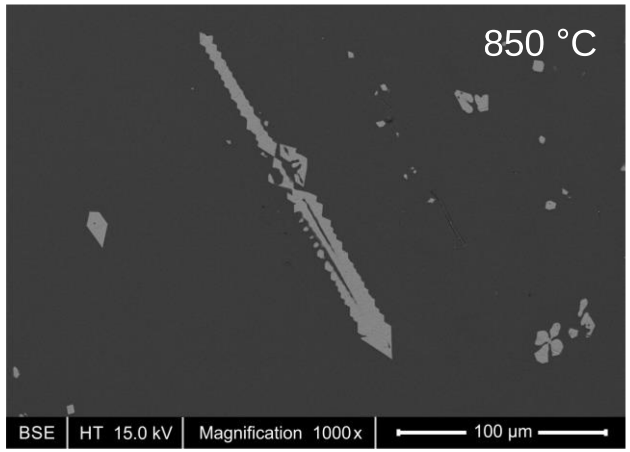

TRANSCEND

Transformative Science and Engineering for Nuclear Decommissioning

VTR samples | Simple Ca/Zn GC samples | **Irradiation experiments**

VTR samples

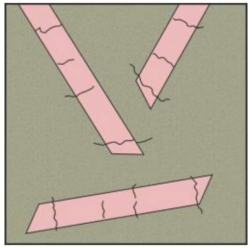

Ni irradiation

+ *SEM, EPMA, EBSD* ✓

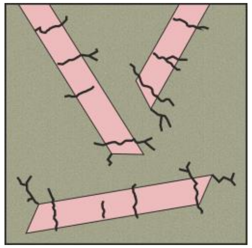

New cracks (?)

Crack propagation (?)

Amorphisation (?)

Irradiation induced strain (?)

Ca/Zn GC samples

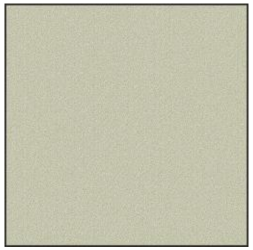

Heat treatment ✓

+ SEM, TGA, DSC

To understand powellite crystallisation and cracking

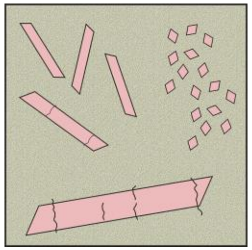

Ni irradiation

+ SEM, EBSD

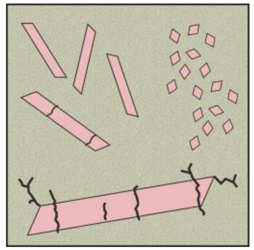

Ca/Zn glass samples

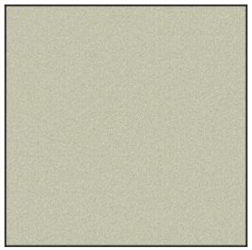

α irradiation ✓

+ *EPR, XAS, UV-VIS*

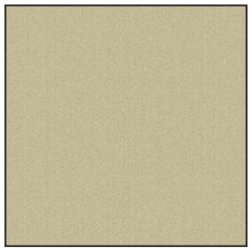

Irradiation induced microstructural changes

Transformative Science and Engineering for Nuclear Decommissioning

Thank you for the help!

Laura Leay
Brian O'Driscoll

Tracey Taylor
Mike Harrison

NATIONAL NUCLEAR LABORATORY

Paul Bingham
Prince Rautiyal
Stuart Bartlett
Györgyi Glodán
Chetna Tyagi
Samir de Moraes Shubeita
Carl Andrews

Special thanks for the support from National Nuclear Laboratory.

NATIONAL NUCLEAR LABORATORY

Thank you

Contact Details
tamas.zagyva@postgrad.manchester.ac.uk